ame	Date Modified	Size	Kind
Golander 1989 Gradient Surfaces Caldwell lin.pdf	Aug 11, 2006, 9:54 PM	1.1 MB	PDF
Golander 1990 Adsorption Gradient Hydrophobic Surfaces lin Hlady .pdf	Aug 11, 2006, 10:00 PM	2.2 MB	PDF
Golander 1992 Harris book Plenum Im…d PEG Herron Lim Claesson Stenius.pdf	Oct 19, 2013, 10:31 AM	3.6 MB	PDF
Golander Jozefowicz fibringogen adsor…ran draft Muller Zhou unpublished.pdf	Oct 2, 2015, 3:37 PM	321 KB	PDF
Gough 1973 Science Enzyme Electrodes.pdf	Aug 11, 2006, 10:05 PM	1.7 MB	PDF
Gough 1974? Electrochemical Society reprint Enzyme Electrodes.pdf	Oct 21, 2013, 4:28 PM	1.1 MB	PDF
Gregonis 1976 Methacrylate Hydrogels ACS Hydrogels bk chen.pdf	Aug 11, 2006, 10:09 PM	1.2 MB	PDF
Gregonis 1982 Wilhelmy Seymour bk Hsu Buerger Smith.pdf	Oct 10, 2006, 5:50 PM	1.9 MB	PDF
Gregonis 1983 Hydrophobic Hydrogel…ngs Preprints Coleman Hsu Buerger.pdf	Oct 31, 2017, 3:13 PM	586 KB	PDF
Gregonis 1984 JP Paul bk Adsorption…odel Surfaces coleman van wagenen.pdf	Aug 11, 2006, 6:18 PM	1.7 MB	PDF
Gregonis 1985 Model Polymers Chap 3.pdf	Aug 11, 2006, 10:47 PM	5.7 MB	PDF

Gola-2

A New Technique to Prepare Gradient Surfaces Using Density Gradient Solutions

C.G. GÖLANDER*, KARIN CALDWELL and Y.-S. LIN

Center for Biopolymers at Interfaces and of Bioengineering, 2480 Merrill Engineering Building, The University of Utah, Salt Lake City, UT 84112 (U.S.A.)

ABSTRACT

We present a new method to prepare quartz slides with a wettability gradient by confining a concentration gradient of dichlorodimethyl silane, the hydrophobation agent, in a density gradient formed by mixing diiodomethane and trichloroethylene. The gradients were characterized by means of contact angle measurements using the Wilhelmy plate technique and by the adsorption of human lysozyme, IgG or fibrinogen as measured by total internal reflectance fluorescence (TIRF) spectroscopy.

INTRODUCTION

Some years ago Elwing et al. [1] described the preparation of surfaces with a wettability gradient formed by the diffusion and reaction of dichlorodimethyl silane (DDS) on hydrophilized silicone wafers. The most obvious reason for the interest in gradient surfaces is that a variety of surfaces differing only with respect to one property can be studied in a single experiment, which saves resources and simplifies experimental comparison and interpretation of the results. This is of particular interest for fundamental studies of the interaction between biological molecules and surfaces. In particular the nature of protein adsorption, the initial event occurring when a foreign material is exposed to blood or tissue, can be studied in more detail on gradient surfaces.

One essential feature in these studies is the shape of the gradient, which is determined by Ficks diffusion equations. In an effort to increase the degrees of freedom to choose gradient shapes and also to make other gradient types, by choosing other suitable surface reactants, we have developed a new preparation technique in which the reactants are present in a density gradient during surface exposure and reaction. In order to characterize the gradients and to demonstrate their value as research tools, we have studied wetting properties

---

*Present address: Institute for Surface Chemistry Box 5607, S-11486 Stockholm, Sweden.

and adsorption, using total internal reflectance fluorescence spectroscopy (TIRF), of human IgG, fibrinogen and lysozyme to three gradients with different shapes.

EXPERIMENTAL

Chemicals

Dimethyldichloro silane (DDS) was purchased from Petrarch Systems Karlsruhe, F.R.G., (lot #703496) and used without further purification. For preparation of the density gradient we used pro analysis grade trichloroethylene (TCE, density $d=1.42$) from Fluka and diiodomethane (DIM, $d=3.34$) from Aldrich.

Lyophilized human placenta lysozyme from Behring Diagnostics, San Diego, CA (lot #703496); human fibrinogen, 65% clottable from US Biochemical Corp., U.S.A. (lot #52364), and chromatographically purified human IgG from Organon-Teknika Corp., U.S.A. (lot #30567) were dissolved in phosphate-buffered saline (pH=7.3, $I=0.19$).

L-5-Hydroxytryptophane methylester hydrochloride·H_2O, Behring (lot #410066) was used for calibration of the intrinsic fluorescence from lysozyme.

Preparation of density gradient surfaces

Quartz cover slips, 25.4×76.2 mm, were exposed to chromosulphuric acid for 40 min at 70°C and subsequently rinsed thoroughly in triply distilled water before final drying by N_2 jet. The sample now showed complete wetting (zero contact angle). Three cover slips were mounted parallel in a 15 mm wide polypropylene chamber. They were kept apart from each other by 1 mm thick protrusions on the walls of the chamber. In the bottom of the chamber, a drainage hole was made and polypropylene tubing was connected and sealed against the chamber using silicone adhesive. From a vigorously stirred mixing flask, initially containing 20 ml pure TCE, solution was pumped peristaltically into the slide chamber while continuously being replaced by DIM solution containing DDS of specified concentration from a second flask, see Fig. 1. Thereby a vertical density gradient containing a DDS concentration gradient is built up in the slide chamber (with increasing concentration towards the bottom). Periods of 10–30 min were allowed for the surface silanization reaction (hydrophobation) before the chamber was drained from the bottom. Each slide was then separately taken out and rinsed thoroughly in 20 ml TCE, 20 ml ethanol and finally in 100 ml triply distilled water. The slope of the wettability gradient established on the surface was controlled by choosing an appropriate DDS concentration in the DIM flask and an appropriate ratio between the volume flow into the mixing flask and the slide chamber. In practice this latter ratio was controlled by using tubes of different internal diameters on the rotor head of the pump. The wettability range was controlled by the reaction time.
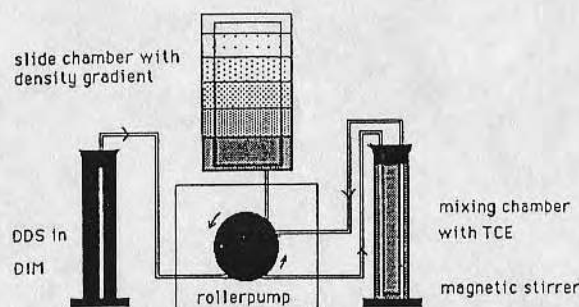
Fig. 1. Schematic illustration of the equipment used for preparation of gradient surfaces by means of a density gradient solution. DDS is dichlorodimethyl silane, DIM is diiodomethane and TCE is trichloroethylene.

Wetting studies

Advancing and receding contact angles were recorded along the gradient by using the Wilhelmy Plate method [2]. The slides were suspended on a thread which was connected to a microbalance and the weight was continuously recorded while the slide was immersed into a water flask. The flask was supported on a table which was moving at a constant speed of 40 mm min^{-1} by means of a stepping motor. The contact angle, ϕ, was calculated from

$$f = p\gamma \cos \phi + (m - V\Delta g)$$

where f is the force on the plate, p the perimeter of the slide, γ the liquid surface tension, m is the weight of the plate in air, Δg is the liquid–vapour density difference and V the displaced volume.

Fluorescein-labelling of the proteins

Fluorescein-isothiocyanate isomer I from Sigma was used for extrinsically labelling IgG and fibrinogen according to the method of Coons et al. [3]. The molar fluorescein/protein ratio was 1.2 for IgG and 1.0 for fibrinogen. The sodium salt of fluorescein (Sigma) was used for the calibration of the extrinsic fluorescence.

Protein adsorption studies

TIRF was used to record the adsorption of proteins on the gradient surface. For intrinsic fluorescence, from lysozyme, a Xenon arc lamp (Model PS150-8, Ion Laser Technology Inc., CA) was used. The excitation wavelength was 280

nm and the emission intensity was recorded at 340 nm. Fluorescein-labelled IgG and fibrinogen were excited by means of the 488 nm line of an air cooled Argon laser (Ion Laser Technology Inc., Model 5490ASL). Here the emission was recorded at 515 nm. The TIRF cell was mounted on a moving table and the position along the gradients were scanned manually by adjustments on a micrometer screw. This TIRF geometry has been described previously [4]. Adsorbed amounts, Γ, were calculated using the quantification procedure of Hlady et al. [5]:

$$\mathcal{O}_a/\mathcal{O}_b \cdot \Gamma = 2d_p c_p N_a/N_{b(ev)}$$

where $\mathcal{O}_a$ is the quantum yield for adsorbed and $\mathcal{O}_b$ from bulk fluors, d_p the penetration depth for the exciting light, c_p the protein concentration, N_a the fluorescence intensity from adsorbed fluors and $N_{b(ev)}$ from fluors in the evanescent bulk region respectively. For both hydroxy tryptophane and fluorescein standards, solutions with absorption values ϵc (ϵ is the extinction coefficient) in the range 0–40 absorption units/cm were prepared and used for making fluorescence calibration curves. These curves were used to distinguish the $N_{b(ev)}$ component from the scattering component, $N_{b(s)}$, of the directly measured total bulk fluorescence, $N_{b(tot)}$.

RESULTS AND DISCUSSION

Using different sets of conditions, three samples with different wetting characteristics (Fig. 2) were made. In all preparations, a volume flow of 10 ml min^{-1} was used for the mixing of TCE and DIM solutions and for filling of the
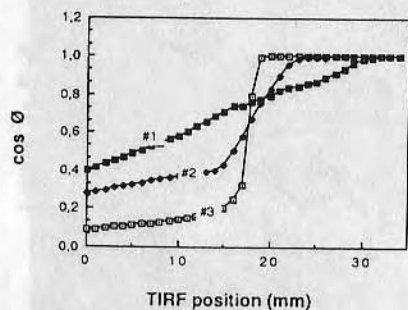

Fig. 2. Cosine of the advancing contact angle, ϕ, on the wettability gradients obtained by using the following preparation conditions. Sample #1: DDS concentration $c_{DDS}=0.3$ vol.%, reaction time $t=15$ min. Sample #2: $c_{DDS}=0.5$ vol.%, $t=10$ min. Sample #3: $c_{DDS}=1.0$ vol.%, $t=20$ min. Position 0 (zero) refers to the hydrophobic end.

slide chamber. The zero contact angle measured on the upper end of all samples in Fig. 2 indicates that the density gradients are quite stable, i.e. the convective and diffusive transport of DDS within the density gradient can, in practice, be neglected. Roughly, two wetting regions can be identified on two of the samples (#2 and #3) of Fig. 2; a low contact angle region characterized by a steep and linear contact angle gradient and a high contact angle region, above 70°, characterized by a more shallow, but still approximately linear, wetting gradient. Since DDS reacts instantaneously with encountered surface silanol groups (Si–OH), one would expect that the wettability range would be completely determined by the linear concentration profile of DDS established in the density gradient and by the diffusion time. The presence of this second wetting region at higher contact angles (lower cos ϕ values) may indicate that the apparent DDS reaction rate is slower at higher DDS surface coverages (probably due to steric hindrance [6]) and that the surface does not reach saturation with regard to the DDS reaction. In this context it is worthwhile to mention that it has recently been shown that only ~50% of the SiOH reaction centers present on amorphous silica reacts with alkylsilanes [6]. For a completely methylated surface $\gamma_s = 50$ dyn cm^{-1} and $\phi = 117°$ [7].

A considerable wetting hysteresis was found on the hydrophobic side of all samples. Hence, the advancing and receding angles of sample 2 differed by almost 20°, see Fig. 3. Although the hysteresis decreases with decreasing immersion velocity, it is still significant at <1 mm min^{-1} (under present investigation). It should be pointed out that the noise level in the original force versus distance recording on the slide was negligible in comparison with the recorded hysteresis. Hysteresis is also present on wettability gradients made by diffusion on quartz [8]. Wetting hysteresis originates either from surface roughness or surface chemical heterogeneity. Scanning electron micrographs of the samples show no evidence of any surface structure in the micron range
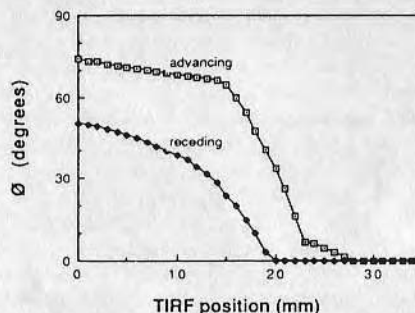

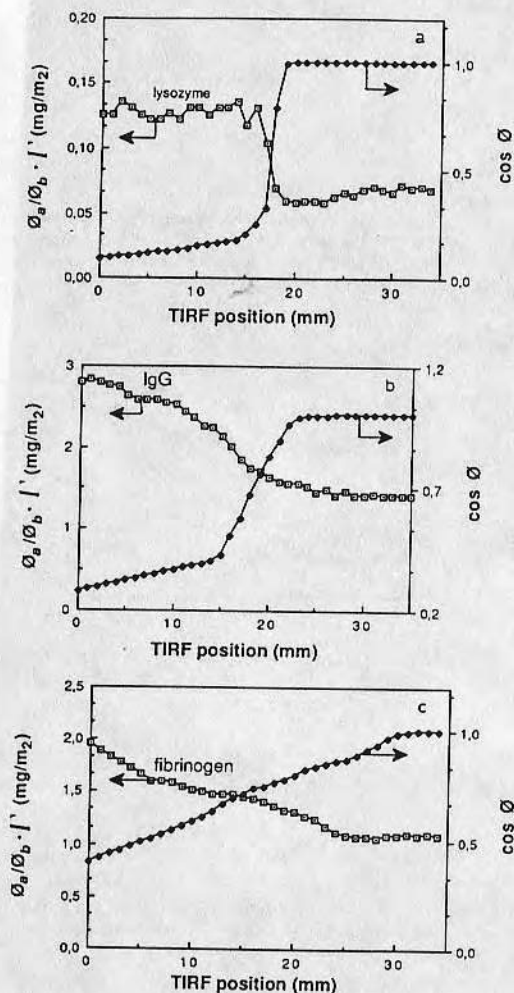Fig. 3. Wetting hysteresis on sample #2 from Fig. 2. (□) Advancing contact angle, (♦) Receeding contact angle.

Fig. 4. Protein adsorption as measured by TIRF on gradient samples from Fig. 2. The measured adsorbed amounts are expressed as $\varnothing_a/\varnothing_b \cdot \Gamma$, where $\varnothing_a/\varnothing_b$ is the ratio between the fluorescence quantum yield for adsorbed and bulk fluors, respectively, and Γ is the surface density in mg m^{-2}. Cosine for the contact angle, ϕ, on the gradient surface in water before protein adsorption. (a) sample #3 exposed to human lysozyme $c=0.1$ mg ml^{-1}, (b) sample #2 exposed to human IgG, $c=1.3$ mg ml^{-1}, (c) sample #1 exposed to human fibrinogen, $c=0.32$ mg ml^{-1}.

(not shown here). One way to rationalize wetting hysteresis is to assume a mosaic surface composed of hydrophilic and hydrophobic domains with sizes larger than ~1000 Å [9]. A more detailed investigation of the wetting characteristics and the surface heterogeneity is presently under way.

Relative adsorption of human lysozyme, IgG and fibrinogen, respectively, on the three gradient surfaces is presented in Fig. 4 as $\varnothing_a/\varnothing_b \cdot \Gamma$. Since the quantum yield change upon adsorption is not known, absolute adsorption values cannot be determined. However, in a recent study of IgG adsorption on trimethoxyaminopropyl silanized surfaces using the intrinsic tryptophane fluorescence, the $\varnothing_a/\varnothing_b$ ratio was in the order of 0.1 as obtained from independent measurements using ^{125}I-labelled proteins [10]. On the other hand, for extrinsic fluors, as used here in the case of IgG and fibrinogen, one expects only minor changes in the quantum yield upon adsorption.

Figure 4 shows that there are correlations between the adsorption of lysozyme, IgG or fibrinogen and the cosine of the contact angle. For both pure lysozyme and IgG solutions the adsorption steadily increases toward the hydrophobic end. Fibrinogen, when freshly dissolved, shows the same trend and the result on lysozyme is in agreement with earlier results on homogeneously acid etched or DDS reacted slides [11].

Some advantages with using the density gradient method presented is the stability of the concentration distribution as mentioned above. Furthermore there is a great flexibility in the choice of gradient shape by proper choice of reactant concentration and reaction time. Also, by proper choice of other functional silanes one would be able to create gradients with other properties, for example charge, H-bonding or hydrocarbon/fluorocarbon character. The applications of the method can be further extended to making two-component gradient surface films of polymers, proteins, etc. When water is the solvent, the density gradient can be made by means of dextran, sucrose or CsCl among others. Such gradients are commonly used in ultracentrifugation.

ACKNOWLEDGEMENTS

REFERENCES

1 H. Elwing, S. Welin, A. Askendahl, U. Nilsson and I. Lundström, J. Colloid Interface Sci., 119 (1987) 1.
2 L. Wilhelmy, Ann. Phys., 119 (1963) 177.
3 A.M. Coons, H.J. Creech, R.N. Jones and E. Berliner, J. Immunol., 45 (1942) 159.
4 V. Hlady, C.-G. Gölander and J.D. Andrade, Colloids Surfaces, 33 (1988) 185.
5 V. Hlady, D.R. Reinecke and J.D. Andrade, J. Colloid Interface Sci., 111 (1986) 555.

Wetting and Plasma-Protein Adsorption Studies Using Surfaces with a Hydrophobicity Gradient

C-G. GÖLANDER*, Y-S. LIN, V. HLADY** and J.D. ANDRADE

Center for Biopolymers at Interfaces, University of Utah, Salt Lake City, UT 84112 (U.S.A.)

ABSTRACT

Wetting gradients on silica were prepared according to the technique developed by Elwing et al. (J. Colloid Interface Sci., 119 (1987) 1). The contact angle, determined by the Wilhelmy-plate method, showed an S-shaped dependence on the position along the gradient. The advancing water contact angle was 0° on the hydrophilic end and 97 ±3° on the hydrophobic end. The receding water contact angles were ~40° smaller in the wetting transition region and ~20° smaller on the hydrophobic side of the gradient. Total internal reflection fluorescence (TIRF) was used to study the adsorption of three fluorescein-labelled proteins: human serum albumin, IgG and fibrinogen. The gradient surface exposed to a single protein solution resulted in an amount of adsorbed protein on the hydrophobic end that approximately corresponded to a monolayer. As a rule, lower adsorption was found on the hydrophilic end. When the proteins were adsorbed from a mixture, the surface concentration of albumin was generally not affected, the fibrinogen adsorption decreased by 40–50% and the IgG adsorption decreased to 10% of the adsorption measured from a single protein solution. The so-called Vroman effect (for example, transient IgG adsorption maximum in adsorption kinetics) was found on the hydrophobic side of the gradient. The desorption experiments were carried out with a nonionic polymeric surfactant, an ethylene oxide–propylene oxide copolymer: EO_{100}–PO_{70}–EO_{100}. The adsorption affinity of albumin to the wetting transition region, as measured by surfactant induced desorption, was extraordinarily high.

INTRODUCTION

A foreign material in contact with blood initially responds by adsorbing plasma proteins. The structure and composition of this "conditioning" layer essentially determine all subsequent blood–material interactions [1]. In the development of blood- and tissue-compatible materials, there is a need for increasing understanding of the detailed relationship between the nature of the surface and its blood response. One expects that a surface with a conditioning layer of albumin or antithrombin III is more blood compatible than a surface with adsorbed fibrinogen, a potential fibrin generator. A dynamic exchange of

*Present address: Institute for Surface Chemistry, Box 5607, S-11486 Stockholm, Sweden.
**On leave of absence from Ruder Boskovic Institute, P.O. Box 1016, 41000 Zagreb, Yugoslavia.

/ last page

5 J.N. Lindon, G. McManama, K. Kusher, E.W. Merrill and E.W. Salzman, Blood, 68 (1986) 355.
6 R. Schmitt, R. Varoqui, S. Uniyal, J.L. Brash and Pysineri, J. Colloid Interface Sci., 92 (1983) 25.
7 J.L. Brash and T.A. Horbett, ACS Symp. Ser., 343 (1986) 290.
8 P. Wojciechowski, P. ten Hove and J.L. Brash, J. Colloid Interface Sci., 111 (1986) 455.
9 H. Elwing, S. Welin, A. Askendahl, U. Nilsson and I. Lundström, J. Colloid Interface Sci., 119 (1987) 1.
10 H. Elwing, B. Nilsson, K.-E. Svensson, A. Askendal, U. Nilsson and I. Lundström, J. Colloid Interface Sci., 125 (1987), 139.
11 D. Axelrod, Ann. Rev. Biophys. Bioeng., 13 (1984) 247.
12 V. Hlady, D.R. Reinecke and J.D. Andrade, J. Colloid Interface Sci., 111 (1986) 555.
13 V. Hlady, J. Rickel and J.D. Andrade, Colloids Surfaces, 34 (1988/89) 171.
14 D. Ausserre, H. Hervet and F. Rondelez, Macromolecules, 19 (1986) 85.
15 V. Hlady and J.D. Andrade, Colloids Surfaces, 32 (1988) 359.
16 V. Hlady, C. Gölander and J.D. Andrade, Colloids Surfaces, 33 (1988) 185.
17 A.M. Coons, H.J. Crech, R.N. Jones and E. Berliner, J. Immunol., 45 (1942) 59.
18 H.B. Pollard, R. Menard, H.A. Brandt, C.J. Pazoles, C.E. Creutz and A. Ramu, Anal. Biochem., 86 (1978) 761.
19 A. Baszkin and D.J. Lyman, J. Biomed. Mater. Res., 14 (1980) 393.
20 J. Gobet and E.Sz. Kova'ts, Adsorption Sci. Technol., 1 (1984) 77.
21 A.B.D. Cassie, Discuss. Faraday Soc., 75 (1952) 5041.
22 B. Blombäck and L.Å. Hansson, Plasma proteins, AWE Gebers, Stockholm, 1976.

proteins occurs in the adsorbed protein layer. Furthermore, even before the steady state composition of adsorbate is reached, proteins may replace each other in a well-defined order; for example: albumin–IgG–fibrinogen–HMW kininogen. This is now called the Vroman effect [2], which has been recently observed by different scientists and extensively studied by Brash et al. [3,4]. One can assume that the rate of this exchange and the extent to which the exchange will occur is dependent on protein affinity to the surface which, in turn, can be modulated by modifying the surface properties. If one protein in the exchange sequence has an exceptionally high surface affinity, further exchange will be blocked. In particular, surface-induced perturbation of protein conformation will affect the exchange and the interactions. Accordingly, it was reported that an adsorbate layer of denatured fibrinogen is inert, while more natural fibrinogen adsorbates trigger coagulation activation [5]. The exact role of surface denaturation in blood interactions is, however, still open to question. A large number of plasma-protein adsorption measurements onto a variety of surfaces has been reported, ranging from studies in single protein solutions, binary or ternary mixtures, to whole plasma [6–8].

A more convenient way to systematically study how surface chemistry affects adsorption and protein exchange is to utilize surfaces with gradient-like varying characteristics [9]. However, if one wishes to study the adsorption from whole plasma then the determination of the exact adsorbate composition presents considerable difficulty since it requires that all plasma proteins are individually separated, labelled, and injected back into the plasma. Alternatively, one can utilize antibody reactions to obtain qualitative adsorption information [10] or two-dimensional electrophoresis of eluted adsorbate proteins. Although the latter technique is not directly applicable to gradient surface studies, it appears to be a valuable technique for post-adsorption protein mixture mapping.

The aim of this paper is to show the usefulness of applying total internal reflection fluorescence (TIRF) to study single and competitive adsorption of proteins on hydrophobic gradient surfaces. TIRF is a well-established in situ method to study, in a quantitative manner [11,12], the adsorption [13] and depletion [14] of polymers and proteins at interfaces or, in a qualitative manner, the surface-induced conformational change in proteins [15].

We have studied the three most abundant plasma proteins: albumin, IgG and fibrinogen. A qualitative measure of protein surface affinity was obtained by adding a non-ionic surfactant during the desorption phase of the experiment.

EXPERIMENTAL

Wettability gradients were prepared on 2.5×7.5 cm fused silica plates (ESCO Product Co.) according to the diffusion technique described by Elwing et al. [9]. Prior to silanization, the plates were etched at 70°C in chromosulphuric

acid for 40 min, rinsed thoroughly in triply-distilled water, dried in an N_2 jet and mounted in a 100 ml glass jar. In the jar, 50 ml p-xylene (Fluka, density, $d=0.9$), was gently layered on top of 50 ml 0.05% w/w solution of distilled dichlorodimethylsilane (DDS) (Petrarch Systems Inc.) in trichloroethylene (Fluka, $d=1.4$). The silane was allowed to diffuse into p-xylene and react with the silica surface for 30 min before the jar was emptied through a drainage pipe. The plates were thoroughly rinsed from above with 100 ml of each trichloroethylene, ethanol and water and finally dried in an N_2 jet.

The contact angle along the gradient surface was measured by the Wilhelmy-plate technique. The plate was attached to the hook of a microbalance and gradually immersed into a water container by vertically moving the supporting table by means of a stepping motor while the plate weight was continuously recorded. A constant immersing speed of 40 mm min^{-1} was used. Both advancing and receding water contact angles were measured.

The TIRF geometry is schematically shown in Fig. 1. The experimental configuration was similar to the one described elsewhere [12]. As the excitation light source an Ar$^+$ laser (Ion-Laser Technology Inc.) with an output power of approximately 10 mW at 488 nm was used. The 488 nm line was selected with an interference filter and the beam intensity was adjusted by neutral density filters. The laser beam was totally reflected at the silica surface/solution interface which created an evanescent surface wave on the solution side of the interface. The fluorescence was collected normal to the interface through the TIRF cell. The internal reflection element was mounted on a micrometer-driven stage which allowed lateral scanning along the longest surface dimensions
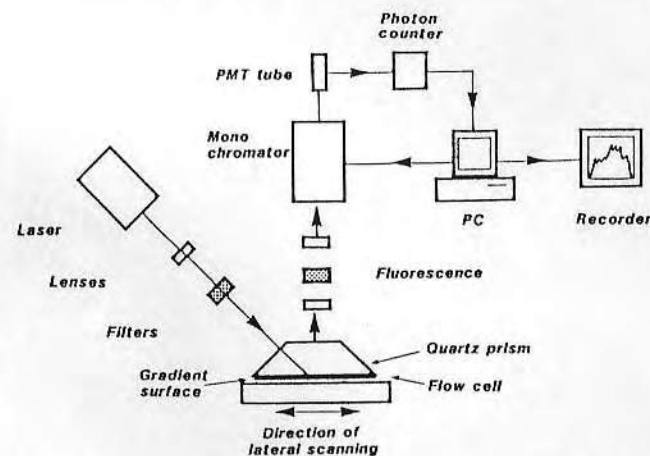

Fig. 1. Schematic illustration of the arrangement of the TIRF equipment used for protein adsorption studies.

[16]. The lateral distance between measuring points was 1 mm; the fluorescence was collected from a 0.5 mm wide spot.

Protein adsorption/desorption. Human albumin (Pentex, Miles Diagnostics), chromatographically purified human IgG (Organon Teknika Corp.) and human fibrinogen (65% clottable, United States Biochemical Corp.) were labelled with fluorescein-isothiocyanate, FITC (Isomer I, Sigma), according to the method of Coons et al. [17]. The degree of labelling was determined from the absorption at 280 and 490 nm and from an independent protein concentration measurement using the Biorad protein assay [18]. The proteins were dissolved in phosphate buffer solution (PBS, pH 7.3, I 0.19), injected into the TIRF cell and adsorbed under static conditions. After 1 h equilibration the fluorescence contributions from the adsorbed proteins, N_a, and the non-adsorbed proteins in the bulk volume, $N_{b\ (tot)}$, respectively, were determined by quickly displacing the protein solution with the buffer. Subsequently, the affinity of adsorbed protein(s) for the surface was studied by measuring, in buffer, the residual fluorescence after allowing 30 min for desorption in a 1% solution on nonionic surfactant in PBS, an ethylene oxide–propylene oxide copolymer (EO_{100}–PO_{70}–EO_{100}, Pluronic F127, BASF).

Quantitation of TIRF adsorption experiments. The quantitation of protein adsorption experiments essentially followed the procedure given elsewhere [12,13]. The sodium salt of fluorescein (Sigma) was used as a fluorescence standard, to obtain a TIRF calibration curve at 488 nm excitation which was needed to separate the scatter-excited part, $N_{b\ (s)}$, from the evanescent wave-excited part, $N_{b\ (ev)}$, of the total, $N_{b\ (tot)}$, measured signal. Quantitation of protein adsorbed amount, Γ, was based on the following equation [12,13]:

$$(F_a/F_b)\Gamma = N_a d_p c_p / 2 N_{b\ (ev)}$$

where F is the fluorescence quantum yield for adsorbed (a) and bulk (b) fluors, N the corresponding fluorescence intensity, d_p the penetration depth at 488 nm and c_p is the protein solution concentration. This quantitation scheme does not account for the change in fluorescence quantum yield upon adsorption often found in the case for intrinsic protein fluorescence [12]. In the case that the fluorescein–isothiocyanate quantum yield is not affected by protein adsorption the TIRF-derived adsorption result, $(F_a/F_b)\Gamma$, will equal the actual adsorption, Γ.

RESULTS

Wetting characterization of surfaces

Advancing contact angles were measured on slides which were immersed in homogeneous DDS solution in trichloroethylene of different concentration for different time (Fig. 2b). Constant contact angle values were generally reached
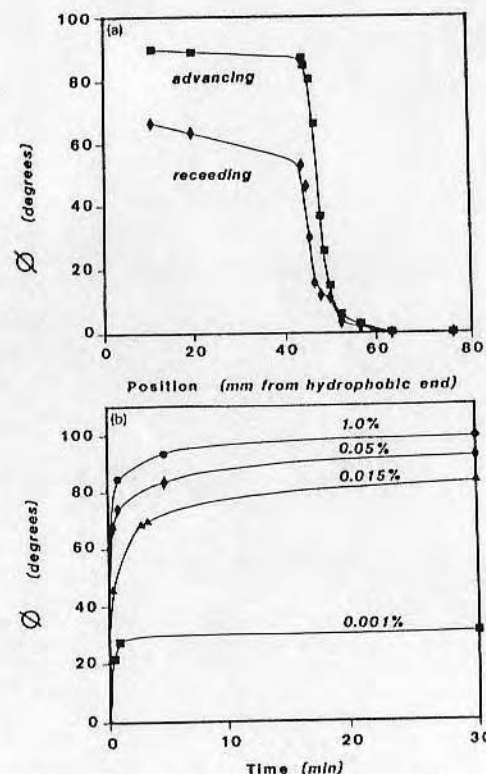
Fig. 2. (a) Advancing and receding contact angles, ϕ, as a function of position on the silica gradient surface. The error bars from results of two independent measurements are smaller than the size of the symbols. The hydrophobic end is referred to as the 0 position, and position 40 corresponds to the interface between the *p*-xylene and the trichloroethylene solvent phases during preparation. (b) Advancing contact angles on DDS-treated silica slides as a function of reaction time at various concentrations of DDS (%w/w) in trichloroethylene.

within 15 min of immersion time. The contact angle showed a strong dependence on the DDS concentration in the range 0.001–0.1% while surface saturation was obtained above 0.1% DDS concentration (contact angle: 98°).

Advancing and receding contact angles of the hydrophobicity gradient surface are shown in Fig. 2a. At chosen standard conditions: $c_{(DDS)} = 0.05\%$ w/w, $t = 30$ min, the hydrophobic side of the gradient was non-wetting, showing 89–92° in advancing water contact angle, while complete wetting was observed on the hydrophilic end. A considerable hysteresis of the contact angle on the hydrophobic side and in the wetting transition region of the gradient was found (Fig. 2a). However, no surface irregularities in the micron range could be observed by scanning electron microscopy (not shown).

Protein adsorption

Adsorption on the gradient surface was initially measured for single protein solutions of albumin, IgG and fibrinogen as a function of the linear position along the hydrophobic gradient surface at low degree of labelling (<1 mole FITC/mole protein), Figs 3a–c. The concentrations were 4.2, 1.3 and 0.32 mg ml^{-1}, respectively, corresponding to one tenth of the protein plasma concen-
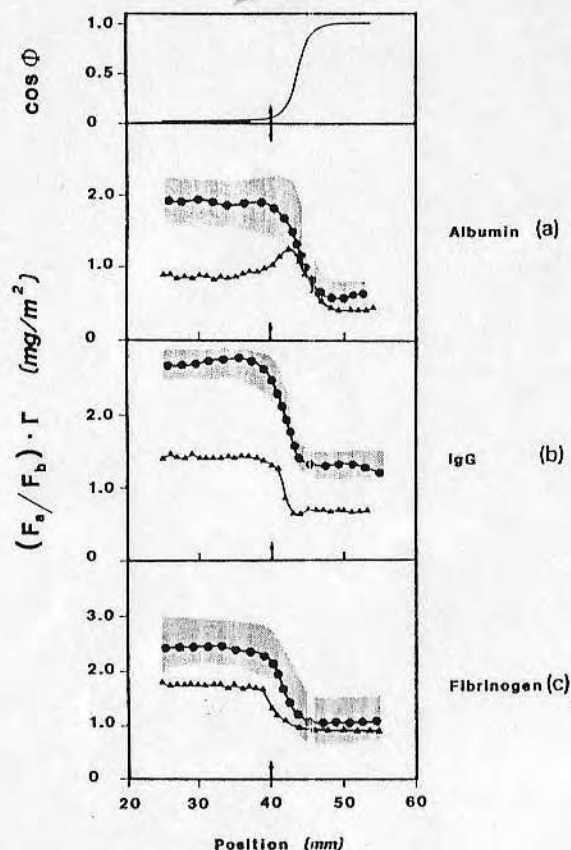

Fig. 3. TIRF-quantified adsorption of single plasma proteins to a hydrophobic gradient surface. The adsorption is expressed as $(F_a/F_b)\Gamma$ (in mg m^{-2}). For clarity, only results from the measurements on one gradient surface are displayed. The shaded area represents scattering in data between three independent measurements. The arrow marks the position of the interface between the p-xylene and trichloroethylene phases at the preparation of the gradient. Adsorption from PBS buffer after surfactant desorption: (a) albumin, $c_{(alb)}=4.2$ mg ml^{-1}, degree of labelling, DL, (mole/mole) $=0.2$; (b) IgG, $c_{(IgG)}=1.3$, mg ml^{-1}, DL$=1.0$; (c) fibrinogen, $c_{(fgn)}=0.32$ mg ml^{-1}, DL$=1.0$.

tration. In the same figure, the cosine of the advancing contact angle, ϕ, measured prior to the adsorption, is displayed.

As a rule, the three proteins were adsorbed to a larger degree on the hydrophobic side compared to the hydrophilic side and a good correlation between the increase in the adsorption values and the decrease in the cos ϕ value was found (Fig. 3).

The adsorption values on the hydrophobic side corresponded roughly to monolayer capacities of the different proteins, $M_{alb}=2.5$ mg m^{-2} [19], $M_{IgG}=2.7$ mg m^{-2} [6] and $M_{fib}=2.1$ mg m^{-2} (calculated for side-on orientation). The variation of the adsorption results, as obtained from the data scatter along a single gradient surface, was typically ± 0.1 mg m^{-2}. The adsorption measurements performed on two identical gradient surfaces and using the same degree of protein labelling showed the maximal variation to be between ± 0.2 and ± 0.5 mg m^{-2}, depending on the type of protein. However, the albumin gave rise to a larger scattering in experimental adsorption results in the mid-region of the gradient and often a minor peak in the adsorbed amount appeared in this region.

The fraction of albumin displaced by the nonionic surfactant from the hydrophobic side was higher than from the hydrophilic side (Fig. 3), which is understandable when considering the fact that the surfactant predominantly interacted via hydrophobic interactions. Furthermore, the adsorption peak in the mid-region became more pronounced after surfactant rising. Fibrinogen was more easily removed from the hydrophobic side as compared to the hydrophilic side, while IgG was equally well displaced across the whole gradient surface.

Table 1 shows how the degree of labelling affects the adsorption on the dif-

TABLE 1

Influence of the degree of labelling (mole fluor/mole protein) on the adsorption values (in mg m^{-2}) for single proteins on gradient surfaces ($c_{(alb)}=4.2$ mg ml^{-1}, $c_{(IgG)}=1.3$ mg ml^{-1}, $c_{(fgn)}=0.32$ mg ml^{-1})

Protein	Labelling degree	Hydrophobic end	Interface	Hydrophilic end
Albumin	0.2	2.0 ± 0.3	1.3 ± 0.6	0.6 ± 0.2
	0.6	1.8 ± 0.2	1.2 ± 0.6	0.5 ± 0.1
IgG	0.5	2.8 ± 0.2	2.0 ± 0.2	1.1 ± 0.2
	1.0	2.7 ± 0.2	2.0 ± 0.3	1.3 ± 0.2
	2.5	1.9 ± 0.2	1.5 ± 0.3	0.9 ± 0.3
Fibrinogen	1.0	2.5 ± 0.5	1.8 ± 0.5	1.2 ± 0.5
	2.5	3.1 ± 1.0	2.9 ± 0.9	2.8 ± 1.5

ferent parts of the gradient. IgG and fibrinogen adsorption was considerably biased at higher degrees of labelling while albumin adsorption was almost unaffected by the degree of labelling.

When the three proteins were mixed to a final concentration of 1/10 of the plasma concentration, the adsorption of IgG and fibrinogen decreased significantly compared to the adsorption from single protein solutions (Fig. 4). The albumin adsorption was not significantly affected on the hydrophobic side and changed only moderately (ca 50% decrease) on the hydrophilic side by the presence of the other two proteins. This is more evident from Fig. 5a where the
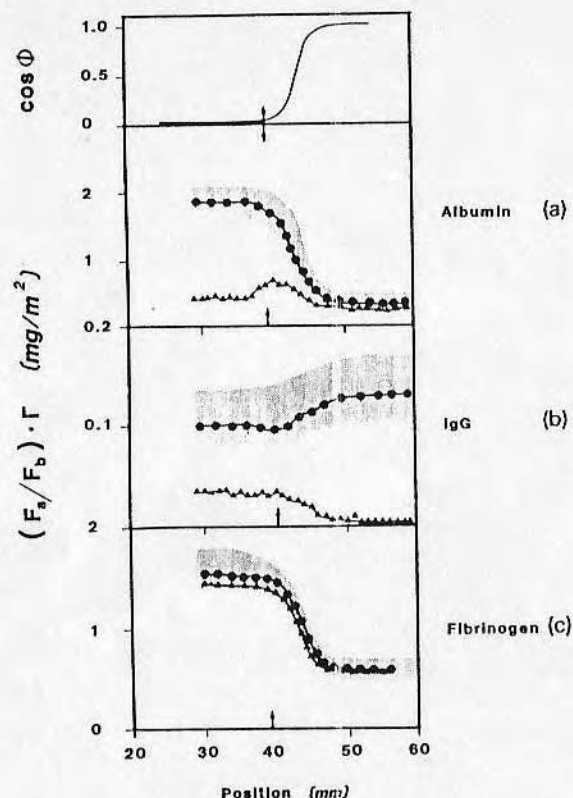
Fig. 4. TIRF-quantified adsorption of plasma proteins from a ternary mixture of albumin, IgG and fibrinogen to a hydrophobic gradient surface. The adsorption is expressed as $(F_a/F_b)\Gamma$ (in mg m^{-2}). For clarity, only results from the measurements on one gradient surface are displayed. The shaded area represents scattering in data between three independent measurements. The arrow marks the position of the interface between the p-xylene and trichloroethylene phases at the preparation of the gradient. Adsorption from PBS buffer after surfactant desorption: (a) albumin, $c_{(alb)} = 4.2$ mg ml^{-1}, DL (mole/mole) = 0.3; (b) IgG, $c_{(IgG)} = 1.3$, mg ml^{-1}, DL = 1.0; (c) fibrinogen, $c_{(fgn)} = 0.32$ mg ml^{-1}, DL = 0.5.
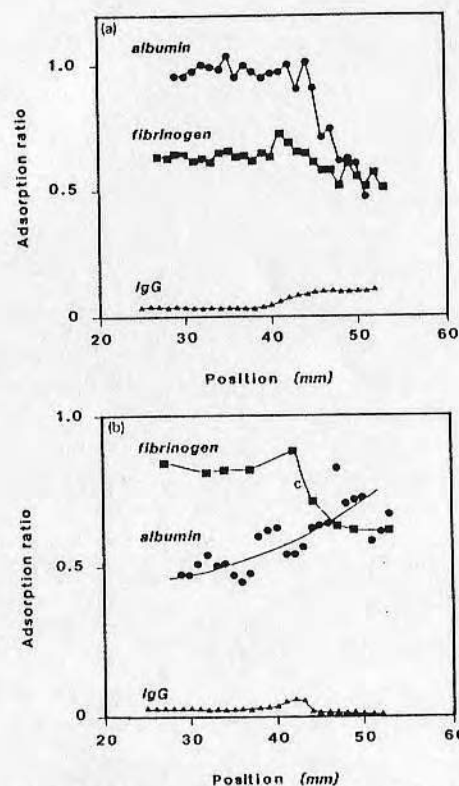
Fig. 5. (a) The ratio between the amount of protein adsorbed from the three protein mixture and the amount of the same protein adsorbed from the single protein solution as a function of gradient position: $c_{(alb)} = 4.2$ mg ml^{-1}; $c_{(IgG)} = 1.3$ mg ml^{-1}; $c_{(fgn)} = 0.32$ mg ml^{-1} for both single protein solution and ternary mixture. (b) The ratio between the amount of protein adsorbed from the three protein mixture after surfactant desorption and the amount of the same protein adsorbed from the single protein solution also after surfactant desorption experiment as a function of gradient position. Protein concentrations as above.

ratio between adsorption in the mixture and in the single protein solution is plotted. The same ratio after displacement by the surfactant is displayed in Fig. 5b. From Fig. 5b we conclude that the amount of albumin displaced by surfactant increased on the hydrophobic side due to the presence of the other two proteins. Furthermore, albumin showed an enhanced preference for the wetting transition region after desorption in surfactant (Fig. 4). IgG was quantitatively displaced on the hydrophobic side in the presence of the two other proteins and was also quantitatively displaced on the hydrophilic side after desorption in surfactant solution. In contrast, the amount of fibrinogen re-

TABLE 2

Influence of the degree of labelling on the adsorption values (in mg m^{-2}) for a ternary mixture of proteins ($c_{(alb)}$ = 4.2 mg ml^{-1}, $c_{(IgG)}$ = 1.3 mg ml^{-1}, $c_{(fgn)}$ = 0.32 mg ml^{-1})

Protein	Labelling degree	Hydrophobic end	Interface	Hydrophilic end
Albumin	0.3	1.9 ± 0.2	1.2 ± 0.4	0.4 ± 0.2
	1.0	1.5 ± 0.2	1.7 ± 0.3	1.1 ± 0.2
IgG	1.0	0.11 ± 0.04	0.12 ± 0.05	0.13 ± 0.05
	3.0	0.10 ± 0.05	0.11 ± 0.05	0.20 ± 0.10
Fibrinogen	0.5	1.8 ± 0.2	1.1 ± 0.3	0.6 ± 0.2
	3.0	1.5 ± 0.2	1.1 ± 0.4	1.0 ± 0.3
	7.0	0.4 ± 0.2	0.6 ± 0.2	0.85 ± 0.3
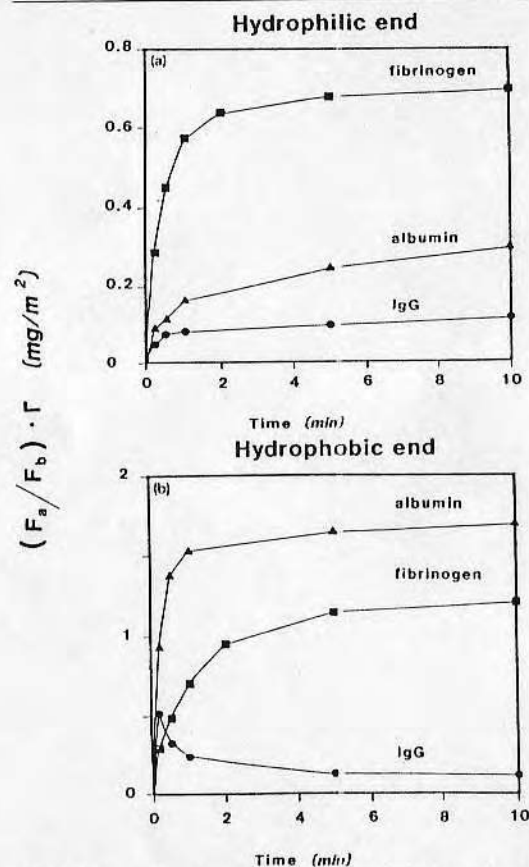
Fig. 6. Adsorption kinetics of three proteins from the ternary mixture of albumin, IgG and fibrinogen (a) on the hydrophilic end (position 55) and (b) on the hydrophobic end (position 30) of the gradient surface: $c_{(alb)}$ = 4.2 mg ml^{-1}; $c_{(IgG)}$ = 1.3 mg ml^{-1}; $c_{(fgn)}$ = 0.32 mg ml^{-1}.

maining after desorption in surfactant solution is not, to any large extent, influenced by the presence of the other two proteins.

In contrast to previous results (Table 1), the adsorption pattern of albumin in the mixture becomes distorted even at a moderate degrees of labelling (1 mole/mole), Table 2. Only at very high labelling degrees (7 mole/mole) was a distortion of fibrinogen adsorption found.

The plateau adsorption was reached in 10 min on the hydrophobic side, and slightly faster on the hydrophilic side, for all three proteins. The adsorption of IgG showed a transient peak on the hydrophobic side (Fig. 6). Judged on the basis of fibrinogen adsorption which was still increasing on a relatively longer time scale, IgG was displaced by fibrinogen.

DISCUSSION

The cos ϕ versus the linear position along the gradient showed an S-shaped dependence which is expected for a diffusion-controlled reaction of DDS at the silica surface. A deviation from the S-shape was found at the far hydrophobic end indicating a kinetically controlled (probably sterically hindered) silanization reaction, at higher surface coverages of DDS.

Similar contact angle hysteresis as seen here on the hydrophobic side of the gradient on silica was also observed on gradient surfaces prepared on atomically smooth silicon wafers (not shown here). Hence, hysteresis is due to chemical surface heterogeneity. A possible explanation would be that it is caused by residual unreacted SiOH groups on the hydrophobic side. Recently, Gobet and Kova'ts showed that only half of all surface SiOH groups on silica are available for reaction with a C$_6$ silane [20]. Polymerization of the silane at the interface, catalyzed by residual moisture associated with SiOH groups on the surface, may also cause wetting hysteresis. Although the reaction of DDS with surface silanol groups (SiOH) occurs instantaneously without any activation energy barrier, surface saturation (constant contact angle) was obtained only at DDS concentrations exceeding 0.1% (Fig. 2b). This indicates that residual water (which consumes DDS) is present in the solvent.

The enhanced wetting hysteresis observed in the wetting transition region of the gradient may indicate that the hydrophobic adsorption sites here appear as larger patches. We put forward in some more detail a hypothesis for the origin of the surface heterogeneity in the wetting transition region.

The surface silanization can be viewed as an analogue of a heterogeneous surface nucleation process in which the number of nucleation sites is constant along the surface and the growth of two-dimensional hydrophobic domains depends on the flux of the silane reagent to the surface, i.e., on DDS concentration, and the diffusion time. If we assume that the experimentally measured cosine value of the contact angle, cos ϕ_{exp}, is a cosine average of two surface

domains [21]: (1) entirely hydrophobic patches of equal size saturated with –CH$_3$ groups (contact angle $\phi = 114°$ as obtained from the Young equation with $\gamma(CH_3/H_2O) = 50$ mN m^{-1} and $\gamma(CH_3/air) = 20$ mN m^{-1}); and (2) the complementary area populated with hydrophilic SiOH groups (contact angle $\phi = 0°$):

$$\cos \phi_{exp} = f \cos 114° + (1-f) \cos 0°$$

one can calculate the fraction of the surface occupied by the hydrophobic groups, f. When the nucleation sites are uniformly distributed over the surface one finds the largest phase boundary density between hydrophobic and hydrophilic domains at $0.50 < f < 0.70$ depending on the shape of the hydrophobic surface domain. In this region of the gradient surface, albumin showed the increased adsorption affinity. Such increased adsorption affinity of an amphiphilic molecule can be envisaged if such a molecule can interact with hydrophobic and hydrophilic adsorption sites simultaneously (albumin is an amphiphilic and easily deformable protein [22]).

The present values on single protein adsorption on the DDS wetting gradient surfaces are in qualitative agreement with the ellipsometric study by Elwing et al. (9). However, the TIRF technique has a higher sensitivity and accuracy for in situ study of protein adsorption from solution than the ellipsometric method [9]. In addition, TIRF can be used to study adsorption of singly labelled protein from a non-labelled protein mixture, whereas in ellipsometry one needs to detect adsorbed protein from a mixture with a specific antibody. The latter may not necessarily react with the adsorbed protein molecules in a constant and quantitative way.

Regarding FITC labelling, the covalent binding of fluorescein label to proteins occurs via lysine residues which are distributed in large numbers around the entire surface of IgG and fibrinogen [22]. This can account for the higher labelling degrees of these two proteins as compared with the labelling of albumin. It can pressumably induce a solution aggregation of highly labelled IgG and fibrinogen since the fluorescein molecule itself has a partially hydrophobic character. We also noted that a longer storage time of fibrinogen after labelling causes aggregation in solution even at lower degrees of labelling. Hence, during aggregation, the hydrophobic driving force for adsorption can be consumed which may account for the observed change in adsorption characteristics for fibrinogen at high degrees of labelling.

The displacement of IgG by fibrinogen observed on the hydrophobic side of the gradient is a manifestation of the Vroman effect. However, this effect was not observed on the hydrophilic side, possibly due to the faster adsorption kinetics of fibrinogen on this side of the gradient. Wojciechowski et al. [8] have demonstrated that fibrinogen also shows a transient adsorption peak due to the displacement by HMW kininogen at longer exposure times and found this displacement to be strongly dependent on the total concentration of plasma proteins.

CONCLUSIONS

The Wilhelmy-plate method was applied to analyze the contact angle, ϕ, and TIRF was used to the study single and competitive protein adsorption across a wettability gradient surface prepared by two-phase solution silanization. Wetting hysteresis was found at the hydrophobic end and in the wetting transition region of the gradient. The adsorption of human albumin, IgG or fibrinogen from single protein solutions, at a concentration of one tenth of that in plasma, increased with decreasing values of cos ϕ (increasing hydrophobicity). On the hydrophobic end of the gradient the adsorption values generally corresponded to monolayer capacities. In the wetting transition region of the surface, an extraordinary affinity for albumin was found as indicated by surfactant desorption studies. Albumin adsorption was almost unaffected by addition of IgG and fibrinogen. In relation to its bulk concentration, fibrinogen, on the other hand, showed a comparatively large affinity toward the whole gradient at the expense of IgG adsorption when adsorbed from the protein mixtures. Furthermore, the Vroman effect was manifested in the IgG adsorption kinetics on the hydrophobic end of the gradient, i.e., a transient adsorption peak occurred during the first minute of exposure.

We conclude that gradient surfaces can be a valuable tool in clarifying the nature of the protein adsorption to foreign surfaces, and the role of protein adsorption for the biocompatibility of artificial materials.

We have demonstrated that on a surface in contact with a protein mixture, some proteins can be competitively displaced, depending on the relative concentration in solution and affinity to the surface. Since the affinity may vary along the gradient, proteins may show characteristic "diagnostic" patterns, e.g., adsorption maximum at different positions, as shown here for albumin. According to the authors knowledge, this is the first time the Vroman effect has been demonstrated for an artificial mixture of plasma proteins.

ACKNOWLEDGEMENTS

REFERENCES

1 J.L. Brash and D.J. Lyman, J. Biomed. Mater. Res., 3 (1969) 191.
2 L. Vroman and A.L. Adams, J. Biomed. Mater. Res., 3 (1969) 43.
3 J.L. Brash and P. ten Hove, Thromb. Haemostas., 51 (1984) 326.
4 J.L. Brash, Makromol. Chem. Suppl., 9 (1985) 69.

22. E. W. Merrill, V. Sa Da Costa, E. W. Salzman, D. Brier-Russell, L. Kuchner, D. R. Waugh, G. Trudel, III, S. Stopper, and V. Vitale, *Adv. Chem. Ser. 199* (Biomaterials: Interfacial Phenomena and Applications), pp. 95–107, A.C.S., Washington, D.C. (1982).

23. N. A. Mahmud, S. Wan, V. Sa da Costa, V. Vitale, D. Brier-Russell, L. Kuchner, E. W. Salzman, and E. W. Merrill, in: *Physico-chemical Aspects of Polymer Surfaces* (K. Mittal, ed.), Vol. 2, pp. 953–968, Plenum Press, New York (1982).

24. E. W. Merrill, V. Sa da Costa, E. W. Salzman, D. Brier-Russell, L. Kuchner, D. R. Waugh, G. Trudel, III, S. Stopper and V. Vitale, in: *Adv. Chem. Ser. 199* (Biomaterials: Interfacial Phenomena and Applications), pp. 95–107, A.C.S., Washington, D.C. (1982).

25. E. W. Merrill, E. W. Salzman, S. Wan, N. Mahmud, and L. Kuchner, *Trans. Soc. Artif. Internal Organs 28*, 482 (1982).

26. N. Mahmud, D.Sc. Thesis submitted to MIT (1984).

27. R. W. Pekala, Ph.D. Thesis submitted to MIT (1984).

28. R. W. Pekala, M. Rudoltz, E. R. Lang, E. W. Merrill, J. Lindon, L. Kushner, G. McManama, and E. W. Salzman, *Biomaterials 7*, 372 (1986).

29. R. W. Pekala, E. W. Merrill, J. Lindon, L. Kushner, and E. W. Salzman, *Biomaterials 7*, 379 (1986).

30. C. Sung, Ph.D. Thesis submitted to MIT (1988).

31. C. Sung, M. R. Sobarzo, and E. W. Merrill, *Polymer 31*, 556–563 (1990).

32. C. Sung, J. E. Raeder, and E. W. Merrill, *J. Pharm. Sci. 79*, 829 (1990).

33. E. L. Chaikof, Ph.D. Thesis submitted to MIT (1989).

34. E. L. Chaikof and E. W. Merrill, *New Polymeric Materials 2*(2), 125–147 (1990).

35. E. L. Chaikof, E. W. Merrill, S. L. Verdon, L. L. Hayes, R. J. Connolly, and A. D. Callow, *Polymer Commun. 31*, 182 (1990).

36. E. L. Chaikof, E. W. Merrill, S. L. Verdon, J. E. Coleman, L. L. Hayes, R. J. Connolly, K. Ramberg, and A. D. Callow, presentation at the 1989 International Chemical Congress of Pacific Basin Societies Symposium on Chain Dynamics at Polymer Interfaces, Session 2: Interface Characterization and Modification, Honolulu (December, 1989).

37. E. L. Chaikof and E. W. Merrill, *J. Colloid Interface Sci. 137*, 340 (1990).

38. S. Laliberté Verdon, E. L. Chaikof, J. E. Coleman, L. Hayes, K. Ramberg, R. J. Connolly, E. W. Merrill, and A. D. Callow, submitted for presentation at the Annual Meeting of the SEM Society of America (1989); *Scanning Microscopy 4*, 341 (1990).

39. E. L. Chaikof, E. W. Merrill, J. E. Coleman, K. Ramberg, R. J. Connolly, and A. D. Callow, *AIChE J. 36*, 994 (1990).

40. A. Z. Okkema, T. G. Grasel, R. J. Zdrahala, D. D. Solomon, and S. L. Cooper, *J. Biomater. Sci., Polymer Ed. 1*, 43 (1989).

41. D. W. Grainger, K. Knutson, S. W. Kim, and J. Feijen, *J. Biomed. Mater. Res. 24*, 403 (1990).

42. M. V. Sefton, oral communication in discussion following his presentation at ACS Boston Meeting, April 1990, Division of Polymer Chem., Session E, Symposium Honoring R. Langer, Paper #41.

43. K. A. Dennison, Ph.D. Thesis submitted to MIT (1986).

44. S.-W. Tay, Ph.D. Thesis submitted to MIT (1986).

45. S.-W. Tay, E. W. Merrill, E. W. Salzman, and J. Lindon, *Biomaterials 10*, 11 (1989).

46. P. Lutz and P. Rempp, *Makromol. Chem. 189*, 1051 (1988).

47. Y. Gnanou, P. Lutz, and P. Rempp, *Makromol. Chem. 189*, 2893 (1988).

48. E. W. Merrill, K. A. Wright, R. W. Pekala, K. A. Dennison, C. Sung, E. Chaikof, P. Rempp, P. Lutz, A. D. Callow, R. Connolly, K. Ramberg, and S. Verdon, in: *Polymers in Medicine: Biomedical and Pharmaceutical Applications* (R. Ottenbrite, ed.), Technomic Publishing Co., Lancaster, PA (in press) (1992).

49. P. Rempp, P. Lutz, and E. W. Merrill, *Polym. Prepr. Am. Chem. Soc. 31*, 215 (1990).

50. E. W. Merrill, P. Rempp, P. Lutz, A. Sagar, R. Connolly, A. D. Callow, K. Gould, and K. Ramberg, *Proceedings*, Society for Biomaterials Annual Meeting, Charleston, S.C. (May 1990).

15

Properties of Immobilized PEG Films and the Interaction with Proteins

Experiments and Modeling

C.-G. GÖLANDER, JAMES N. HERRON, KAP LIM, P. CLAESSON, P. STENIUS, and J. D. ANDRADE

15.1. INTRODUCTION

Poly(ethylene oxide), or as it is frequently denoted in the literature, poly-(ethylene glycol) (PEG), is a nonionic, water-soluble polymer widely used for stabilizing colloids in food and paints and in formulating pharmaceuticals and cosmetics. The reason for the extensive use of this polymer is that it acts as a dispersant and yet is inert, e.g., it does not interfere adversely with other functional ingredients in the dispersion.

Recently, some other potential applications have been identified within the biotechnology area (see Figure 1). It has been shown that substances covered with a PEG coating do not show antigenic activity. This can be utilized for camouflaging drugs that may otherwise cause allergic reactions in the body. In particular, successive therapy has been reported with PEG-encapsulated enzymes such as adenosin-deaminase (immunodeficiency disease), superoxide-dismutase (kidney transplanta-

C.-G. GÖLANDER and P. STENIUS • Institute for Surface Chemistry, S-11486 Stockholm, Sweden. JAMES N. HERRON and KAP LIM • Center for Biopolymers at Interfaces, and Departments of Bio-engineering and Pharmaceutics, University of Utah, Salt Lake City, Utah 84112.   P. CLAESSON • The Surface Force Group, The Royal Institute of Technology, S-10044 Stockholm; and Institute for Surface Chemistry, S-11486 Stockholm, Sweden.   J. D. ANDRADE • Center for Biopolymers at Interfaces, and Department of Bioengineering, University of Utah, Salt Lake City, Utah 84112.

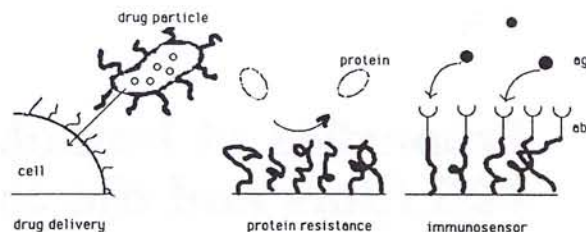222   C.-G. Gölander *et al.*

Figure 1. Three biotechnical applications for PEG coatings.

tion), and streptokinase (heart surgery). Other important areas are targeting of cytostatics in cancer therapy and the use of PEG/dextran mixtures in protein separation by affinity partitioning. In diagnostic assays and biosensors based on specific recognition of antigen–antibody (ag–ab) pairs, unspecific adsorption of proteins will cause a background noise. This can be avoided by covering the voids on the surface with PEG. Still another application of PEG is to incorporate this substance in a protein layer, which will keep the functional properties of the protein intact even when the protein film is stored in air. PEG here acts as a moisture preserver so that the native environment around the protein is retained. This property of PEG is also utilized in humectants.

It will be shown below that the molecular origin of these properties is quite intricate. We will start this PEG essay by describing some basic routes via which stable PEG films can be prepared and how the films can be studied physically and chemically by various surface analysis techniques. An important feature is that aqueous solutions of PEG show a lower consolute temperature (LCT), i.e., the solution splits into two phases (one with a very low concentration of PEG) above a critical temperature, called the cloud point. The correlation between this phase separation and the surface forces measured between two PEG-covered mica sheets will be discussed. The molecular behavior of PEG has also been studied by molecular dynamic simulations. The different theories for the molecular origin of PEG/water interaction will be briefly reviewed. Finally, we discuss how the properties of PEG are expressed in the interaction with proteins. A tentative explanation will be given as to the generally low protein adsorption found on PEG-coated surfaces.

15.2. PREPARATION OF PEG FILMS

The properties of PEG films, such as chemical stability, film thickness, and film composition, are influenced by the way they are prepared. It is difficult to cover a surface with a dense PEG film, because at temperatures below LCT, PEG molecules naturally repel each other in water. In most cases, other compounds, such as crosslinkers and film-forming agents, are also present in the film and may, particularly in thick films, induce chemical segregation both vertically and laterally in the

film and also, in extreme cases, cause phase separation on the surface. Effects due to swelling in thick films may also obliterate the true PEG properties of the surfaces. In the following we discuss in some detail three different ways to realize a PEG film on a solid substrate: preparation of PEG hydrogels, chemical immobilization, and quasi-irreversible adsorption (see Figure 2).

15.2.1. PEG Hydrogels

A PEG hydrogel can be created by incorporating PEG in a polymerizable resin, which is first deposited on a substrate and then polymerized *in situ*. Acrylate or methacrylate resins, polymerized by a free radical mechanism, are suitable. The polymerization can be initiated thermally by azobisisobutyronitrile (AIBN) or peroxides (see, for example, Gregonis *et al.*[1]) or photochemically using photoinitiators like benzophenones, hydroxipropiophenones, or thioxanthones.[2] In many cases bifunctional (diacrylated) PEG has been incorporated into a crosslinked network. In such cases, as a consequence of the presence of the hydrophobic crosslinking agent, the final polymer backbone will have a mixed hydrophilic–hydrophobic character.

In order to obtain a coating with pendant PEG chains, we have utilized the monomethoxy PEG and prepared PEG-monoacrylate.[2] Coating resins containing
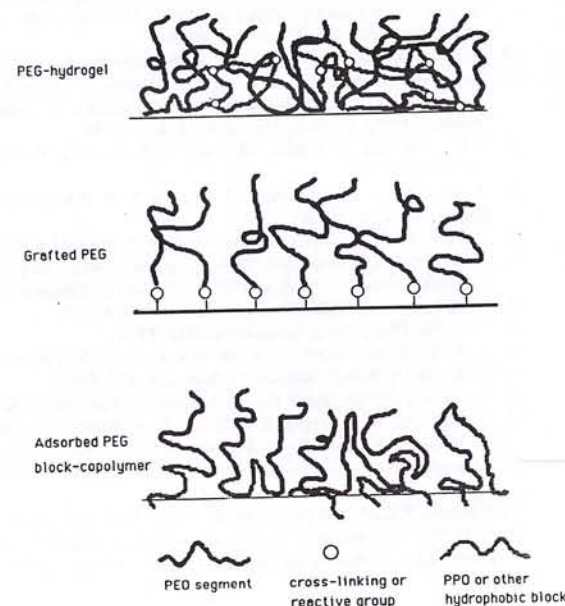

Figure 2. Schematic drawing showing the structural features of PEG layers obtained by different coating techniques.

either PEG-acrylate with molecular weight of 550, 1900, or 5000, or diacrylated ethoxylated trimethylolpropane [TMP (EO)$_{20}$], together with a crosslinker, hexanediol-diacrylate (HDDA), and 2-hydroxy-2-propiophenone (photoinitiator), are prepared in a toluene/ethanol/tetrahydrofurane mixture. A 1% solution was applied to a polymer surface with a 20-μm rod applicator. The film was allowed to dry and was then photocured. In order to maximize the ethylenoxide (EO) content in the film deposited on PVC, the molar ratio PEG-acrylate/HDDA was varied. The relative EO content was measured as the ratio between the electron intensity from carbon bound to a single oxygen (C—O) to that from CH$_2$ carbon in the C1s peak of the ESCA spectrum of the film. The EO content shows a maximum at a PEG/HDDA ratio between 1 and 2.[2] At higher ratios, the degree of crosslinking is lower. Consequently, film adhesion becomes poor. The EO content of the film increases with the molecular weight of the PEG monomer. However, beyond MW 1900, steric hindrance causes the EO content of the film to increase only slowly with molecular weight. Hence, molecular weights around 2000 seem to be sufficient for obtaining a high grafting yield and a high PEG content on the surface. At this MW the C—O/CH$_2$ ratio does not change much with the PEG/HDDA ratio. In all coatings prepared, the experimentally found C—O/CH$_2$ ratio was significantly lower than expected from stoichiometry. The most likely reason is that the polymer in the layer tends to minimize the free energy by migration of hydrophilic moieties to the bulk of the film, where a higher refractive index environment is offered than at the air interface. Consequently, hydrophobic segments will accumulate at the air interface. This process will be particularly pronounced in vacuum, where ESCA analysis occurs.

However, in water the situation is the reverse and polar groups migrate to the interface; this shows up in the low contact angles (around 15°) for these PEG hydrogels. The measured contact angle decreases as the C—O/CH$_2$ ratio increases.[2] The low contact angle measured for these hydrogels is also due to contributions from surface roughness, swelling, and capillary forces in porous structures. This is particularly clear when considering that higher values are measured for chemically immobilized monolayers of PEG (see below). For a constant C—O/CH$_2$ ratio, the contact angle decreased with increasing molecular weight of the PEG, which indicates that the PEG/water surface tension decreases in comparison to the PEG/air surface tension with increasing molecular weight (see below). Hydrogels are characterized by a high water uptake. The water content in swelled films of PEG 1900/HDDA 1:1 was around 45–50% w/w. A structural model of the PEG hydrogel is displayed in Figure 2.

To increase the EO content of the surface layer beyond the limits of the method described above, we have developed a two-step curing procedure shown in Figure 3. The coating is precured at low UV dosage to obtain a gel-like PEG coating, characterized by a polymer network with low crosslinking density, high mobility, and yet low water solubility. The substrate coated with the PEG gel is then exposed to water. This leads to migration of polar EO groups to the water interface. Finally, the layer is subjected to a high-dosage UV flash. The two-step procedure enhances the EO content at the interface, which increases the C—O/CH$_2$ ratio observed by ESCA approximately a factor of two for PEG gels with MW 1900.
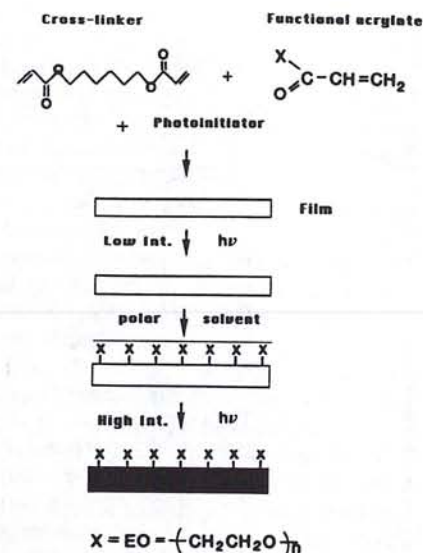
Figure 3. Two-step procedure for the photocuring of a PEG–acrylate layer for enhancement of the surface density of EO groups.

$X = EO = -(CH_2CH_2O)_n$

A layer containing equimolar amounts of PEG-acrylate (MW 1900) and HDDA coated onto PVC has excellent *barrier properties* against migration of hydrophobic substances like plasticizers. Hence, while the surface concentration of a dioctyl-phthalate plasticizer (measured by the fraction of CH$_2$ carbon in the C1s spectra) increased significantly with time on bare PVC (within hours at 20 °C and minutes at 60 °C) due to surface migration from the bulk, no change of the elementary composition with time occurred when PVC was covered with a PEG film.

15.2.2. Chemical Immobilization and Grafting

Various methods for covalent attachment of PEG to surfaces have been proposed. They usually require chemical derivatization of the terminal OH groups of PEG prior to reaction with a functionalized surface. Abuchowski *et al.*[6] introduced cyanuric chloride activation of PEG for reactions with enzymes in order to render them nonimmunogenic. Bückmann *et al.*[7] described the preparation of PEG ligands with bromide, amine, sulfonate and *N*-hydroxy succinimide for affinity partitioning of proteins, and Zalipsky *et al.*[8] prepared amino-, isocyanato-, and carboxylated PEG for attachment to drugs. Harris *et al.*[9] developed some improved and versatile methods to prepare PEG derivatives such as tosylate, amine, and aldehyde. They also studied how various PEG coupling reactions influence the activity of enzymes.[10] In one of our groups, Yee *et al.* tried to use the thiol–disulfide interchange reaction with

a dithiolated PEG to immobilize a protein to quartz via a PEG spacer.[23] An excellent overview of various derivatization reactions has been given by Harris.[11]

We have used the aldehyde–amine reaction for immobilization of PEG–aldehyde to aminated solid surfaces. This reaction is convenient to use in aqueous media and can be driven to completion by addition of NaCNBH$_3$, a reducing agent that selectively reduces the imine product —CH=N—) in the presence of aldehyde. The only side reaction that occurs is polymerization of PEG–aldehyde by aldol condensation. PEG–aldehyde can be prepared by various reactions, some of which are shown in Table 1.

Of the first four reactions that we tried, the best yield (NMR) was found with the partial oxidation in acetic anhydride/DMSO (#4), proposed by Harris *et al.*[9,12] Harris has pointed out that the PEG–CHO is not chemically stable but may polymerize by aldol condensation. This does not occur with PEG–benzaldehyde or PEG–propionaldehyde (see reaction #5). However, the experimental results presented below are all based on PEG–CHO prepared by the #4 procedure.

A very important aspect of the properties of PEG surfaces is the surface density. The interpretation of results on PEG surfaces becomes ambiguous if only partial coverage of the surface is obtained. In order to increase the surface coverage we have performed the immobilization reaction under solution conditions close to the cloud point, where repulsion between PEG chains are small.

Figure 4 shows schematically the coupling procedure and Figure 2 the structural model of the PEG surface. The cloud point of PEG 1900 is around 180 °C. To induce clouding at realistic reaction temperatures, "salting out" with potassium sulfate was

Table 1.   Some Derivatization Reactions for Preparing PEO–CHO

1.   Oxidation Ce^{4+} or pyridinium chloroformate (PCC)

$C_5H_5N + CrO_3 \xrightarrow{H} (PCC)$

$CH_3—(EO)_n—OH + PCC \xrightarrow{toluene} CH_3 (EO)_n—O—CH_2—CHO + (CrO_2)$

2.   Choloracetaldehyde diacetal

$CH_3—(EO)_n—OH + ClCH_2CH (OCH_3)_2 \xrightarrow{NaOH} CH_3—(EO)_n—O—CH_2CH (OCH_3)_2$
$\xrightarrow{H_2SO_4} CH_3—(EO)_n—O—CH_2CHO + 2CH_3OH$

3.   Aluminum tert-butoxide

$CH_3—(EO)_n—OH + (CH_3)_2C=O \xrightarrow{Al(OC_4H_{10}-t)} CH_3—(EO)_n—CHO + (CH_3)_2CHOH$

4.   DMSO/(CH$_3$CO)$_2$O

$(CH_3)_2S=O + (CH_3CO)_2O + CH_3—(EO)_n—OH$
$\rightarrow CH_3—(EO)_{n-1}—OCH_2CHO + 2CH_3COOH + (CH_3)_2S$

5.   Propanedithiol/chloropropionaldehyde diacetal

$HS—CH_2CH_2CH_2—HS \xrightarrow{NaOCH_3} Na—S—CH_2CH_2CH_2—S—Na$
$\xrightarrow{Cl—CH_2CH_2CH—(OC_2H_5)_2} Na—S—CH_2CH_2CH_2—S—CH_2CH_2CH—(OC_2H_5)_2 \ (+NaCl)$
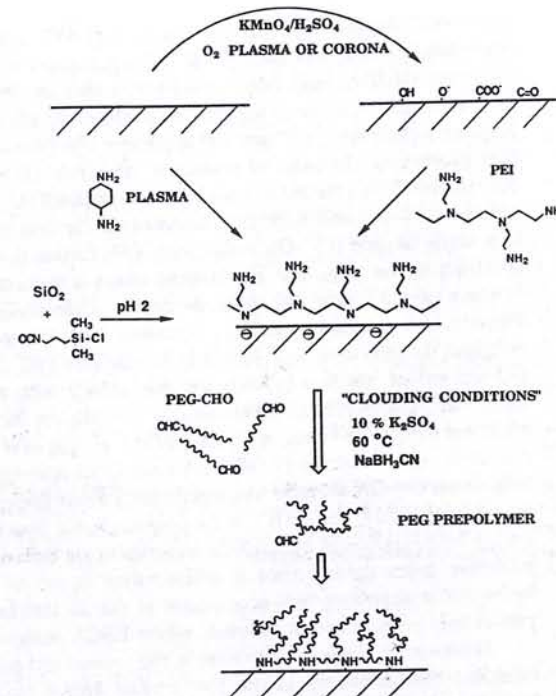$\xrightarrow{(EO)_n—OTs,H_2SO_4} (EO)_n—S—CH_2CH_2CH_2—S—CH_2CH_2—CHO \ (+NACl)$

Figure 4. Grafting of PEG by the Schiff base reaction between PEG–CHO and surface-NH$_2$ on surfaces aminated in various ways.

used.[14] However, due to steric hindrance, the reaction is sluggish. In order to find the conditions that give maximum PEG coverage, we determined both the C—O/CH$_2$ ratio in the layer and the attenuation of the signals from substrate atoms in the ESCA analysis. The optimal conditions for coupling aldehyde–PEG to aminated surfaces were found to be pH6,[14] 60 °C, 10% K$_2$SO$_4$, and 40 hours reaction time.

Figure 5 compares the carbon 1s peak from PEG surfaces prepared under optimal conditions with the peak obtained when immobilization was accomplished in pure water at 20 °C and in a 10% w/w K$_2$SO$_4$ solution at 60 °C for the same reaction time. In both cases NaBH$_3$CN (reducing agent) was added. The figure clearly shows the improvement in PEG grafting density (C—O/CH$_2$ ratio) when using close to phase separation conditions. These PEG grafted surfaces are chemically very stable in the sense that no significant change occurred in the ESCA spectra after prolonged rinsing with water, 0.1M NaOH, 0.1M HCl, ethanol, or 10% trifluoroacetic acid; see Figure 6.

To prepare a substrate surface with amino groups for PEG immobilization is not trivial. Yet it is critical, since a high density of amino groups is required if a dense
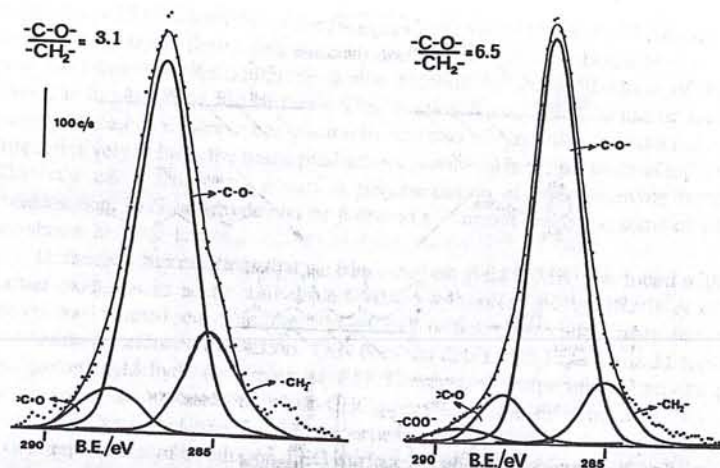
C.-G. Gölander *et al.*

$\dfrac{\text{-C-O-}}{\text{-CH}_2\text{-}} = 3.1$

$\dfrac{\text{-C-O-}}{\text{-CH}_2\text{-}} = 6.5$

Figure 5. Carbon 1s spectrum from PEG films obtained by immobilization of PEG-aldehyde to an aminofunctional surface. Left, in pure water, 20 °C; right, in a 10% w/w K_2SO_4 solution, pH 6, 60 °C. The signal is dominated by a peak centered at 286.5 eV corresponding to C—O carbon in PEG. The C—C peak at 285 eV originates from the substrate (and contaminants) and the peak at 289.2 eV originates from carboxylate species.

packing of PEG is to be obtained (at least 1 NH_2 per nm^2). These groups must also be accessible for reaction. We have used three ways to achieve this (see Figure 4): *"irreversible" adsorption* of polyethyleneimine on an oxidized polymer surface,[16,17] *plasma polymerization* of diaminocyclohexane (DACH)[19] on any surface (allylamine was used by Gombotz *et al.*[18]) and *silanization* of silicon oxide with aminopropyl trimethoxy silane (APS)[21] or isocyanatopropyl dimethyl monochlorosilane (IPS), (hydrolyzed to $-NH_2$ after immobilization)[20] yielding densities well above $1-2$ NH_2 per nm^2.

PEG–CHO was reacted in the way described above with the aminated surfaces.

The agreement between the amounts of immobilized PEG measured using various methods is good (see Table 2). However, measurements in wet and dry states give different thickness and refractive index values. The standard procedure using PEI as an amino functional substrate results in a layer with 2 mg per m^2 PEG or 1.5 nm^2 per molecule. In the dry state this means a thickness of approximately 2.5 nm and a refractive index which agrees with the bulk value for PEG ($n = 1.44$). The low refractive thickness ($n = 1.36$) and relatively thick film $d = 10$ nm measured in water indicates considerable swelling. The calculated water content in this PEG monolayer (from refractive index) is >70% w/w, which is considerably higher than for the hydrogels. The contact angles are much higher than for the PEG hydrogels: $\Theta_{adv} = 56 \pm 3°$ and $\Theta_{rec} = 35 \pm 2°$. The high values indicate a nonzero surface tension against water and/or a rather low surface tension against air. Hence, at 20 °C we obtained

---

Properties and Interactions of Immobilized PEG Films

Table 2. Quantification of Covalently Attached PEG Layers (MW 1900) on Various Substrates

Method	Substrate	NH_2 layer	Γ (mg m^{-2})	d (nm)	n
Ellips[a] (dry state)	SiO_2	DACH[19], 5 nm	1.2	1.5	1.44
Ellips[a] (wet state)	SiO_2	PEI, 3 nm	2.0[b]	10	1.36
Ellips[a] (dry state)	SiO_2	PEI, 3 nm	2.0[b]	2.5	1.44
Ellips[a] (dry state)	SiO_2	IPS silane	1.2[b]	1.6	1.44
SFA[c] (wet state)	Mica	PEG–lysine	1.1[d]	3.5	
SFA[c] (wet state)	Mica–OH	IPS silane	1.1[d]	4.0	
ESCA	Mica–OH	IPS silane	1.2[d]		
QCM[e]	SiO_2	APS > 10 nm	7.0		

[a]Obtained from ellipsometry.[3]
[b]Calculated from Cuypers model.[50]
[c]Obtained from surface force measurement.[4]
[d]Obtained from quantitative ESCA analysis.[5] Agrees well with values obtained from ellipsometry on the same surface film on a silicon wafer.
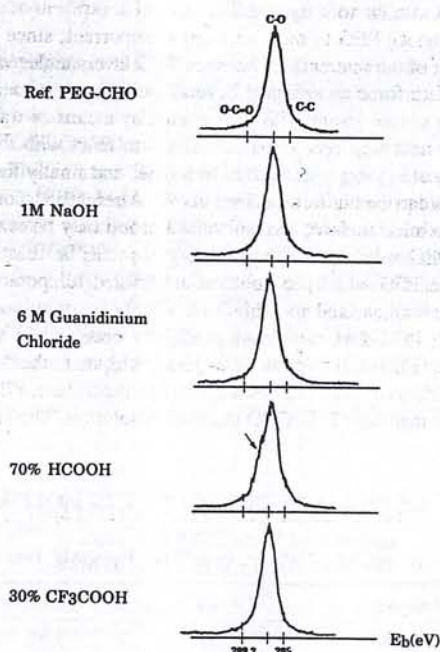[e]Obtained from measurements with a surface acoustic wave (SAW) device.

Figure 6. Carbon 1s spectra from a PEG film immobilized on polyethylene and rinsed in water 1 hour (Ref. PEG–CHO), 1 M NaOH, 6 M guanidinium chloride, 70% HCOOH, or 30% CH_3COOH. Only in the case of formic acid rinsing is there a small asymmetry in the peak indicating interaction between the formic acid and ether in PEG.

$\gamma = 44$ mN m^{-1}, by straight line extrapolation from pendant drop measurements on melts of PEG, MW 1900.[51] The surface tension decreases with temperature to 36 mN m^{-1} at 140 °C. We also measured a (small) surface tension increase with molecular weight [41 mN m^{-1} for monomethoxy PEG (MW 550) and 47 mN m^{-1} for PEG (MW 6000)]. This is most likely due to purely entropic factors.

Adsorption of a cationically modified PEG (PEG–lysine) to (negatively charged) mica at room temperature resulted in an adsorbed amount of 1.1 mg per m^2 PEG. An increase in temperature to 55 °C (close to the conditions used above during immobilization) increased the adsorbed amount to the vicinity of 2 mg per m^2, obtained above for grafted layers.

Table 2 shows that less PEG can be attached to IPS or DACH layers[19] (1.2 mg per m^2 or 2.5 nm^2 per molecule) although they carry >1 reactive amino group per nm^2 than PEI or APS layers. It is likely that, on the compact and rigid IPS or DACH films, the amino groups are less accessible to reaction than the mobile side chains in the PEI or APS films.[16]

The polymerizable APS results in an extremely thick (>20 monolayers) and rough layer. The large amounts of PEG in this layer indicate a three-dimensional PEG–APS network similar to a hydrogel.

To covalently attach PEG to mica surfaces is important, since this would allow direct measurement of the interactions between PEG layers under various conditions employing the surface force technique.[4] Several methods have been tried. One way is to first introduce silanol groups (SiOH) on mica by means of water vapor plasma treatment.[15] In the next step IPS vapor is allowed to react with the modified mica surface, the isocyanato group is converted to amine, and finally the PEG–aldehyde coupling reaction is carried out as described above. Alternatively, once the silane has been bonded to the mica surface, the isocyanate group may be reacted with a PEG melt (110 °C) or PEG solution, or the amine group can be reacted with a PEG–aldehyde melt or a PEG–aldehyde solution at elevated temperatures. The results obtained so far are summarized in Table 3.

Reaction with PEG–OH melt gave a slightly better yield than the solution reaction. However, PEG–CHO melt gave less yield than the solution reaction, probably due to oxidation of PEG–CHO at elevated temperature. PEG–benzaldehyde also gave less yield than the PEG–CHO reaction in solution. The comparatively low

Table 3. ESCA Quantification of PEG Layers Immobilized by the Aldehyde–Amine or Isocyanate–Hydroxyl Reactions on Mica

Sample	Reactant	Γ (mg m^{-2})
Mica–IPS	PEO–OH melt	1.5
Mica–NH$_2$	PEG–CHO melt	0.6
Mica–NH$_2$	PEG–CHO solution	1.1
Mica–NH$_2$	PEGΦCHO solution	0.6

chemical "stability" of the monomeric PEG–CHO hence seems to be advantageous. A possible explanation is that the aldol condensation in solution leads to oligomers with residual reactive aldehyde groups, so that more PEG is bound by a single reaction event at the surface (Figure 4).

15.2.3. Quasi-Irreversible Adsorption

By this term we denote physical adsorption of high molecular weight copolymers of PEG which attach at multiple adsorption sites. Although the free energy of adsorption for each site may be relatively small, the attachment of a molecule to several sites leads to a multiplication effect, so that the total free energy of adsorption of a polymer becomes quite large. For this reason, polymers tend to be adsorbed either very strongly or not at all. Frequently, the adsorption isotherm will rise steeply at such low concentrations that, for all practical purposes, adsorption appears to be irreversible.

In one of our groups, we have studied how the structure of block-copolymers of PEO/PPO/PBO (polyethyleneoxide/polypropyleneoxide/polybutyleneoxide) influences the adsorption/desorption kinetics at the water/air and at the polyethylene/water interface.[24]

The block-copolymers that were used and the amounts adsorbed after 30 minutes at 20 °C, as well as the amount of polymer remaining on the surface after desorption for 30 minutes, are shown in Figure 7.

While the PEO/PBO/PEO triblock adsorbs in large amounts, the film also easily desorbs in water. This is most likely due to the self-aggregation properties induced by the hydrophobic PBO block. With preferentially hydrophilic PEO segments (which are very weakly attached to the surface) on the outside, these aggregates will readily desorb. For PEO/PPO star copolymers, close packing is severely restricted as a result of the high mobility of PEO tails. However, the (thin) films formed are quite stable against dissolution, evidently due to strong interaction between the hydrophobic core of the star polymer and the hydrophobic surface. A PEO/PPO alternate block obviously offers the largest hydrophobic contact area with the surface, so that a stable film with reasonable PEO density results. The PEO/PPO/PEO triblock hardly adsorbs at all.

15.3. INTERACTION BETWEEN PEG AND WATER

15.3.1. Theories and Models Describing the PEG–Water Interaction

The solubility of PEG in water is characterized by a closed immiscibility loop, i.e., there exists both a lower and a higher consolute temperature. This is the result of the unusual temperature dependence of the molecular interaction between PEG and water. We now proceed to discuss the origin of this behavior starting with a brief thermodynamical discussion.
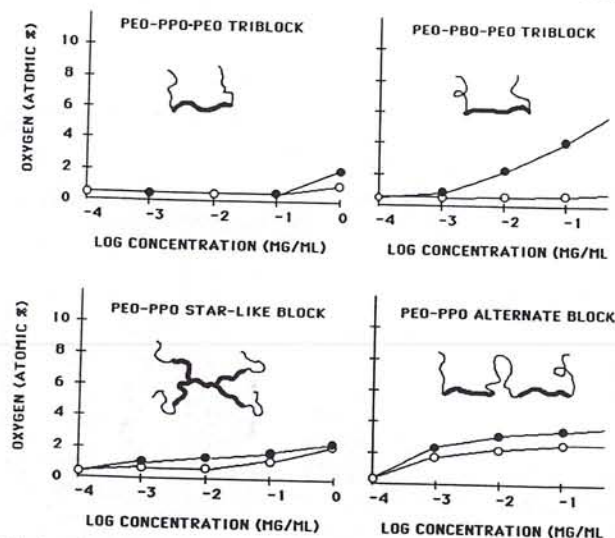
Figure 7. Relative adsorption of various PEG block-copolymers on polyethylene as determined from the relative oxygen content from ESCA analysis. The following block-copolymers were used: $PEO_{13}PPO_{30}PEO_{13}$ triblock; $PEO_{13}PBO_{25}PEO_{13}$ triblock; $(PEO_{26}PPO_{29})_2NCH_2CH_2N(PEO_{26}PPO_{29})_2$ star-like; $(PEO_{13}PPO_{30})_3$ alternate block. Redrawn from Ref. 24 and published with permission from John Wiley & Sons.

Hydrophobic molecules dissolved in aqueous solutions cannot form hydrogen bonds with water. As a consequence the surrounding water has to associate into "cage"-like structures in order to minimize the free energy of the system. The hydration of hydrophobic molecules results in an increase in water–water hydrogen bonds, a lowering of the entropy, and a lowering of the enthalpy. Consequently, when two hydrophobic units are brought together in water it results in a large increase in entropy ($\Delta S > 0$), a large compensating increase in enthalpy ($\Delta H < 0$), and a decrease in free energy ($\Delta G < 0$). This is the so-called "hydrophobic effect" which is also characterized by a decrease in heat capacity ($d\Delta H/dT < 0$), i.e., as temperature increases the process becomes enthalpically more and entropically less favorable in a manner such that $\Delta G < 0$ becomes almost independent of temperature.[25]

Kjellander and Florin-Robertsson[26] started from the idea that the PEG chain can be perfectly accommodated in a hexagonal water lattice. They argued that the hydration of a PEG chain is essentially hydrophobic, but a modification is imposed by the ether oxygen that can participate in hydrogen bonds with water. In Kjellander's model the enthalpy change (ΔH repulsive) and the entropy change (ΔS, attractive) caused by the association of two PEG chains are both large, but they nearly cancel in the expression for the free energy. To explain the phase behavior of the PEG–water system one must consider these two contributions and the ideal entropy of mixing

---

(ΔS_i). It is assumed that ΔS_i is small compared to ΔS at room temperature. Hence, the free energy change (ΔG) due to association can be written as: $\Delta G = \Delta H - T\Delta S - T\Delta S_i$.

At low temperatures (T) the free energy is negative and no phase separation takes place. As the temperature increases, the entropy term ($T\Delta S$) becomes more important and, above the cloud point, will cause the free energy of association to become negative. For PEG with a molecular weight of 1900 g mol^{-1} this occurs at a temperature of 180 °C.[27] It is important to realize that in Kjellander's model the phase separation of the PEG–water system is a consequence of the hydrated structure around the PEG chain. Only at temperatures considerably above the cloud point does the hydration of the PEG chain begin to vanish due to the increased thermal energy. When this occurs, both ΔH and $T\Delta S$ become less important. Instead the $T\Delta S_i$ term will eventually dominate, and the entropy of mixing will make the PEG–water system completely miscible again at high enough temperatures. Theoretical phase diagrams that agreed well with experiment could be calculated from Kjellander's model.

Two other models for the near-anomalous temperature behavior have been proposed (see Figure 8). Goldstein[28] suggested a two-state model with water hydrogen bonded or nonbonded to PEG, giving rise to repulsive and attractive domains in the PEG molecule. By treating the mixture by the Flory–Huggins statistical mechanical theory for solutions, with a temperature-dependent χ parameter, he was able to predict the presence of a solubility gap. At low temperatures repulsive hydrogen-bonded domains dominate, and at elevated temperature nonhydrogen-bonded domains dominate.

Karlström suggested a completely different explanation[29] for the phase separation of PEG in water and other polar solvents.[30] In his view, the change in interaction is related to temperature-induced conformational changes in the PEG chain. The oxygen atoms prefer a *gauche* conformation around the C—C bond and a *trans* conformation is preferred around the C—O bond. This leads to a high dipole moment for the segment, and consequently a strong interaction with water. As the temperature increases, more segments adopt conformations with smaller dipole moments, causing the interaction with water to become less favorable. Karlström's calculations predicted a phase diagram in reasonable agreement with experiment.

Karlström's model was further developed for application to PEG molecules *terminally attached* to surfaces. Using Scheutjen and Fleer's mean-field theory based on a lattice model and discrete description of layers, the same group[31] demonstrated that this two-state model gives a segment distribution where the nonpolar state dominates close to the surface while the polar state dominates further out. The segment density close to the surface and far out is large, and in the intermediate range it is lower. An increased grafting density results in a more extended conformation, which decreases the segment fraction close to the surface.

To model how adsorbed or *grafted PEG* layers interact, the scaling approach[32] based on self-similarity is very useful. It provides a simplified statistical mechanical description of adsorbed or grafted polymers without predicting precise numerical values for all adherend parameters. Considering van der Waals and steric forces and
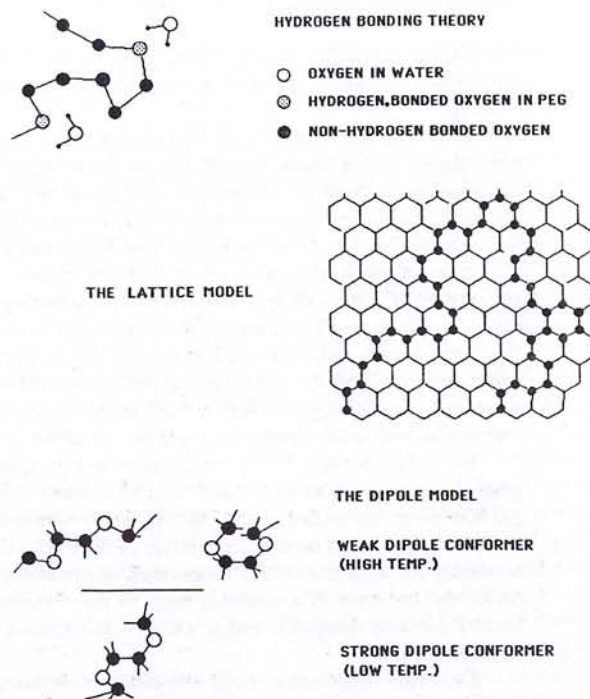
HYDROGEN BONDING THEORY

○   OXYGEN IN WATER

◎   HYDROGEN-BONDED OXYGEN IN PEG

●   NON-HYDROGEN BONDED OXYGEN

THE LATTICE MODEL

THE DIPOLE MODEL

WEAK DIPOLE CONFORMER
(HIGH TEMP.)

STRONG DIPOLE CONFORMER
(LOW TEMP.)

Figure 8. Simplified picture for three different models for the interaction between PEG and water as proposed in the literature; see text.

using this approach, Jeon *et al.*[33] could describe how the range of the steric repulsion between grafted polymer "brushes" of PEG varies as a function of packing density, thickness of the layer, and size of the PEG molecule (see Figure 9).

15.3.2. Computer Modeling of the Properties of PEG in Solution

Although statistical mechanical methods such as scaling concepts and self-consistent field theories of polymer chains are useful in predicting macroscopic properties of grafted PEG of high molecular weight[32] modeling of smaller PEGs at atomic scale can give further insight into the behavior of individual chains.

We have performed molecular dynamic (MD) simulations with 14 EO unit PEG chains and octadecane chains, respectively, at 300 K *in vacuo* and in water using the DISCOVER program (Biosym, USA).[34] The partial charge used was -0.30 eu for PEG oxygen and -0.82 eu for water oxygen. The nonbonding interaction is the most
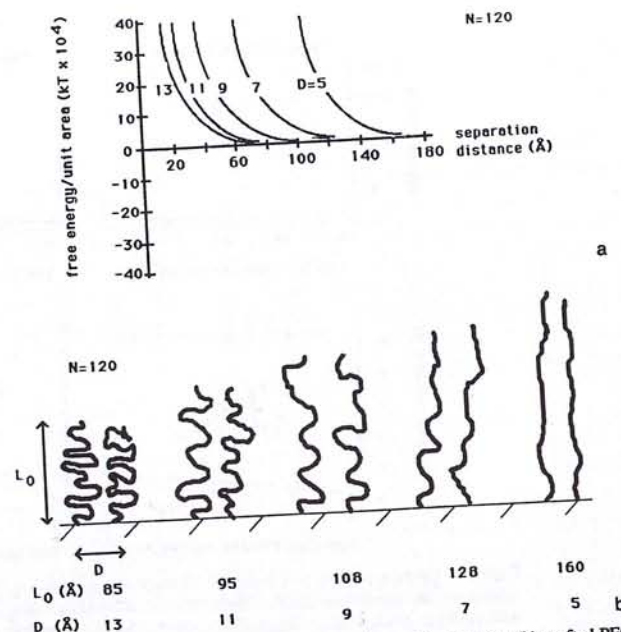
Figure 9. (a) Calculated force versus distance plots for the interaction between (b) grafted PEG-brushes obtained from de Gennes scaling theory, where N is the number of EO units in the molecule (redrawn from Ref. 33). D is the distance between attachment points and L_0 the extension of the PEG molecule from the surface.

difficult aspect of the potential function used in the molecular simulation. As with other molecular mechanics program, the DISCOVER program has the Lennard-Jones function and an electrostatic function to describe the nonbonding interaction.[38] The selection of parameters used in these calculations is important to describe the intermolecular interaction accurately. Although DISCOVER uses no explicit function for hydrogen bonds, it is at least partially considered in the electrostatic function.

The results for octadecane and PEG were compared in terms of chain flexibility and interaction with water. For an *octadecane* molecule *in vacuo*, with C—C bonds that are initially in the all-*trans* conformation, the torsional energy barrier is higher than the thermal energy level ($RT = 0.60$ kcal mol^{-1}). However, cooperative conversion between neighboring torsion bonds and deformations in bond length and bond angles may occur. This results in an overall oscillating motion of the hydrocarbon chain. In contrast, the motion of a *PEG* chain *in vacuo* is significantly different due to the fact that the C—O bond has a lower energy barrier between *gauche*$^-$, *trans*, and *gauche*$^+$ conformations (see Figure 4 in Chapter 3, this volume). However, the

most favorable conformation for the C—O bond is *trans*. Since *in vacuo* a PEG chain can only interact with itself, each of the atoms in the molecule is attracted by others and soon the chain adopts a compact, coiled form. Simulations *in vacuo* thus demonstrate large differences in the internal structure of a PEG and an octadecane chain.

Differences of intermolecular interactions for octadecane and PEG can also be recognized with MD simulations in water. For the octadecane–water system, phase separation occurred in the simulation. The first layer of water molecules around the hydrocarbon chain was aligned parallel along the axes of the chain. The radial distribution function $g(r)$ of *octadecane in water* is illustrated in Figure 10a, as determined from the 10-picosecond molecular trajectories of one octadecane and 478 water molecules in a $20 \times 20 \times 35$ Å box with periodic boundary condition. The first maximum of the pair correlation function $g(r)$ for C—O and C—H are located at almost the same distance, which indicates that the plane formed by the H—O—H bond angle in water is parallel to the axis of the hydrocarbon molecule. The low intensity of the two closest maxima as compared to that of the O—O pair correlation function for the water–water interaction shows that the density of water molecules in the first shell around octadecane is lower than that around a water molecule. These results are consistent with a previous Monte Carlo study of n-butane in water.[35]

The radial distribution functions for *PEG–water*, obtained by MD simulations, were (as shown in Figures 10b and c) different than those for octadecane–water. These data were obtained from a 10-picosecond simulation of one PEG and 579 water molecules in a $20 \times 20 \times 45$ Å box with the periodic boundary condition. The structural order of the first shell of water around the carbon atoms of PEG is not as rigid as that for octadecane. Further, functions $g(r)$ for C—O and C—H are, as compared with the case of octadecane–water, more distinguishable from each other (Figure 10b) with a higher and narrower first maximum for C—O. The reason for the reduced ordering of water around the carbon atoms of PEG is the helical structure of the PEG chain and the presence of oxygen atoms in PEG. The PEG oxygen–water interaction disrupts the water structure around the carbon atoms in PEG. The small first intensity maximum in $g(r)$ for PEG oxygen and water shows that the hydrogen bond is not fully established between these two elements (Figure 10c). It has been shown that the greater partial charge of an alcohol group enables stronger binding of water.[36] The small distance between the adjoining pair of oxygen atoms of PEG (≥ 2.84 Å) also contributes to the lack of full hydrogen bonding with water.[37] However, unlike polyoxymethylene (POM) that has only one methylene group between the adjoining pair of oxygen atoms, an additional CH_2 group in PEG prevents exclusive oxygen–oxygen interactions. *Gauche* conformation is preferred in POM due to this oxygen–oxygen interaction, while *trans* is preferred for C—O of PEG. These differences are reflected in molecular ball models where POM shows two "faces": one hydrophobic and one hydrophilic, while PEG is more symmetric with evenly distributed polar (C—O) and nonpolar (C—C) groups facing water.[46] Water molecules dampen the motion of PEG, as its conformation changed very little after a 20-picosecond MD run (Figure 11). Hence, simulation results with PEG and
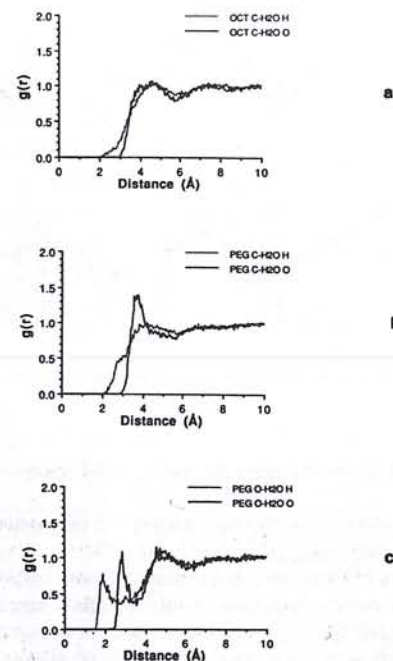
Figure 10. The radial distribution functions for PEG-water obtained from 10-ps molecular dynamics trajectories.

octadecane indicate that molecular differences of these two molecules can be demonstrated at least in a qualitative manner. Simulation of *grafted* PEG *in vacuo* shows that the PEG chains can adopt various equilibrium conformations with different densities depending on initial conformation, temperature, etc. This is described in more detail by Lim and Herron in Chapter 3 of this volume. Briefly, twenty 40-unit PEG chains fixed at one end collapsed to a thickness of 15–20 Å when the initial conformation was all-*gauche⁻*. Such a thickness conforms to experimental data obtained from the air interface. The *gauche* conformation of the C—O bond is energetically unfavorable compared to *trans*, and when the PEG chains of this conformation interact with each other, the chains are forced to assume a more compact overall structure. However, when the initial PEG conformation is the crystal structure with *trans–gauche⁺–trans* (CO as *trans* and C—C as *gauche⁺*), the grafted PEG chain remains in its extended helical form throughout the duration of the simulation (the equilibrated thickness is 50 Å).
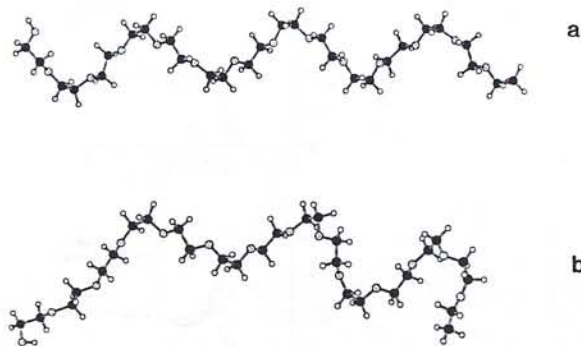
Figure 11. Conformation of a helical PEG molecule (a) before and (b) after a 20-ps MD run in water.

15.3.3. Direct Force Measurements between PEG Layers

Some investigations of the forces acting between PEG-coated mica surfaces have been reported. In a first study, PEG 1900 with a terminally attached positively charged lysine group, PEG–lysine, was adsorbed from solution.[22] The forces between mica surfaces without any PEG coating in dilute electrolyte solutions are dominated at large separations by a repulsive double-layer force. At a separation of less than 2–3 nm, this force is overcome by a van der Waals attraction in perfect agreement with predictions based on the DLVO theory.

In 10^{-4} M PEG–lysine, the long-range force is, at room temperature, still dominated by a double-layer force originating from an incomplete neutralization of the mica lattice charge. However, at separations less than 10 nm an additional repulsion appears. This repulsion, which completely overcomes the van der Waals attraction, is due to the interaction between adsorbed PEG chains, in particular the tails. The same forces were measured on approach and on separation, indicating a quasi-equilibrium situation.

The interaction becomes much more complicated when the PEG–lysine concentration is increased to 5×10^{-3} M (Figure 12). The force is purely repulsive and considerably stronger on compression than on decompression. The reason for this hysteresis can be either that PEG–lysine molecules loosely associated with the surface (e.g., as counterions) are forced to leave the gap between the surfaces as they are brought together, or that slow conformational changes take place in the adsorbed layer. For this low molecular weight PEG chain we favor the former interpretation. Klein and Luckham[39] have observed a similar hysteresis in the force curve between mica surfaces carrying adsorbed homopolymers of PEO (MW 40,000 g mol^{-1}).

Interestingly, when inorganic salt is added (0.1 M KBr) or when the temperature is increased to 55 °C, the hysteresis in the force–distance profile between PEG–lysine coated mica surfaces disappears. When salt is added, the range of the force decreases
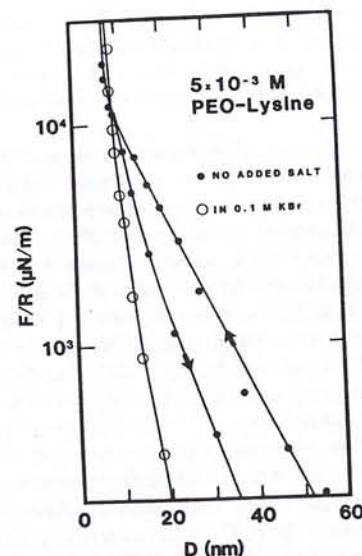
Figure 12. The influence of an addition of electrolyte on the force versus distance profile for electrostatically adsorbed PEG-lysin. (From Ref. 22, published with permission from Academic Press.)

dramatically from 50 nm to 20 nm (Figure 12). This is due to a reduction in the double layer and to a replacement of large PEG–lysine counterions for smaller potassium ions. This also explains the disappearance of the hysteresis in the force–distance profile. When the temperature is increased the PEG chain becomes more hydrophobic, which results in an increased adsorption and a more compact layer. The increased adsorption also results in a lowering of the surface charge density and less associated PEG–lysine counterions, which rationalizes the disappearance of the hysteresis.

For *grafted* PEG-OH 1900 (to isocyanatopropyl silanized water-vapor plasma treated mica surface), so far only forces in pure water at 20 °C have been investigated.[42] A repulsion similar to that observed between adsorbed PEG–lysine layers is present at separations below 30 nm. However, in comparison with adsorbed PEG, a less repulsive interaction was observed down to a separation of 9 nm (Figure 13). This supports the suggestion that hysteresis in the force–distance curve is largely due to displacement of polymers from between the surfaces. In fact, it is possible that the hysteresis between surfaces with grafted PEG is due to the presence of a small presence of some polymers not covalently attached to the surface (due to insufficient rinsing after the last reaction step). The compressed layer thickness (about 4 nm on each surface) is the same for adsorbed and grafted PEG.[41,42] The layer thickness is larger than twice the solution radius of gyration, $R_g = 7$–8 Å. Rather, it is in better agreement with the approximately $6R_g$ (here around 4 nm Å). This indicates a rather
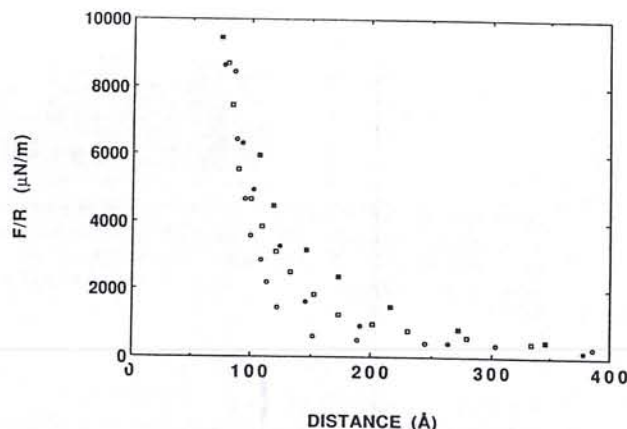
Figure 13. Normalized force (*F/R*) versus distance (*D*) measured between mica surfaces bearing anchored PEG layers with MW 1900. ●, ■, electrostatically attached PEG-lysine; ○, □, grafted PEG, MW 1900. Squares, measured on approach; circles: measured on separation. From Ref. 42. Published with permission from Steinkopf Verlag Darmstadt.

extended conformation, in qualitative agreement with the results obtained by Taunton *et al.*[47] and with de Gennes's scaling considerations for a polymer brush in a good solvent.[32,48]

The behavior of PEG 1900 close to the cloud point temperature (about 180 °C) could not be investigated for practical reasons. However, a similar study has been performed for a nonionic surfactant, $C_{12}EO_5$, which has a cloud point at 27 °C.[40] The force between $C_{12}EO_5$ layers adsorbed to mica which had been hydrophobed by Langmuir–Blodgett deposition of a layer of dioctadecyl dimethylammonium ions is, at large separations, dominated by a weak double-layer force which does not change with temperature. At separations larger than 4.5 nm, the force shows a dramatic temperature dependence as indicated in Figure 14. At 15 °C the measured repulsion becomes much larger than the extrapolated double-layer force at distances below 3.5 nm. At 20 °C a weak minimum occurs, but still in the repulsive regime.

As temperature increases, the short-range hydration repulsion decreases in range and the minimum shifts to smaller separations and becomes attractive at 30 °C. The layer thickness increases with temperature to approximately 2.6 nm at 37 °C. The most plausible explanation for the increased thickness is that decreased repulsion between the EO chains leads to a closer packing (increased adsorption) of the $C_{12}EO_5$ molecules at the surface. The decreased repulsion is also manifested in the temperature dependence of the relatively short-range interaction between the adsorbed layers. There is no general agreement in the molecular mechanism underlying this tempera-
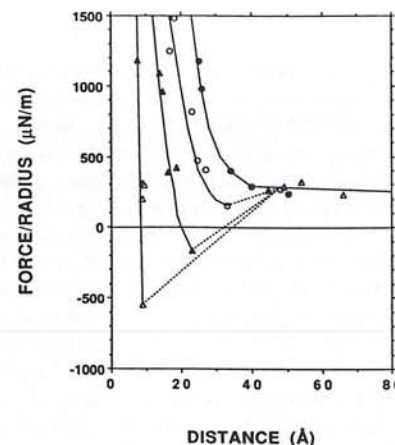
Figure 14. The force between $C_{12}EO_5$-coated surfaces as a function of separation at various temperatures (°C). ●, 15; ○, 20; ▲, 30; △, 37. (From Ref. 40.)

ture dependence. It is noteworthy, however, that it correlates directly with the cloud point of the surfactant/water system.

15.4. PROTEIN INTERACTION WITH PEG SURFACES

One of the first to study, in some detail, the adsorption of biomolecules to PEG surfaces was Nagaoka *et al.*[43] They found comparatively low platelet adhesion and protein adsorption to PEG hydrogels.

We have undertaken an extensive ellipsometry study on how proteins with isoelectric points in the range 4 to 10, i.e., with different charge at physiological conditions, adsorb on PEG grafted to silicon. The results were compared with the adsorption to hydrophobic PVC and to anionic polymethacrylate (PMA).[14] For these latter two surfaces, adsorption values in the order of a monolayer were generally found. For the (at pH 7) negatively charged (albumin) and neutral (IgG) proteins, adsorption is presumably driven by hydrophobic and van der Waals interactions while electrostatics is more important for the adsorption of poly-lysine to negatively charged PMA surfaces. Although PEG forms coaservate with polyacrylic acid, no such tendency was observed with the anionic protein on the PEG surface. Instead, generally, adsorption values below 0.1–0.2 mg m⁻² (less than one tenth of a monolayer) were observed, indicating that steric repulsion dominates the interaction between PEG and proteins at physiological conditions. Also, in contrast to the other surfaces no pronounced plateau in the adsorption isotherms was found on PEG-coated surfaces. Rather, a slowly progressing increase in this "background level" adsorption

was observed other the whole concentration range; see, for example, results for IgG in Figure 13.

The proteins that do adsorb to PEG-coated surfaces can not all be displaced by extensive rinsing. This may either be the result of interaction of protruding parts on the protein and bare substrate sites not covered with PEG, or due to mere physical entanglement of PEG and protein segments. Fibrinogen, the largest protein studied, gives slightly higher adsorbed amounts after rinsing compared to albumin, IgG, and poly-lysine. Similarly, low adsorption values on a PEG surface were found for complement proteins (C3 and C1q) when compared with adsorption values on a variety of other polymer films with different functionality prepared by plasma polymerization;[44] see Figures 15 and 16. Although one expects from studies of PEG–protein conjugates in solution that proteins on a PEG surface may be in a more native state than on hydrophobic or ionic surfaces, no such experimental evidence exists to date.

The adsorption of proteins to PEG surfaces decreases with increasing degree of polymerization. This is indicated by the N/C ratio from ESCA after adsorption of human albumin (0.1% w/w) to hydrogels with PEG 550, 1900, and 5000;[5] see Table 4. Similar results have been found for fibrinogen[45] and for the total amount of proteins adsorbed from blood plasma.[42]

The adsorption decrease with increasing PEG molecular weights is large up to 1500, above which only a marginal decrease is observed. This correlates with a decreasing grafting efficiency with increasing molecular weight, yielding a rather constant EO content at molecular weights above 2000.[5]

Protein adsorption on PEG surfaces increases with temperature, as shown in Table 5 for the total amount of protein adsorbed from plasma (ellipsometry) and for
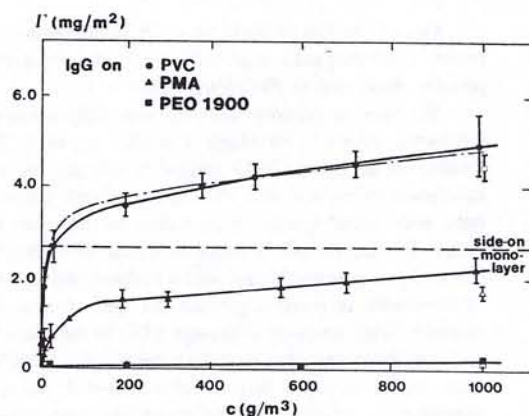
Figure 15. Adsorption isotherms at 20 °C for human IgG on various surfaces. (From Ref. 14.)
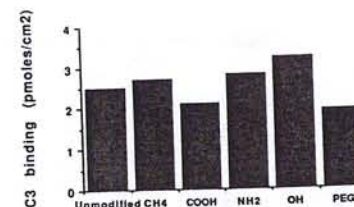
Figure 16. Comparison of the active adsorption (total minus unspecific adsorption) of radiolabeled complement factor C3 on a PEG surface and other functionalized surfaces as obtained from various gas-plasma treatments. Unspecific adsorption was measured after addition of 10 mM EDTA, i.e., measurements took place in the absence of Ca^{2+} and Mg^{2+} ions (essential for activation of complement) (see Ref. 44).

pure fibrinogen adsorption (0.1% in buffer, ESCA). The increase is almost linear over the whole temperature range studied (20–60 °C). This is most likely due to the temperature-dependent interactions of PEG, as discussed above. It is noteworthy that no dramatic changes of the fibrinogen structure are expected below 45 °C.

Finally, it should be mentioned that dextran also shows protein-repellant properties. However, in this case significantly higher molecular weight of the polymer must be used to obtain similar effects.

15.5. HYPOTHESIS ON THE PROTEIN INERTNESS OF PEG SURFACES

From this experimental and theoretical description, the following hypothesis evolves: The nonionic EO building unit in PEG is a dipole. The dipole moment depends on the conformation and an equilibrium between different states develops. At room temperature, the *gauche–trans–gauche* conformation dominates and gives rise to maximum dipole moment, a helical structure in vacuum,[49] and extensive hydration of the PEG chain in water. Since water is a better than theta solvent for PEG, this gives

Table 4. Relative Amounts of Human Albumin Remaining on PEG Surfaces after Rinsing as Determined by the Nitrogen/Carbon Ratio from ESCA Analysis

Sample	N/C (%)	Sample	N/C (%)
PVC	8.8	PEG 5000	0.9
PEG 550	5.5	TMP (EO)$_{20}$ *branched* 7.7	7.7
PEG 1900	2.2	Pure albumin	16

Table 5. The Influence of Temperature on the Adsorption of Proteins on PEG (MW 1900) Surfaces[a]

Temperature	Γ_{tot} (mg m^{-2})	$(N/C)_{fib}$ (%)
17	0.4	1.3
25	0.7	2.0
37	1.5	2.8
50	2.5	4.3
71	4.9	6.4

[a]The total amount of proteins adsorbed from serum (diluted 1/10) was determined by ellipsometry on PEG-treated silicon wafers. The relative amounts of fibrinogen adsorbed (from a single protein solution, $c = 0.1\%$ w/w) onto PEG-modified polyethylene was calculated from the nitrogen/carbon ratio obtained from ESCA analysis.

rise to a general and dominating steric repulsion force (osmotic and excluded volume contributions) between PEG and protein in aqueous solutions, since the extensive hydration causes the van der Waals force contribution to be very small and electrostatic interactions are not present. The effective range of the steric repulsion, reflected in lowering of the residual protein adsorption found on PEG surfaces, increases with molecular weight and surface coverage with PEG. A temperature rise as well as an addition of electrolyte changes the distribution of conformer states. As we have discussed above, this is accompanied by changes in the dipole strength of the EO units and a decreased repulsion between PEG chains which shows up as a decreased hydration and, eventually, phase separation. The consequence is that PEG is not such a good steric stabilizer at elevated temperature. As a result, protein adsorption increases with temperature and electrolyte addition.

REFERENCES

1. D. E. Gregonis, C. M. Chen, and J. D. Andrade, in: *Hydrogels for Medical and Related Applications* (J. D. Andrade, ed.), *ACS Symp. Ser. 31*, 88 (1973).
2. C.-G. Gölander, S. Jönsson, T. Vladkova, P. Stenius, and J.-C. Eriksson, *Colloids and Surfaces 21*, 149 (1986).
3. P. Drude, *Ann. Phys. 272*, 532, 865 (1889).
4. J. N. Israelachvili and G. E. Adams, *J. Chem. Soc., Faraday Trans. 1, 74*, 975 (1978).
5. P. C. Herder, P. M. Claesson, and C. E. Herder, *J. Colloid Interface Sci. 119*, 240 (1988).
6. A. Abuchowski, T. van Es, N. C. Palczuk, and F. Davis, *J. Biol. Chem. 252*, 3578 (1977).
7. A. F. Bückmann, M. Morr, and G. Johansson, *Makromol. Chem. 182*, 1379 (1981).
8. S. Zalipsky, C. Gilon, and A. Zilkha, *Eur. Polym. J. 19*, 1177 (1983).
9. J. M. Harris, E. C. Struck, M. G. Case, and M. S. Paley, *J. Polym. Sci. 22*, 341 (1984).
10. J. M. Harris, K. Yoshinaga, M. S. Paley, and M. R. Herati, in: *Advances in Separations Using Aqueous Phase Systems in Cell Biology and Biotechnology* (D. Fisher and I. A. Sutherland, eds.), Plenum Press, London (1988).
11. J. M. Harris, *Rev. Macromol. Chem. Phys. C25*, 325 (1985).
12. M. S. Paley and J. M. Harris, *J. Polym. Sci. 25*, 2447 (1987).
13. F. E. Bailey, Jr. and R. W. Callard, *J. Appl. Polym. Sci. 1*, 56 (1959).
14. E. Kiss, C-G. Gölander, and J. C. Eriksson, *Progr. Colloid & Polymer Sci. 74*, 113–119 (1987).
15. J. L. Parker, D. L. Cho, and P. M. Claesson, *J. Phys. Chem. 93*, 6121 (1989).
16. C.-G. Gölander and J.-C. Eriksson, *J. Colloid Interface Sci. 119*, 38 (1987).
17. J.-C. Eriksson, C.-G. Gölander, A. Baszkin, and L. Ter-Minassian-Saraga, *J. Colloid Interface Sci. 100*, 2 (1984).
18. W. R. Gombotz, W. Guanghui, and A. S. Hoffman, *J. Appl. Polym. Sci. 37*, 91 (1989).
19. C.-G. Gölander, M. W. Rutland, D. L. Cho, A. Johansson, H. Ringblom, S. Jönsson, and H. K. Yasuda, *J. Appl. Polym. Sci.*, submitted.
20. E. Kiss and E. Gölander, *Colloids and Surfaces 49*, 335–342 (1990).
21. C.-G. Gölander and E. Kiss, *Colloids and Surfaces*, submitted.
22. P. M. Claesson and C.-G. Gölander, *J. Colloid Interface Sci. 117*, 366 (1987).
23. John Yee, *Synthesis and Interfacial Coupling of Mercapto Activated Poly(ethyleneoxide) via Thiol-Disulphide Interchange*, M.Sc. Thesis, Dept. of Bioengineering, University of Utah, Salt Lake City.
24. H. L. Lee, J. Kopecek, and J. D. Andrade, *J. Biomed. Mater. Res. 23*, 351 (1989).
25. R. Silverstone and K. Kronberg, *J. Phys. Chem. 93*, 6241 (1989).
26. R. Kjellander and E. Florin-Robertsson, *J. Chem. Soc., Faraday Trans. 1, 77*, 2053 (1981).
27. S. Saeki, N. Kuwahara, M. Nakata, and M. Kaneko, *Polymer 17*, 685 (1976).
28. R. E. Goldstein, *J. Chem. Phys. 80*, 5340 (1984).
29. G. Karlström, *J. Phys. Chem. 89*, 4962 (1985).
30. A. A. Samii, B. Lindman, and G. Karlström, *Prog. Colloid Polym. Sci. 82*, 1 (1990).
31. M. Björling, P. Linse, and G. Karlström, *J. Phys. Chem. 94*, 471 (1990).
32. P. G. de Gennes, *Macromolecules 13*, 1069 (1980).
33. S. I. Jeon, J. H. Lee, J. D. Andrade, and P. G. de Gennes, in press.
34. *DISCOVER*. A molecular simulation program from Biosym Technologies, 10065 Barnes Canyon Road, San Diego, CA 92121.
35. W. L. Jörgensen, *J. Chem. Phys. 77*, 5757 (1982).
36. J. L. Valles and J. W. Halley, *J. Chem. Phys. 92*, 694 (1990).
37. P. J. Flory, *Statistical Mechanics of Chain Molecules*, Chapter 5, Hanser Publishers, New York (1989).
38. P. Dauber-Osguthorpe, V. A. Roberts, D. J. Osguthorpe, J. Wolff, M. Genest, and A. T. Hagler, *Proteins, Structure, Function and Genetics 4*, 31 (1988).
39. J. Klein and P. F. Luckham, *Macromolecules 17*, 1041 (1984).
40. P. M. Claesson, R. Kjellander, S. Stenius, and H. K. Christensen, *J. Chem. Soc., Faraday Trans. 82*, 2735 (1986).
41. P. M. Claesson, D. L. Cho, C.-G. Gölander, E. Kiss, and J. L. Parker, *Prog. Colloid Polym. Sci. 82*, 330–336 (1990).
42. E. Kiss and C.-G. Gölander, *J. Colloid and Interface Sci. 117*, 366–374 (1987).
43. Y. Mori, S. Nagaoka, H. Takiuchi, T. Kikuchi, N. Noguchi, H. Tanzawa, and Y. Noishiki, *Trans. Am. Soc. Artif. Internal Organs 28*, 459 (1982).
44. K. Nilsson Ekdahl, B. Nilsson, C.-G. Gölander, B. Lassen, H. Elwing, and U. R. Nilsson, *J. Biomed. Mater. Res.*, submitted.
45. W. R. Gombotz, W. Guanghui, A. S. Hoffman, and T. A. Horbett, *Proc. The Third World Biomater. Congr.*, Kyoto, Japan (April 21–25, 1988).
46. Y-S. Yeh, Y. Iriyama, Y. Matsuzawa, S. R. Hanson, and H. Yasuda, *J. Biomed. Mater. Res. 22*, 795 (1988).
47. H. J. Taunton, C. Toprakciouglu, L. J. Fetters, and J. Klein, *Macromolecules 23*, 571 (1990).
48. S. Patel, M. Tirell, and G. Hadziioannou, *Colloids and Surfaces 31*, 157 (1988).
49. F. E. Bailey and J. V. Koleske, *Polyethyleneoxide*, Academic Press, New York (1976).
50. P. A. Cuypers, W. T. Hermens, and H. C. Hemker, *N.Y. Acad. Sci. 283*, 77 (1977).
51. E. Kiss and C.-G. Gölander, *Colloids and Surfaces 58*, 263–270 (1991).

Andrade
Nov. Feb
8/92

Themes:

Merrill – complete coverage
Goranson – opt. tactical cont
S CR = Nagaoka S

_____

Hey Joe:
I hope as many
people read this as
read your books!
But,
Milton

POLY(ETHYLENE GLYCOL) CHEMISTRY (spine)

POLY(ETHYLENE GLYCOL) CHEMISTRY

Biotechnical and Biomedical Applications
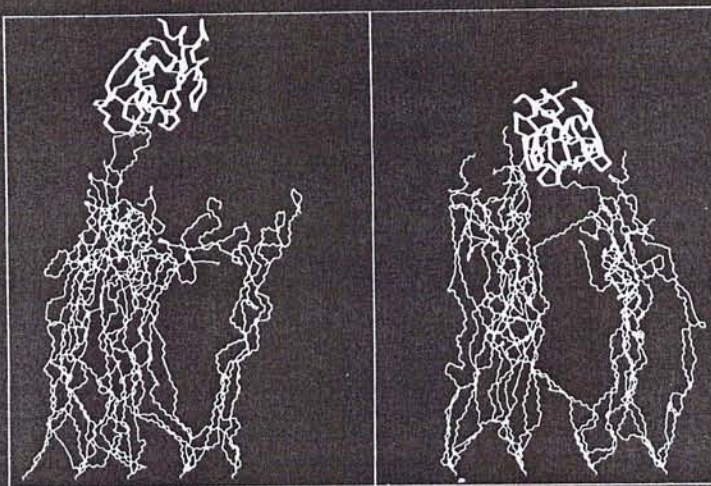
Edited by

J. MILTON HARRIS

PLENUM

FIBRINOGEN ADSORPTION ON DEAE-DEXTRAN FUNCTIONALIZED GLASs

Golander CG, Andrade J and ~~Josefowitz~~ Muller D. and Jozefonvicz J

or → Zhou F.L., Muller D. and Jozefonvicz J

ABSTRACT

Diethylaminoethyl (DEAE) modified dextran of molecular weights 40000 and 500000 respectively, were adsorbed to a chromosulphuric acid cleaned amorphous quartz slide and cross-linked with 1,4-butanediol diglycidyl ether. Both unmodified and dextrane derivatized slides showed zero contact angle in water. Adsorption of FITC-labelled human fibrinogen to the surfaces was measured by means of Total Internal Reflection Fluorescence (TIRF). Compared to bare silica the adsorbed amount on both DEAE-dextran derivatized surfaces was reduced almost one order of magnitude. Reduced double layer interaction caused by surface charge neutralization and polymer-protein repulsion caused by configurational entropy loss may tentatively explain this result.

INTRODUCTION

Protein resistant or protein inert surfaces have recently gained a lot of interest in biomedical science and technology. It has obvious applicability in soft contact lenses to reduce opacity caused by protein adsorbate and to keep the lens permanently wetting. Furthermore, one might expect that a low interaction potential with proteins could be generalized to other biological species so that tissue and blood biocompatibility would follow. Promising result has been found using layers of hydrofilic non-charged polymers like polyethyleneoxide (1,2).

Most surfaces naturally carries a small negative surface charge. Even after hydrofobation by means of silanization of glass or LB deposition on mica a residual charge is present which in direct force measurements has showed to give considerable contribution to the overall interaction (3). One might expect that a repulsive double layer potential from the substrate can cause conformational perturbation of biomolecules in close proximity to the surface, resulting in bioactivation allthough the molecules themselves never touch the surface. It is therefore important to reduce the surface charge in connection with the surface modification.

In this short communication , we have studied the applicability of dextran as protein resistant surface coating on amorphous quartz. By using diethylaminethyl (DEAE) modified dextran, we anticipate that it would be possible to match the density of DEAE groups in the polymer with the negative surface charge density of the silica, so that substrate surface charge neutralization could be effectuated. Consequently, the interaction potential originates from the inherent properties of the non-charged, hydrophilic polymer itself.

EXPERIMENTALS

Preparation of surfaces

Diethylaminoethyl (DEAE) modified dextrans with parent molecular weights of 40000 and 500000 were purchased from Pharmacia AB, Sweden. The nitrogen content was 0.5% and 1.8% and the equivalent DEAE content 4-5% and 12% respectively. Of the total number of DEAE groups, 30% existed as doubly charged "tandem groups" $-OCH_2CH_2N^+(C_2H_5)_2-CH_2CH_2N^+H(C_2H_5)(Cl^-)_2$.

DEAE-dextran, 0.2g, was dissolved in 2.5 ml triply distilled water. By using NaOH, pH was adjusted to 11.5. A quartz cover slip, 2.54*7.62 mm, previously etched in chromosulphuriic acid at 70^0 C for 40 minutes, rinsed thoroughly in water and finally dried by N_2 jet, was immersed 30 mm into the DEAE-dextran 40000 (DDT 40) solution and kept there for 30 min. After thorough rinsing in water, the slide was dried in vaccum at 80^0 C overnight. The slide was now turned around and 30 mm of the other side was treated with DEAE-dextran 500000 (DDT 500) using the same procedure. Subsequently , the DEAE dextran adsorbate film was crosslinked by means of 1,4-butanediol diglycidyl ether (6 µl in 6 ml diethyl ether, 40^0 C, 30 minutes) and finally rinsed in water and dried at 80^0 C overnight. The contact angle was measured along the whole slide with the Wilhelmy technique.

Protein adsorption studies
Human fibrinogen (65% clottable, lot #52364, United States Biochemical Corp., OH) was FITC labelled by using the method of Coons et al (4).[6] The concentration was measured independently by the Biorad assay (5).[7] The labelling degree, as calculated from the concentration and the absorption at 280 nm and 490 nm (8)[8] was 3 moles/mole fibrinogen. FITC-labelled fibrinogen was dissolved in PBS buffer, (pH=7.3, I=0.19) to a final concentration of 0.32 mg/ml. (One tenth of the plasma concentration.) Protein adsorption was measured by means of Total Internal Reflection Fluorescence Spectroscopy (TIRF). Principles and TIRF geometry has been described elsewhere (7)[9] The TIRF cell was mounted on a micrometer-driven stage which allowed us to make lateral scanning of the fluorescence emission along the surface as described in a recent paper (8)[10]. The excitation source was a Ar laser (emitting 45 mW at 488 nm) and fluorescence was measured at 515 nm. Background fluorescence was measured as a function of position before fibrinogen solution was injected. Two hours were allowed for adsorption. No measure of the kinetics was made. Subsequently, we scanned the fluorescence, flushed quickly with 20 ml buffer and scanned again. A 5% water solution of a pleuronic surfactant (F-127, BASF) with structural formula, $HO-(CH_2CH_2O)_{98}-(CH_2CH_2CH_2O)_{69}-(CH_2CH_2O)_{98}-OH$, was then injected and exposed to the surface for 30 min. After flushing with buffer another fluorescence scan was recorded. Finally, non-labelled fibrinogen was injected and the exchange was recorded after 30 minutes exposure and subsequent rinsing with buffer. The quantitative determination of adsorbed proteins is based on the following equation (7): (3):

$$\varnothing_a/\varnothing_b T = d_p C_p N_a/2 N_b, ev$$

Here $\varnothing$ is the fluorescence quantum yield for adsorbed (a) and bulk (b) fluors respectively, T the adsorbed amount, d_p the penetration depth of the excitation light, C_p the protein concentration and N the fluorescence intensity from adsorbed (a) fluors and from fluors present in the evanescent region of the bulk(b) respectively. A calibration curve, based on measurements of fluorescence (in the TIRF mode) from standard solutions of known (c:s), was used to sort out the evanescent part from the total bulk fluorescence measured, Nb(tot). Absolute values of adsorbed amounts,T, could not be determined since the quantum yield ratio $\varnothing_a/\varnothing_b$ has not been determined. (This requires independent measurements of adsorption or fluorescence lifetime studies.) Data is therefore rather presented as "relative"values $\varnothing_a/\varnothing_b T$.

RESULTS AND DISCUSSION

According to the preparation procedure above, the slide can be devided into three regions: DDT 40-SiOH-DDT 500. All three regions of the slide were hydrofilic and showed zero (advancing) contact angle in water. One may object that partial dipping of the slide in the DEAE dextran solution may result in an extended zone of partial surface coverage of polymer at the solution/air contact position due to some solution turbulence and also diffusion of the polymer along the surface. On the other hand, the polymer is expected to adsorb ~~almost~~ irreversibly. Furthermore, we have the advantage to be able to directly compare the adsorption to three different surfaces.

As indicated by the adsorption result in Fig.1, the borderline between the regions seems fairly sharp. The adsorption of fibrinogen is almost seven times higher to SiOH than to both DEAE-dextran polymers. The comparatively high figure for SiOH indicates that fluorescein-labelled fibrinogen was partly aggregated. Comparing the SiOH surface with the DEAE polymer film, there are some features that are different and which can at least partly explain the difference in behavior: the pK values of the functional groups (SiOH versus mainly C-OH) and the related surface charge, the hydrogen bonding capacity and the mobility of the hydrofilic groups. The surface charge of the silica surface probably constitutes the most important mechanism for protein interaction since ~~hydrofobic~~ interaction is not possible. Furthermore, protein-polymer interactions would lead to an unfavorable entropy decrease which in practice means a repulsive force.

There is a slightly lower fibrinogen adsorption to DDT 40 compared to DDT 500. If the entropy effect was dominating one would expect the opposite, that the higher molecular weight DDT 500 should yield lower adsorption. This might indicate that the surface charge is more efficiciently compensated when using DDT 40 due to a more efficient packing of the smaller polymer molecules and/or a better matching of distances between the positive charges of the polymer and the negative charges of the SiOH surface. (Figures for close-packing densities) OK.

About 15% of the fibrinogen was desorbed from all regions after 30 minutes exposure to surfactant F-127. If electrostatics were dominating the interaction, an ion-exchange mechanism for desorption would be more efficient. Another 10-15% was consequently exchanged with unlabelled fibrinogen. However, these are comparatively low values and may indicate at least a partial irreversible adsorption.

** see p4

REFERENCES

1. Golander C-G and Kiss E. J Colloid Interface Sci, 121 (1988) 240-253.
2. Lee's dissertation or one of the incuded papers.
3. Claeson P M, Blom C, Herder P and Ninham B. J Colloid Interface Sci, 114 (1986) 234-242
4. Coons A M , Creech H J, Jones R N and Berliner E.J Immunol. 45, (1942)159-170
5. Biorad^R assay manual.
6. Wells A F, Miller C E and Nadel M K. Applied Microbiology, vol 14 no 2, (1966), 271-275.
7. Hlady V, Reinecke D R and Andrade J.J Colloid and Interface Science, vol111, no2, (1986), 555-569.

position from DDT 40 derivatized end (mm)
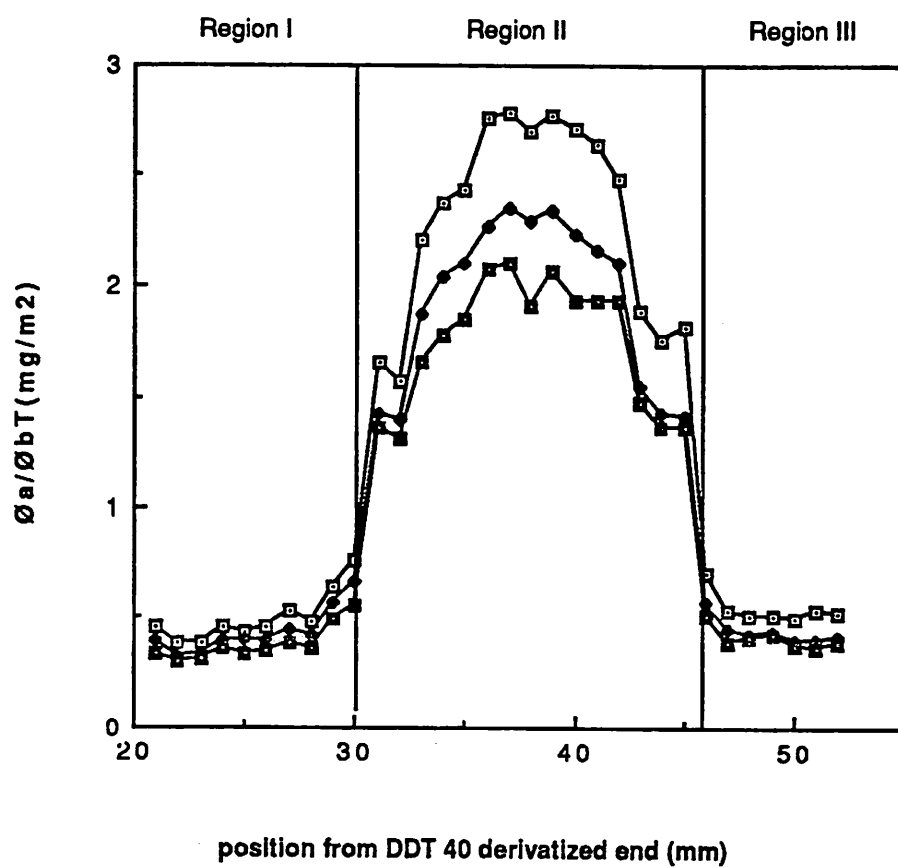
8. Hlady V, Golander C-G and Andrade J. Colloids and Surfaces, 33 (1988), 185-190

9. Golander C-G, Andrade J, Hlady V and Lin Y-S. To be published.

FIGURE CAPTIONS

Figure 1. Adsorption of FITC-labelled human fibrinogen to a quartz slide partly modified with DEAE-dextran. The adsorption values are expressed as $\emptyset_a/\emptyset_bT$ in mg/m2. Region I: DEAE-dextran 40000; Region II: bare silica; Region III: DEAE-dextran 50000. After quick flush with PBS buffer. After 30 minutes exposure to pleuronic F-127 and buffer rinsing. After 30 minutes exposure to non-labelled fibrinogen (c=0.32 mg/ml) followed by buffer rinsing.

DEAE - dextran 403

DEAE - dextran 50011

4. Santarelli X., Muller D., and Jozefonvicz J. J. Chromatogr., 443 (1988), 55-62.

5. Santarelli X., Zhou F.L., Muller D. and Jozefonvicz J. Proceedings on Biotechnology of plasma proteins - INSERM Symposia (in press).

SCIENCE

Enzyme Electrodes

Electrodes containing immobilized enzymes could be
used to monitor specific metabolites.

David A. Gough and Joseph D. Andrade

There is currently considerable interest in the development of biochemical-specific electrodes that could be used to monitor and regulate the concentrations of biochemicals in body fluids. Some very selective biochemical sensors have been made recently in which conventional solute-specific electrodes are used to monitor reactions

catalyzed by immobilized enzymes. These devices can theoretically be made to determine metabolites, enzymes, coenzymes, or enzyme inhibitors, in situ, without special preparation of the sample. Widespread application can be predicted for such electrodes in both experimental and clinical medicine if they can be made to function specifically and accurately, and if they can be used for nondestructive, instantaneous, and continuous determinations in situ. Enzyme electrodes must not promote undesirable physiological responses, such as antigenic re-

sponses, thrombosis, or tissue reaction. In addition, they must be inexpensive, easy to operate, and have a long lifetime.

In this article we discuss the development of biochemical-specific electrode systems, present some of the foreseeable problems that might be associated with their use, and review the essential literature.

The basic functional concept of the "enzyme electrode" is the continuous, instantaneous, electrochemical monitoring of enzyme-catalyzed reactions, in which a substrate, coenzyme, or inhibitor is converted into a product by means of an enzyme. The relative concentration of the reactants can be varied so that analytical techniques are obtained in which the reaction rates or equilibrium concentrations are proportional to the limiting components. Electroactive species either produced or consumed by the reaction may be detected by commercial solute-specific electrodes, the signal thus produced being related to the limiting reactant. If a system can be designed such that the enzymes are immobilized or constrained to the immediate vicinity of the electrode—these enzymes being capable of continuous catalysis in complex physiological fluids—a new bio-

Mr. Gough is a research assistant in the Division of Materials Science and Engineering of the College of Engineering, University of Utah, Salt Lake City 84112. Dr. Andrade is an associate professor in the colleges of Engineering and Pharmacy and an assistant research professor in the College of Medicine, University of Utah.

chemical-specific electrode is feasible. Obviously, the term "enzyme electrode" is not rigorously accurate because these devices may be made sensitive to substrate, product, enzymic effectors, or enzymes themselves. We prefer to use the term, however, to describe biochemical-specific electrodes that are dependent on immobilized enzymes, until more accurate terms become familiar.

Electrode Characteristics

The most commonly known solute-specific electrode is the glass pH electrode. When referenced against a standard reference electrode, a potential difference is produced which is proportional to the pH of the solution, according to the Nernst equation. Such an electrode may be useful for following enzyme reactions in which hydrogen ions are a product. Their use is limited, however, because most enzyme reactions are not linear over a broad pH range and for accurate results the reaction media must have a low buffering capacity, the opposite of many physiological fluids.

The composition of the electrode glass may be varied experimentally so that the resultant potential is proportional to the potassium, sodium, ammonium, or other cations in solution. In some other types of specific ion electrodes, ingenious liquid or solid ion exchange membranes are employed. Descriptions of these electrodes and their mechanisms of operation have been discussed in detail (1, 2). Of the more than 20 specific ion electrodes available commercially, only those sensitive to species participating in enzymic reactions will be useful in this application. The electrodes that will be of most immediate use are those specific for pH, ammonium, and other monovalent cations (3), and cyanide (4). A phosphate-specific electrode has been reported (5), but does not appear to be adequately selective or reproducible.

The electrodes now available are not generally completely selective for the desired species. For example, if the enzyme reaction produces NH_4^+ which is to be measured, the electrode may respond not only to NH_4^+, but also to Na^+, K^+, and other cations in solution, as well as pH. This effect may be eliminated by referencing against another cation electrode, which cannot

respond to the NH_4^+ formed from the reaction because of diffusional or flow effects, but responds to everything else. By determining electronically the difference between the two, a signal that is only proportional to the NH_4^+ produced by the enzyme reaction will be obtained.

Truly continuous measurements can be made only when the signal-bearing species is continuously removed or converted by the electrode, such as in polarographic or amperometric systems. Most ion-selective electrodes are potentiometric, however.

The response of specific ion electrodes has been discussed elsewhere (1). Ideally, specific ion electrodes provide a linear Nernstian response of 0.059 volt at 25°C per decimal change in activity of monovalent cation over a certain range of concentration. Response times are on the order of seconds or less for most electrodes, making electrode kinetics a minimal concern.

Polarographic measurements are made by measuring a change in current as a function of changing potential between two inert metal electrodes, and are useful for detecting several species in solution that have a characteristic plateau at a known potential. Although polarography itself may not be very useful to the system of interest, constant potential polarography, or amperometry (in which the current is proportional to a certain species reduced or oxidized at a fixed potential), has application. This is the basis for the operation of the well-known Clark pO_2 electrode (6), wherein oxygen diffuses through a gas-permeable polymer membrane and is reduced at a platinum electrode, which is kept at a fixed potential with respect to a silver-silver chloride reference electrode. Response time is on the order of seconds when membranes highly permeable to oxygen are used.

It is also possible to use metal electrodes in the form of an analytical fuel cell, the short circuit current being proportional to the biochemical substrate. The effect of interfering species may be minimized by selective membranes. Relatively high currents may be obtained by efficient electrochemical coupling.

The pCO_2 electrode is also a well-known clinical tool (7). The basis of this electrode is diffusion of carbon dioxide through a gas-permeable polymer membrane into an internal

aqueous solution of fixed bicarbonate concentration. The carbon dioxide is hydrated to carbonic acid in a slower, rate-determining step, then rapidly ionized to bicarbonate and hydrogen ion. This causes a change in the pH of the internal solution, as determined by a potentiometric pH electrode. This electrode has some limitations for enzyme electrode applications. It responds only to carbon dioxide, while the product of many enzyme reactions is bicarbonate. The response time may also be too long for many applications. Membranes of higher permeability, and possibly membranes with enzymatic activity, may significantly reduce the response time of this electrode.

Metal electrodes have been used to measure enzymatic oxidation-reduction reactions in which the oxidation state of a coenzyme or intermediate compound is directly changed at the electrode (8). Such systems will be operable if precautions are taken to prevent excessive adsorption or interference when the metal electrodes are placed in multicomponent systems.

Immobilized Enzymes

Numerous methods of enzyme immobilization have been reported in the literature (9–11). Several techniques are useful in the design of electrodes. The enzyme can be entrapped within a synthetic hydrophilic gel, cross-links can be formed between the molecules of the enzyme to make membranes, the enzyme can be chemically bound to membranes or other surfaces, the enzyme can be copolymerized with other enzymes or proteins, or the enzyme can be physically entrapped between membranes. Other techniques are available and may be useful for certain design requirements. Acidic or basic groups may be polymerized in the supporting polymer matrix in such a way that the pH in the immediate vicinity of the enzyme is optimum, while that of the bulk solution is different. Such techniques can optimize kinetics and possibly make an otherwise inoperable system workable. The method of immobilization will depend on the particular enzyme electrode system.

Some enzyme reactions may require the immobilization of substrates or coenzymes. The high cost of many coenzymes makes prohibitive the simple

addition of non–rate-limiting excesses to each sample to be measured. Probably the most practical techniques will be the covalent bonding of the coenzyme to a surface in such a way that reaction is still possible, as reported recently (*12*), or the covalent bonding of the coenzyme directly to the enzyme or other immobilized particle by techniques which permit catalytic action. Containment by a membrane of selective pore size or slow release through a glass frit to which the enzyme is bound may be necessary in some cases.

An important problem is heat inactivation of many enzymes at physiological temperatures. The long-term usefulness of biochemical electrodes will be seriously limited if methods of thermal stabilization cannot be found. One approach to this problem may be the use of only partially purified enzyme extracts, or the enzyme might be mixed with stabilizing species which will not interfere with the reaction. Some immobilization methods are reported to stabilize certain enzymes for periods longer than their lifetimes in vivo (*11, 13*). However, while perhaps not all enzymes of immediate interest are now capable of being stabilized for performance under the desired conditions, many can be adequately stabilized and current research into new techniques holds much promise (*14*).

Some enzymes that do not produce electroactive species may be linked to other enzymes in such a way that the product of the first enzyme reaction becomes the substrate for the second enzyme which involves an electroactive participant, thus greatly expanding the number of species that can be monitored. Studies indicate that these systems may be most efficient if the enzymes are mixed in the same phase to avoid unnecessary diffusional effects (*15*). Such multistep systems show some similarity to processes in vivo.

Although electrodes will operate under equilibrium or steady-state conditions, they must be characterized kinetically in order to determine the range and rate of response. Enzyme kinetics in the liquid phase (where diffusional effects are absent during the initial stages of the reaction) have been well studied. Some studies relating diffusional (*10, 16*), charge (*17*), and boundary layer effects (*18*) to heterogenous phase enzyme kinetics have been made; product inhibition (*18*) and two-enzyme systems (*19*) have

also been studied. The data indicate that immobilized enzymes can be characterized kinetically by the turnover number, concentration and Michaelis constant (K_m) of the enzyme, the nature and dimensions of the catalytic layer, the diffusivities of participating species, and the estimated thickness of the boundary layer. Diffusion of substrate through the physiological media may also have a limiting effect. Response of an immobilized enzyme electrode can therefore be predicted.

Many solute-specific electrodes cannot respond to very low concentrations of solute, such as concentrations less than $10^{-6}M$. This may limit the feasibility of certain enzyme electrodes since the critical concentrations of some compounds in physiological fluids are quite low. Another important consideration is that electrodes determine activities, not concentrations. In many instances, the clinical significance of activities measured in situ is not known. However, this may lead to some useful investigations.
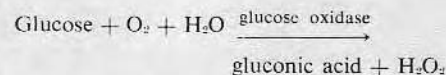
Applications of enzyme electrodes in flowing systems will require consideration of boundary layer artifacts and streaming potentials. This has been studied with glass electrodes in physiological solutions (*20*).

The electrode will also have to be designed to avoid any undesirable physiologic responses, such as protein deposition, thrombosis, antigenic reaction, or the formation of a diffusion-resistant tissue capsule around the electrode (*21*). A hydrophilic biocompatible membrane that excludes compounds of given molecular weight could be placed between the reactive layer and the physiological environment. Such a membrane should result in minimal protein deposition and thrombosis and should prevent species of larger molecular weight from passing while at the same time providing a highly aqueous medium for optimal substrate diffusion.
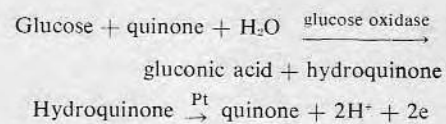
Literature

An excellent review of electrochemical methods of monitoring conventional enzymatic reactions has been published (*22*). In the present article we describe only self-contained biochemical electrode systems in which the enzyme or substrate has been physically immobilized in the vicinity of the sensor or bonded to it.

Probably the first account of an enzyme electrode was given by Clark and Lyons (*23*). They obtained potentiometric determinations of glucose and proposed that glucose could also be determined amperometrically by means of glucose oxidase immobilized between Cuprophane membranes, according to the equation
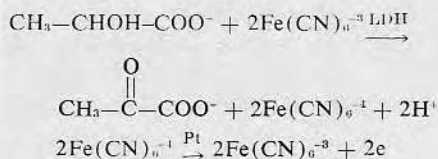
$$\text{Glucose} + O_2 + H_2O \xrightarrow{\text{glucose oxidase}}$$
$$\text{gluconic acid} + H_2O_2$$

Determinations were made from a solution of low buffering strength. Updike and Hicks (*24*) introduced the term "enzyme electrode" and made a dual cathode Clark-type oxygen electrode with glucose oxidase immobilized in polyacrylamide gel. The electrode was used to determine glucose from whole blood and plasma, and thus demonstrated the feasibility of measurements being obtained from complex solutions. The response time was approximately 30 seconds. Clark (*25*) suggested changing the potential across the electrodes so that they would respond to hydrogen peroxide production instead of oxygen uptake, thus reducing the problem of interference from oxygen in solution. Erroneous readings caused by small amounts of catalase or peroxidase found in most enzyme preparations or in physiological solutes can be minimized by suitable membrane-electrode design (*25*) or by inhibitors. Williams *et al.* (*26*) replaced oxygen as the hydrogen acceptor with quinone, to monitor glucose according to the following equations

$$\text{Glucose} + \text{quinone} + H_2O \xrightarrow{\text{glucose oxidase}}$$
$$\text{gluconic acid} + \text{hydroquinone}$$
$$\text{Hydroquinone} \xrightarrow{\text{Pt}} \text{quinone} + 2H^+ + 2e$$

where the reaction potential is 0.4 volt with reference to a standard calomel electrode. Glucose oxidase was held between layers of dialysis paper. The enzyme from *Aspergillus niger* was used because it can utilize quinone as a hydrogen acceptor and does not require other coenzymes, as does the enzyme from other sources. Determinations required the addition of buffer salts and quinone to maintain adequate *p*H and prevent the diffusion of quinone out of the enzyme layer. An electrode to determine lactate was also reported in the same communication (*26*), based on the oxidation of lactate by ferricyanide. The reaction is catalyzed by lactate dehydrogenase (cyto-
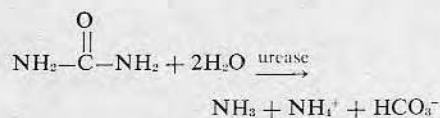
chrome b$_2$, E.C. 1.1.2.3), which does not require nicotinamide adenine dinucleotide as hydrogen acceptor, according to the following equations

$$CH_3-CHOH-COO^- + 2Fe(CN)_6^{-3} \xrightarrow{LDH}$$

$$\underset{\substack{\| \\ O}}{CH_3-C-COO^-} + 2Fe(CN)_6^{-4} + 2H^+$$

$$2Fe(CN)_6^{-4} \xrightarrow{Pt} 2Fe(CN)_6^{-3} + 2e$$

where the reaction potential is 0.4 volt with reference to a standard calomel electrode. The enzyme was held between dialysis membranes. Because of the low K_m of this enzyme ($K_m = 1.2$ mM), it was necessary to dilute the sample with buffered $K_3Fe(CN)_6$. Steady-state measurements were made in 3 to 10 minutes. The authors claimed that this system demonstrated increased sensitivity over spectral techniques (26).

Wingard et al. (27) have proposed constant current voltametry as a method for evaluation of electrodes containing immobilized oxidative enzymes as catalysts. This design was originally suggested as a fuel cell. Bessman and Schultz (13) have used the fuel cell concept to monitor glucose.

Several enzyme electrodes based on potentiometric cation- and ammonium-ion specific electrodes have been reported. Guilbault and Montalvo (28) made a urea transducer by immobilizing urease in a thin layer of acrylamide gel held over the surface of a cation electrode by cellophane film. The reaction is

$$\underset{\substack{\| \\ O}}{NH_2-C-NH_2} + 2H_2O \xrightarrow{urease}$$

$$NH_3 + NH_4^+ + HCO_3^-$$

The electrode was used for periods of up to 3 weeks at 25°C with no loss of activity and it responded to urea concentrations from 5×10^{-5} to $1.6 \times 10^{-1} M$ in tris(hydroxymethyl)aminomethane buffer, with an optimal response time of approximately 25 seconds. Many parameters affecting the function of the electrode were characterized (29). The response was not independent of Na$^+$ and K$^+$ ions when the Na$^+$ ion concentration was greater than one-half of the urea concentration and the K$^+$ ion concentration was greater than one-fifth of the urea concentration, placing limitations on the buffer that could be used. The enzyme gel layer had to be washed after each determination, making truly continuous or rapid measurements impossible. Similar electrodes were evaluated for the determination of urea in blood and urine (3). The sample was diluted and ion exchange resin added directly to eliminate cation interference. The electrode showed precision and accuracy comparable with spectral methods.
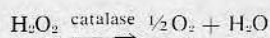
Electrodes specific for amino acids have been described (30). L-Amino acid oxidase (L-AAO) was immobilized by several methods at the tip of a commercially available cation electrode. The reaction is
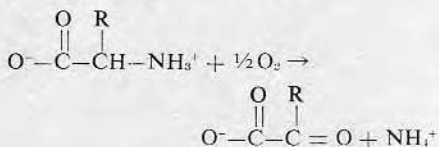
$$\underset{\substack{\|\ \ | \\ O\ R}}{O^--C-CH-NH_3^+} + H_2O + O_2 \xrightarrow{L-AAO}$$

$$\underset{\substack{\|\ \ | \\ O\ R}}{O^--C-C} = O + NH_4^+ + H_2O_2$$

The further nonenzymatic release of CO$_2$ by the following equation

$$\underset{\substack{\|\ \ | \\ O\ R}}{O^--C-C} = O + H_2O_2 \longleftrightarrow$$

$$\underset{\substack{| \\ R}}{O} = C-O^- + CO_2 + H_2O$$

is prevented by adding a small amount of catalase to the enzyme layer, which catalyzes the reaction

$$H_2O_2 \xrightarrow{catalase} \tfrac{1}{2} O_2 + H_2O$$

to give the total reaction

$$\underset{\substack{\|\ \ | \\ O\ R}}{O^--C-CH-NH_3^+} + \tfrac{1}{2} O_2 \rightarrow$$
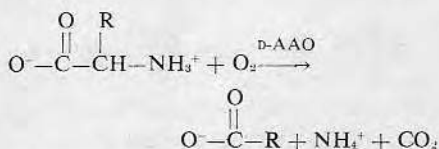
$$\underset{\substack{\|\ \ | \\ O\ R}}{O^--C-C} = O + NH_4^+$$

The addition of catalase seems to improve the electrode, probably because oxygen is generated, which is necessary for the oxidase reaction. These electrodes were reported to remain stable for about 2 weeks, and showed 1- to 2-minute response times to amino acids in dilute buffer solutions (30).

Electrodes specific for D-amino acids which are catalyzed by D-amino acid oxidase (D-AAO) have been reported (31). The reaction is

$$\underset{\substack{\|\ \ | \\ O\ R}}{O^--C-CH-NH_3^+} + O_2 \xrightarrow{D-AAO}$$

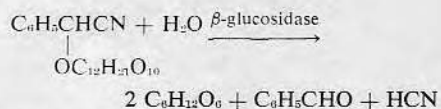$$\underset{\substack{\| \\ O}}{O^--C-R} + NH_4^+ + CO_2$$

where the cation is monitored by a potentiometric cation electrode. It was found that stability of the acrylamide enzyme gel or liquid layer could be maintained for 21 days if it were stored in buffered flavine adenine dinucleotide solution, a weakly bound diffusible coenzyme. The response was not increased by high concentrations of oxygen but was dependent on pH. A very similar electrode for asparagine was also reported (31), asparaginase being used as the catalyst. The addition of a coenzyme was not necessary.

A potentiometric electrode for glutamine has been reported and characterized (32). The electrode response was reproducible for up to 8 hours. The catalytic reaction was dependent on pH and inhibited by cations; measurements were made in dilute aqueous solutions.

An interesting approach to the determination of enzyme activity with potentiometric cation electrodes has been reported (33) in which immobilized substrates were used. A liquid layer of urea was passed between the electrode tip and a dialysis membrane in a continuous or interrupted flow process. Urea diffused through the membrane and was catalyzed by urease in dilute aqueous solutions. The ammonium ion produced was detected by the cation electrode. Although this approach probably requires much more study before it can be of significant practical use, it suggests some interesting applications.

An electrode specific for amygdalin based on a solid-state potentiometric cyanide electrode has been reported and characterized (4). β-Glucosidase, immobilized in acrylamide gel, hydrolyzes amygdalin by the following reaction

$$\underset{\substack{| \\ OC_{12}H_{21}O_{10}}}{C_6H_5CHCN} + H_2O \xrightarrow{\beta\text{-glucosidase}}$$

$$2\ C_6H_{12}O_6 + C_6H_5CHO + HCN$$

The lifetime of this electrode is limited by the dissolution of the cyanide-sensing crystal membrane, which is claimed to have a working lifetime of 200 hours (4).

Summary

From the discussion of electrodes and enzymes herein, and from the accounts of enzyme electrodes that have appeared in the literature, clinical determinations of certain metabolites and soluble enzymes by means of enzyme electrodes seem quite feasible. Such devices may be made highly specific by the use of appropriate enzymes and

a high degree of accuracy can be obtained. Instantaneous and continuous determinations can be made from physiological fluids, and undesirable physiologic responses can theoretically be minimized, thus making long-term clinical monitoring a possibility. Enzyme electrodes may also have a useful lifetime and meet other practical requirements.

References and Notes

1. G. Eisenman, Ed., *Glass Electrodes for Hydrogen and Other Cations* (Dekker, New York, 1967); R. A. Durst, Ed., *Nat. Bur. Stand. Spec. Publ. No. 314* (1969).
2. R. P. Buck, *Anal. Chem.* 44, 270R (1972).
3. G. G. Guilbault and E. Hrabankova, *Anal. Chim. Acta* 52, 287 (1970).
4. G. A. Rechnitz and R. Llenado, *Anal. Chem.* 43, 283 (1971).
5. G. G. Guilbault and P. J. Brignac, Jr., *Anal. Chim. Acta* 56, 139 (1971).
6. L. C. Clark, *Trans. Amer. Soc. Artif. Inter. Organs* 2, 41 (1956).
7. J. W. Severinghaus and A. F. Bradley, *J. Appl. Physiol.* 13, 515 (1958).
8. L. R. Blinks and R. K. Shaw, *Proc. Nat. Acad. Sci. U.S.A.* 24, 420 (1938).
9. I. Silman and E. Katchalski, *Annu. Rev. Biochem.* 35, 873 (1966); S. Avrameas, *Immunochemistry* 6, 43 (1969); R. Axen and S. Ernbach, *Eur. J. Biochem.* 18, 351 (1971).
10. R. Goldman, L. Goldstein, E. Katchalski, in *Biochemical Aspects of Reactions on Solid Supports*, G. R. Stark, Ed. (Academic Press, New York, 1971).
11. L. B. Wingard, Ed., *Enzyme Engineering* (Interscience, New York, 1972).
12. M. Weibel, H. H. Weetal, H. Bright, *Biochem. Biophys. Res. Commun.* 44, 347 (1971).
13. S. Bessman and R. Schultz, personal communication.
14. *Chem. Eng. News* (3 January 1972), p. 24.
15. K. Mosbach and B. Mattiasson, *Acta Chem. Scand.* 24, 2093 (1970).
16. R. Goldman, O. Kedem, I. H. Silman, S. R. Caplan, E. Katchalski, *Biochemistry* 7, 486 (1968); E. Selegny, G. Broun, D. Thomas, *Physiol. Veg.* 9, 25 (1970).
17. R. Goldman, O. Kedem, E. Katchalski, *Biochemistry* 7, 4518 (1968); W. E. Hornby, M. D. Lilly, E. M. Crook, *Biochem. J.* 107, 669 (1968); Y. Levin, M. Pecht, L. Goldstein, E. Katchalski, *Biochemistry* 3, 1905 (1964); K. J. Laidler and P. V. Sundaram, in *Chemistry of the Cell Interface*, H. D. Brown, Ed. (Academic Press, New York, 1971), part A.
18. R. Goldman, O. Kedem, E. Katchalski, *Biochemistry* 10, 165 (1971).
19. R. Goldman and E. Katchalski, *J. Theor. Biol.* 32, 243 (1971).
20. S. Friedman, J. D. Jamieson, M. Nakashima, C. L. Friedman, *Science* 130, 1252 (1959); H. D. Portnoy, L. M. Thomas, E. S. Gurdjian, *J. Appl. Physiol.* 17, 175 (1962).
21. J. D. Andrade, *J. Ass. Advan. Med. Instrum.*, in press.
22. G. D. Christian, *Advan. Biomed. Eng. Med. Phys.* 4, 95 (1971).
23. L. C. Clark and C. Lyons, *Ann. N.Y. Acad. Sci.* 102, 29 (1962).
24. S. J. Updike and G. P. Hicks, *Nature* 214, 986 (1967).
25. L. C. Clark, "Membrane polarographic electrode system and method with electrochemical compensation," U.S. Patent No. 3,539,455.
26. D. L. Williams, A. R. Doig, A. Korosi, *Anal. Chem.* 42, 118 (1970).
27. L. B. Wingard, C. C. Liu, N. L. Nagda, *Biotechnol. Bioeng.* 13, 629 (1971).
28. G. G. Guilbault and J. G. Montalvo, *J. Amer. Chem. Soc.* 92, 2533 (1970).
29. G. G. Guilbault, *Pure Appl. Chem.* 25, 727 (1971).
30. ——— and E. Hrabankova, *Anal. Chem.* 42, 1779 (1970).
31. ———, *Anal. Chim. Acta* 56, 285 (1971).
32. G. G. Guilbault and F. R. Shu, *ibid.*, p. 333.
33. J. C. Montalvo, *Anal. Chem.* 41, 2093 (1969); *Anal. Biochem.* 38, 357 (1970).
34. Portions of this work have been supported by NSF grant GK 29382 and Biomedical Sciences support grant FR 07092. We thank our colleagues in the Division of Artificial Organs, the Division of Materials Science and Engineering, and the Department of Biochemistry of the University of Utah for many helpful discussions. We thank D. Rose for interest and support.

ENZYME ELECTRODES

David A. Gough, Research Assistant
Division of Materials Science & Engineering
College of Engineering
University of Utah
Salt Lake City, Utah 84112

Joseph Andrade, Associate Professor
Colleges of Engineering and Pharmary
and
Assistant Research Professor
College of Medicine
University of Utah
Salt Lake City, Utah 84112

There is currently considerable interest in the development of biochemical-specific electrodes that could be used to monitor and regulate the concentrations of biochemicals in body fluids. Some very selective biochemical sensors have been made recently in which conventional solute-specific electrodes are used to monitor reactions catalyzed by immobilized enzymes. These devices can theoretically be made to determine metabolites, enzymes, coenzymes, or enzyme inhibitors, in situ, without special preparation of the sample. Widespread application can be predicted for such electrodes in both experimental and clinical medicine if they can be made to function specifically and accurately, and if they can be used for nondestructive, instantaneous, and continuous determinations in situ. Enzyme electrodes must not promote undesirable physiological responses, such as antigenic responses, thrombosis, or tissue reaction. In addition, they must be inexpensive, easy to operate, and have a long lifetime.

In this article we discuss the development of biochemical-specific electrode systems, present some of the foreseeable problems that might be associated with their use, and review the essential literature.

The basic functional concept of the "enzyme electrode" is the continuous, instantaneous, electrochemical monitoring of enzyme-catalyzed reactions, in which a substrate, coenzyme, or inhibitor is converted into a product by means of an enzyme. The relative concentration of the reactants can be varied so that analytical techniques are obtained in which the reaction rates or equilibrium concentrations are proportional to the limiting components. Electroactive species either produced or consumed by the reaction may be detected by commercial solute-specific electrodes, the signal thus produced being related to the limiting reactant. If a system can be designed such that the enzymes are immobilized or constrained to the immediate vicinity of the electrode-these enzymes being capable of continuous catalysis in complex physiological fluids-a new biochemical-specific electrode is feasible. Obviously, the term "enzyme electrode" is not rigorously accurate because these devices may be made sensitive to substrate, product, enzymic effectors, or enzymes themselves. We prefer to use the term, however, to describe biochemical-specific electrodes that are dependent on immobilized enzymes, until more accurate terms become familiar.

Electrode Characteristics

The most commonly known solute-specific electrode is the glass pH electrode. When referenced against a standard reference electrode, a potential difference is produced which is proportional to the pH of the solution, according to the Nernst equation. Such an electrode may be useful for following enzyme reactions in which hydrogen ions are a product. Their use is limited, however, because most enzyme reactions are not linear over a broad pH range and for accurate results, the reaction media must have a low buffering capacity, the opposite of many physiological fluids.

The composition of the electrode glass may be varied experimentally so that the resultant potential is proportional to the potassium, sodium, ammonium, or other cations in solution. In some other type of specific ion electrodes, ingenious liquid or solid ion exchange membranes are employed. Descriptions of these electrodes and their mechanisms of operation have been discussed in detail (1,2). Of the more than 20 specific ion electrodes available commercially, only those sensitive to species participating in enzymic reactions will be useful in this application. The electrodes that will be of most immediate use are those specific for pH, ammonium, and other monovalent cations (3), and cyanide (4). A phosphate-specific electrode has been reported (5), but does not appear to be adequately selective or reporducible.

The electrodes now available are not generally completely selective for the desired species. For example, if the enzyme reaction produces NH_4^+ which is to be measured, the electrode may respond not only to NH_4^+, but also to Na^+, and other cations in solution, as well as pH. This effect may be eliminated by referencing against another cation electrode, which cannot respond to the NH_4^+ formed from the reaction because of diffusional or flow effects, but responds to everything else. By determining electronically the difference between the two, a signal that is only proportional to the NH_4^+ produced by the enzyme reaction will be obtained.

Truly continuous measurements can be made only when the signal-bearing species is continuously removed or converted by the electrode, such as in polarographic or amperometric systems. Most ion-selective electrodes are potentiometric, however.

The response of specific ion electrodes has been discussed else-where (1). Ideally, specific ion electrodes provide a linear Nernstian response of 0.059 volt at 25°C per decimal change in activity of monovalent cation over a certain range of concentration. Response times are on the order of seconds or less for most electrodes, making electrode kinetics a minimal concern.

Polarographic measurements are made by measuring a change in current as a function of changing potential between two inert metal electrodes, and are useful for detecting several species in solution that have a characteristic plateau at a known potential. Although polarography itself may not be very useful to the system of interest, constant potential polarography, or amperometry (in which the current is proportional to a certain species reduced or oxidized at a fixed potential), has application. This is the basis for the operation of the well-known Clark pO_2 electrode (6), wherein oxygen diffuses thru a gas-permeable polymer membrane and is reduced at a platinum electrode which is kept at a fixed potential with respect to a silver-silver chloride reference electrode. Response time is on the order of seconds when membranes highly permeable to oxygen are used.

It is also possible to use metal electrodes in the form of an analytical fuel cell, the short circuit current being proportional to the biochemical substrate. The effect of interfering species may be minimized by selective membranes. Relatively high currents may be obtained by efficient electrochemical coupling.

The pCO_2 electrode is also a well-known clinical tool (7). The basis of this electrode is diffusion of carbon dioxide through a gas-permeable polymer membrane into an internal aqueous solution of fixed bicarbonate concentration. The carbon dioxide is hydrated to carbonic acid in a slower, rate-determining step, then rapidly ionized to bicarbonate and hydrogen ion. This causes a change in the pH of the internal solution, as determined by a potentiometric pH electrode. This electrode has some limitations for enzyme electrode applications. It responds only to carbon dioxide, while the product of many enzyme reactions is bicarbonate. The response time may also be too long for many applications. Membranes of higher permeability, and possibly membranes with enzymatic activity, may significantly reduce the response time of this electrode.

Metal electrodes have been used to measure enzymatic oxidation-reduction reactions in which the oxidation state of a coenzyme or intermediate compound is directly changed at the electrode (8). Such systems will be operable if precautions are taken to prevent excessive adsorption or interference when the metal electrodes are placed in multicomponent systems.

Immobilized Enzymes

Numerous methods of enzyme immobilization have been reported in the literature (9-11). Several techniques are useful in the design of electrodes. The enzyme can be entrapped within a synthetic hydro-philic gel, cross-links can be formed between the molecules of the enzyme to make membranes, the enzyme can be chemically bound to membranes or other surfaces, the enzyme can be copolymerized with other enzymes or proteins, or the enzyme can be physically entrapped between membranes. Other techniques are available and may be useful for certain design requirements. Acidic or basic groups may be polymerized in the supporting polymer matrix in which the enzyme is immobilized in such a way that the pH in the immediate vicinity of the enzyme is optimum, while that of the bulk solution is different. Such techniques can optimize kinetics and possibly make an otherwise inoperable system workable. The method of immobilization will depend on the particular enzyme electrode system.

Some enzyme reactions may require the immobilization of substrates or coenzymes. The high cost of many coenzymes makes prohibitive the simple addition of non-rate limiting excesses to each sample to be measured. Probably the most practical techniques will be the covalent bonding of the coenzyme to a surface in such a way that reaction is still possible, as reported recently (12), or the covalent bonding of the coenzyme directly to the enzyme or other immobilized particle by techniques which permit catalytic action. Containment by a membrane of selective pore size or slow release through a glass frit to which the enzyme is bound may be necessary in some cases.

An important problem is heat inactivation of many enzymes at physiological temperatures. The long-term usefulness of biochemical electrodes will be seriously limited if methods of thermal stabilization cannot be found. One approach to this problem may be the use of only partially purified enzyme extracts, or the enzyme might be mixed with stabilizing species which will not interfere with the reaction. Some immobilization methods are reported to stabilize certain enzymes for periods longer than their lifetimes in vivo (11, 13). However, while perhaps not all enzymes of immediate interest are now capable of being stabilized for performance under the desired conditions, many can be adequately stabilized and current research into new techniques holds much promise (14).

Some enzymes that do not produce electroactive species may be linked to other enzymes in such a way that the product of the first enzyme reaction becomes the substrate for the second enzyme which involves an electroactive participant, thus greatly expanding the number of species that can be monitored. Studies indicate that these systems may be most efficient if the enzymes are mixed in the same phase to avoid unnecessary diffusional effects (15). Such multistep systems show some similarity to processes in vivo.

Although electrodes will operate under equilibrium or steady-state conditions, they must be characterized kinetically in order to determine the range and rate of response. Enzyme kinetics in the liquid phase (where diffusional effects are absent during the initial stages of the reaction) have been well studied. Some studies relating diffusional (10, 16), charge (17), and boundary layer effects (18) to heterogeneous phase enzyme kinetics have been made; product inhibition (18) and two-enzyme systems (19) have also been studied. The data indicate that immobilized enzymes can be characterized kinetically by the turnover number, concentration and Michaelis constant (K_m) of the enzyme, the nature and dimensions of the catalytic layer, the diffusivities of participating species, and the estimated thickness of the boundary layer. Diffusion of substrate through the physiological media may also have a limiting effect. Response of an immobilized enzyme electrode can therefore be predicted.

Many solute-specific electrodes cannot respond to very low concentrations of solute, such as concentrations less than 10^{-6} M. This may limit the feasibility of certain enzyme electrodes since the critical concentrations of some compounds in physiological fluids are quite low. Another important consideration is that electrodes determine activities, not concentrations. In many instances, the clinical significance of activities measured in situ is not known. However, this may lead to some useful investigations.

Applications of enzyme electrodes in flowing systems will require consideration of boundary layer artifacts and streaming potentials. This has been studied with glass electrodes in physiological solutions (20).

The electrode will also have to be designed to avoid any undesirable physiologic responses, such as protein deposition, thrombosis, antigenic reaction, or the formation of a diffusion-resistant tissue capsule around the electrode (21). A hydrophilic biocompatible membrane that excludes compounds of given molecular weight could be placed between the reactive layer and the physiological environment. Such a membrane should result in minimal protein deposition and thrombosis and should prevent species of larger molecular weight from passing while at the same time providing a highly aqueous medium for optimal substrate diffusion.
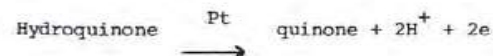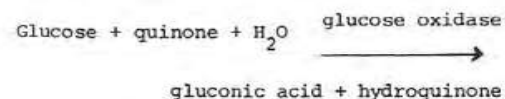
68

Literature

An excellent review of electrochemical methods of monitoring conventional enzymatic reactions has been published (22). In the present article, we describe only self-contained biochemical electrode systems in which the enzyme or substrate has been physically immobilized in the vicinity of the sensor or bonded to it.

Probably the first account of an enzyme electrode was given by Clark and Lyons (23). They obtained potentiometric determination of glucose and proposed that glucose could also be determined amperometrically by means of glucose oxidase immobilized between Cuprophane membranes, according to the equation
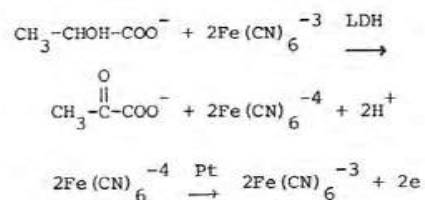
$$\text{Glucose} + O_2 + H_2O \xrightarrow{\text{glucose oxidase}} \text{gluconic acid} + H_2O_2$$

Determinations were made from a solution of low buffering strength. Updike and Hicks (24) introduced the term "enzyme electrode" and made a dual cathode Clark-type oxygen electrode with glucose oxidase immobilized in polyacrylamide gel. The electrode was used to determine glucose from whole blood and plasma, and thus demonstrated the feasibility of measurements being obtained from complex solutions. The response time was approximately 30 seconds. Clark (25) suggested changing the potential across the electrodes so that they would respond to hydrogen peroxide production instead of oxygen uptake, thus reducing the problem of interference from oxygen in solution. Erroneous readings caused by small amounts of catalase or peroxidase found in most enzyme preparations or in physiological solutes can be minimized by suitable membrane-electrode design (25) or by inhibitors. Williams et al (26) replaced oxygen as the hydrogen acceptor with quinone, to monitor glucose according to the following equations

$$\text{Glucose} + \text{quinone} + H_2O \xrightarrow{\text{glucose oxidase}} \text{gluconic acid} + \text{hydroquinone}$$

$$\text{Hydroquinone} \xrightarrow{\text{Pt}} \text{quinone} + 2H^+ + 2e$$

where the reaction potential is 0.4 volt with reference to a standard calomel electrode. Glucose oxidase was held between layers of dialysis paper. The enzyme from *Aspergillus niger* was used because it can
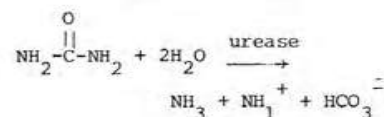
69

utilize quinone as a hydrogen acceptor and does not require other co-
enzymes, as does the enzyme from other sources. Determinations re-
quired the addition of buffer salts and quinone to maintain adequate
pH and prevent the diffusion of quinone out of the enzyme layer. An
electrode to determine lactate was also reported in the same communi-
cation (26), based on the oxidation of lactate by ferricyanide. The
reaction is catalyzed by lactate dehydrogenase (cytochrome b_2, E.C.
1.1.2.3), which does not require nicotinamide adenine dinucleotide
as hydrogen acceptor, according to the following equiations

$$CH_3-CHOH-COO^- + 2Fe(CN)_6^{-3} \xrightarrow{LDH}$$

$$CH_3-\overset{O}{\overset{||}{C}}-COO^- + 2Fe(CN)_6^{-4} + 2H^+$$

$$2Fe(CN)_6^{-4} \xrightarrow{Pt} 2Fe(CN)_6^{-3} + 2e$$

where the reaction potential is 0.4 volt with reference to a standard
calomel electrode. The enzyme was held between dialysis membranes.
Because of the low K_m of this enzyme (K_m = 1.2mM), it was necessary
to dilute the sample with buffered $K_3Fe(CN)_6$. Steady-state measure-
ments were made in 3 to 10 minutes. The authors claimed that this
system demonstrated increased sensitivity over spectral techniques
(26).

Wingard et al. (27) have proposed constant current voltammetry
as a method for evaluation of electrodes containing immobilized
oxidative enzymes as catalysts. This design was originally suggested
as a fuel cell. Bessman and Schultz (13) have used the fuel cell
concept to monitor glucose.

Several enzyme electrodes based on potentiometric cation- and
ammonium-ion specific electrodes have been reported. Guilbault and
Montalvo (28) made a urea transducer by immobilizing urease in a
thin layer of acrylamide gel held over the surface of a cation
electrode by cellophane film. The reaction is

$$NH_2-\overset{O}{\overset{||}{C}}-NH_2 + 2H_2O \xrightarrow{urease}$$

$$NH_3 + NH_1^+ + HCO_3^-$$

The electrode was used for periods of up to 3 weeks at 25°C with no
loss of activity and it responded to urea concentrations from
5×10^{-5} to 1.6×10^{-1}M in tris(hydroxymethyl)aminomethane buffer,
with an optimal response time of approximately 25 seconds. Many
parameters affecting the function of the electrode were characterized
(29). The response was not independent of Na^+ and K^+ ions when the
Na^+ ion concentration was greater than one-half of the urea concen-
tration and the K^+ ion concentration was greater than one-fifth of
the urea concentration, placing limitations on the buffer that could
be used. The enzyme gel layer had to be washed after each determi-
nation, making truly continuous or rapid measurements impossible.
Similar electrodes were evaluated for the determination of urea in
blood and urine (3). The sample was diluted and ion exchange resin
added directly to eliminate cation interference. The electrode
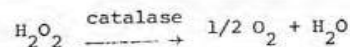showed precision and accuracy comparable with spectral methods.

Electrodes specific for amino acids have been described (30).
L-Amino acid oxidase (L-AAO) was immobilized by several methods at
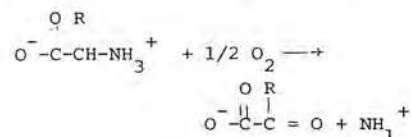the tip of a commercially available cation electrode. The reaction
is

$$O^--\overset{O}{\overset{||}{C}}-\overset{R}{\overset{|}{CH}}-NH_3^+ = H_2O + O_2 \xrightarrow{L-AAO}$$

$$O^--\overset{O}{\overset{||}{C}}-\overset{R}{\overset{|}{C}} = O + NH_1^+ + H_2O_2$$

The further nonenzymatic release of CO_2 by the following equation

$$O^--\overset{O}{\overset{|}{C}}-\overset{R}{\overset{|}{C}} = O + H_2O_2 \leftarrow \rightarrow$$

$$O = \overset{R}{\overset{|}{C}}-O^- + CO_2 + H_2O$$

is prevented by adding a small amount of catalase to the enzyme
layer, which catalyzes the reaction

$$H_2O_2 \xrightarrow{catalase} 1/2\ O_2 + H_2O$$

to give the total reaction

$$O^- -\overset{\overset{\displaystyle O}{\|}}{C}-\overset{\overset{\displaystyle R}{|}}{C}H-NH_3^+ + 1/2\ O_2 \longrightarrow$$

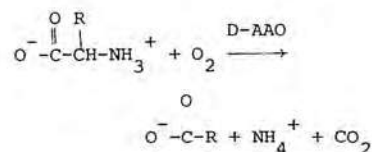$$O^- -\overset{\overset{\displaystyle O}{\|}}{C}-\overset{\overset{\displaystyle R}{|}}{C} = O + NH_1^+$$

The addition of catalase seems to improve the electrode, probably because oxygen is generated, which is necessary for the oxidase reaction. These electrodes were reported to remain stable for about 2 weeks, and showed 1- to 2-minute response times to amino acids in dilute buffer solutions (30).

Electrodes specific for D-amino acids which are catalyzed by D-amino acid oxidase (D-AAO) have been reported (31). The reaction is

$$O^- -\overset{\overset{\displaystyle O}{\|}}{C}-\overset{\overset{\displaystyle R}{|}}{C}H-NH_3^+ + O_2 \xrightarrow{\ D-AAO\ }$$

$$O^- -\overset{\overset{\displaystyle O}{\|}}{C}-R + NH_4^+ + CO_2$$

where the cation is monitored by a potentiometric cation electrode. It was found that stability of the acrylamide enzyme gel or liquid layer could be maintained for 21 days if it were stored in buffered flavine adenine dinucleotide solution, a weakly bound diffusible coenzyme. The response was not increased by high concentrations of ocygen but was dependent on pH. A very similar electrode for asparagine was also reported (31), asparaginase being used as the catalyst. The addition of a coenzyme was not necessary.

A potentiometric electrode for glutamine has been reported and characterized (32). The electrode response was reproducible for up to 8 hours. The catalytic reaction was dependent on pH and inhibited by cations; measurements were made in dilute aqueous solutions.

An interesting approach to the determination of enzyme activity with potentiometric cation electrodes has been reported (33) in which immobilized substrates were used. A liquid layer of urea was passed between the electrode tip and a dialysis membrane in a continuous or interrupted flow process. Urea diffused through the membrane and was catalyzed by urease in dilute aqueous solutions. The ammonium ion produced was detected by the cation electrode. Although this approach probably requires much more study before it can be of significant practical use, it suggests some interesting applications.

An electrode specific for amygdalin based on a solid-state potentiometric cyanide electrode has been reported and characterized (4). β-Glucosidase, immobilized in acrylamide gel, hydrolyzes amygdalin by the following reaction

$$C_6H_5\overset{\overset{\displaystyle |}{}}{C}HCN + H_2O \xrightarrow{\ \beta\text{-glucosidase}\ }$$
$$OC_{12}H_{21}O_{10}$$

$$2C_6H_{12}O_6 + C_6H_5CHO + HCN$$

The lifetime of this electrode is limited by the dissolution of the cyanide-sensing crystal membrane, which is claimed to have a working lifetime of 200 hours (4).

Summary

From the discussion of electrodes and enzymes herein, and from the accounts of enzyme electrodes that have appeared in the literature, clinical determinations of certain metabolites and soluble enzymes by means of enzyme electrodes seem quite feasible. Such devices may be made highly specific by the use of appropriate enzymes and a high degree of accuracy can be obtained. Instantaneous and continuous determinations can be made from physiological fluids, and undesirable physiologic responses can theoretically be minimized, thus making long-term clinical monitoring a possibility. Enzyme electrodes may also have a useful lifetime and meet other practical requirements.

Acknowledgements

References and Notes

(1) G. Eisenman, Ed., *Glass Electrodes for Hydrogen and Other Cations* (Dekker, New York, 1967); R. A. Durst, Ed., *Nat. Bur. Stand. Spec. Publ.* No. 314 (1969).

(2) R. P. Buxk, *Anal. Chem.* 44, 270R (1972).

(3) G. G. Guilbault and E. Hrabankova, *Anal. Chim. Acta* 52, 287 (1970).

(4) G. A. Rechnitz and R. Llenado, *Anal. Chem.* 43, 283 (1971).

(5) G. G. Guilbault and P. J. Brignac, Jr., *Anal. Chim. Acta* 56, 139 (1971).

(6) L. C. Clark, *Trans. Amer. Soc. Artif. Inter. Organs* 2, 41 (1956).

(7) J. W. Severinghaus and A. F. Bradley, *J. Appl. Physiol.* 13, 515 (1958).

(8) L. R. Blinks and R. K. Shaw, *Proc. Nat. Acad. Sci. U.S.A.* 24, 420 (1938).

(9) I. Silman and E. Katchalski, *Annu. Rev. Biochem.* 35, 873 (1966); S. Avrameas, *Immunochemistry* 6, 43 (1969); R. Axen and S. Ernbach, *Eur. J. Biochem.* 18, 351 (1971).

(10) R. Goldman, L. Goldstein, E. Katchalski, in *Biochemical Aspects of Reactions on Solid Supports*, G. R. Stark, Ed. (Academic Press, New York, 1971).

(11) L. B. Wingard, Ed., *Enzyme Engineering* (Interscience, New York, 1972).

(12) M. Weibel, H. H. Weetal, H. Bright, *Biochem. Biophys. Res. Commun.* 44, 347 (1971).

(13) S. Bessman and R. Schultz, personal communication.

(14) *Chem. Eng. News* (3 January 1972), p. 24.

(15) K. Mosbach and B. Mattiasson, *Acta Chem. Scand.* 24, 2093 (1970).

(16) R. Goldman, O. Kedem, I. H. Silman, S. R. Caplan, E. Katchalski, *Biochemistry* 7, 486 (1968); E. Selegny, G. Broun, D. Thomas, *Physiol. Veg.* 9, 25 (1970).

(17) R. Goldman, O. Kedem, E. Katchalski, *Biochemistry* 7, 4518 (1968); W. E. Hornby, M. D. Lilly, E. M. Crook, *Biochem. J.* 107, 669 (1968); Y. Levin, M. Pecht, L. Goldstein, E. Katchalski, *Biochemistry* 3, 1905 (1964); K. J. Laidler and P. V. Sundaram, in *Chemistry of the Cell Interface*, H. D. Brown, Ed., (Academic Press, New York, 1971), part A.

(18) R. Goldman, O. Kedem, E. Katchalski, *Biochemistry* 10, 165 (1971).

(19) R. Goldman and E. Katchalski, *J. Theor. Biol.* 32, 243 (1971).

(20) S. Friedman, J. D. Jamieson, M. Nakashima, C. L. Friedman, *Science* 130, 1252 (1959); H. D. Portnoy, L. M. Thomas, E. S. Gurdjian, *J. Appl. Physiol.* 17, 175 (1962).

(21) J. D. Andrade, *J. Ass. Advan. Med. Instrum.*, in press.

(22) G. D. Christian, *Advan. Biomed. Eng. Med. Phys.* 4, 95 (1971).

(23) L. C. Clark and C. Lyons, *Ann. N.Y. Acad. Sci.* 102, 29 (1962).

(24) S. J. Updike and G. P. Hicks, *Nature* 214, 986 (1967).

(25) L. C. Clark, "Membrane Polarographic Electrode System and Method with Electrochemical Compensation," U.S. Patent No. 3,539,455.

(26) D. L. Williams, A. R. Doig, A. Korosi, *Anal. Chem.* 42, 118 (1970).

(27) L. B. Wingard, C. C. Liu, N. L. Nagda, *Biotechnol. Bioeng.* 13, 629 (1971).

(28) G. G. Guilbault and J. G. Montalvo, *J. Amer. Chem. Soc.* 92, 2533 (1970).

(29) G. G. Guilbault, *Pure Appl. Chem.* 25, 727 (1971).

(30) _____ and E. Hrabankova, *Anal. Chem.* 42, 1779 (1970).

(31) _____, *Anal. Chim. Acta* 56, 285 (1971).

(32) G. G. Guilbault and F. R. Shu, *ibid.*, p. 333.

(33) J. C. Montalvo, *Anal. Chem.* 41, 2093 (1969); *Anal. Biochem.* 38, 357 (1970).

ELECTROCHEMICAL BIOSCIENCE AND BIOENGINEERING

Edited by

Herbert T. Silverman

TRW Incorporated

Redondo Beach, California

Irving F. Miller

University of Illinois

Chicago, Illinois

Alvin J. Salkind

ESB Incorporated

Yardley, Pennsylvania

and

Rutgers Medical School (CMDNJ)

ELECTROCHEMICAL BIOSCIENCE AND BIOENGINEERING

Edited by

Herbert T. Silverman
TRW Incorporated
Redondo Beach, California

Irving F. Miller
University of Illinois
Chicago, Illinois

Alvin J. Salkind
ESB Incorporated
Yardley, Pennsylvania
and
Rutgers Medical School (CMDNJ)

7

The Chemistry of Some Selected Methacrylate Hydrogels

DONALD E. GREGONIS, CHWEN M. CHEN, and JOSEPH D. ANDRADE

Department of Materials Science and Engineering, University of Utah,
Salt Lake City, Utah 84112

Hydrogels have been described as biocompatible materials[1].
Polymers of hydroxyethyl methacrylate (HEMA) are the most studied
synthetic hydrogels [2]. At present, polymers of this material
are widely used in corrective contact lenses [3]; it has been
used as a coating for catheters and other medical devices [4-6].
In our investigations, we wanted to study a variety of hydrophilic
methacrylate polymers to evaluate their biological behavior in
relation to the concentration and type of groups incorporated in-
to the polymer. In order to pursue this goal, a thorough under-
standing of the bulk properties of the hydrogels is required. In
this work the equilibrium water content of the gels is regulated
by varying copolymer ratios. Charged groups are incorporated
into the polymer by copolymerization with acidic or basic meth-
acrylates. The monomers that are being investigated are shown in
Table I. The amount of water in the equilibrated polymers
covered the range from 3.5% to greater than 90% (Table II). For
this study, hydroxyethyl methacrylate was selected as the funda-
mental monomer because of past work and availability.

TABLE I.

Hydrophilic Methacrylate Monomers
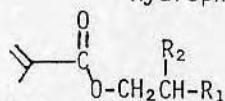
1. R_1 = OH, R_2 = H; hydroxyethyl methacrylate (HEMA).
2. R_1 = OCH_2CH_2OH, R_2 = H; hydroxyethoxyethyl methacrylate(HEEMA).
3. R_1 = $OCH_2CH_2OCH_2CH_2OH$, R_2 = H; hydroxydiethoxyethyl methacryl-
   ate (HDEEMA).
4. R_1 = $-OCH_3$, R_2 = H; methoxyethyl methacrylate (MEMA).
5. R_1 = $OCH_2CH_2OCH_3$, R_2 = H; methoxyethoxyethyl methacrylate
   (MEEMA).
6. R_1 = $OCH_2CH_2OCH_2CH_2OCH_3$, R_2 = H; methoxydiethoxyethyl meth-
   acrylate (MDEEMA).
7. R_1 = CH_2OH, R_2 = OH; 2,3-dihydroxypropyl methacrylate(DHPMA).

TABLE II.
#### Equilibrium Water Swelling of Pure Homopolymers

1.	pHEMA	-	0.40*	5.	pMEEMA	-	0.62
2.	pHEEMA	-	0.80	6.	pMDEEMA	-	>0.90
3.	pHDEEMA	-	>0.90	7.	pDHPMA	-	0.70 to >0.90 (7)
4.	pMEMA	-	0.035				

*Water fraction (W_f) = weight of water in polymer/weight of
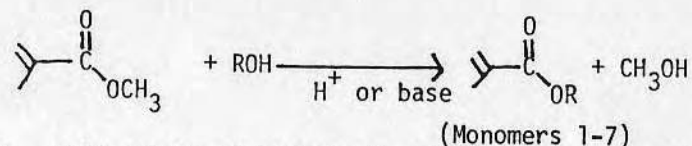hydrated polymer

Monomers (See Table I)

The laboratory synthesis of these monomers is accomplished
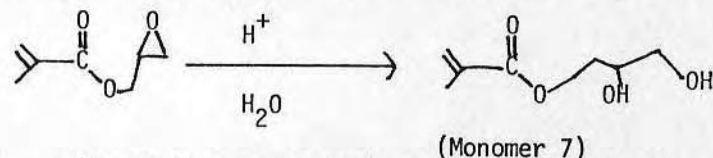by the following classical chemical reactions:
1. Reaction of methacryl chloride with the corresponding
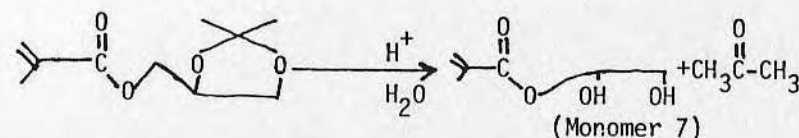alcohol:

(Monomers 1-7)
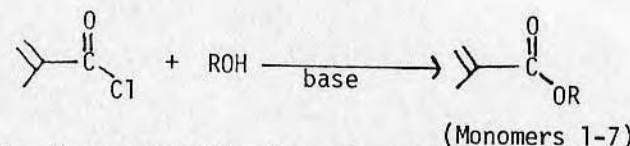
2. Transesterification of methyl methacrylate with the
corresponding alcohol:

(Monomers 1-7)

3. Acid catalyzed hydrolysis of glycidyl methacrylate ([7]):

(Monomer 7)

4. Acid catalyzed hydrolysis of isopropylidineglyceryl
methacrylate ([8-9]).

(Monomer 7)

the use of water or alcohols as solvents. The anionic initiators are organometallic compounds, such as n-butyl lithium, or strong bases, such as lithium t-butoxide. Although there are disadvantages to these initiators, they are used to polymerize methacrylates in a wide range of tacticities from chains having high syndiotactic triads to chains having high isotactic triads. Our group is investigating such polymers to determine the effect of tacticity on the properties of the hydrogels (21).

For certain studies soluble polymers were required (22). Radical polymerization of the methacrylate system without solvent gives a polymer that swells to a high degree in good solvents, but does not dissolve. It is felt that some crosslinking of the polymer occurs by radical chain transfer mechanisms (23). Soluble methacrylate polymers may be obtained with a radical initiator at high dilutions of the monomer. We routinely polymerize the monomers in ethanol (1:10,v/v). These solutions have been used for solvent casting (24) and gel coatings (22).

Preparation of Gel Membranes

Gel membranes were required for our diffusion studies (13) and were used for our work on water swelling of gels. Polymerization of the monomer was initiated by azobis (methyl isobutyrate) using the same concentration used for the polymerization of bulk gels, 7.84 micromoles per milliliter of monomer. This ratio is independent of water concentration. All gel modifiers and crosslinking agents are expressed as molar quantities in terms of the monomer volume. The membranes were prepared by polymerization of the monomer solution between flat plates using a silicone rubber spacer to regulate thickness. The polymerization conditions were standarized at 60°C for 24 hr. At low water concentrations (W_f <0.20), polyethylene or polypropylene mold plates are used; at higher water concentrations, glass plates are used. This is because gels polymerized at low water concentration adhere strongly to the glass surface. Polymerization of membranes on a glass surface is prefered since it has a more uniform surface. The thickness of the gel membranes is 0.75 mm unless otherwise stated.

Synthesis and Polymerization of C^{14}-labeled HEMA

To determine the relative stability of the methacrylate gels in various media, C^{14}-labeled HEMA was synthesized by reacting methacryl chloride and 1,2-C^{14}-ethylene glycol, using excess carrier ethylene glycol to prevent the formation of excessive amounts of C^{14}-labeled diester (ethylene glycol dimethacrylate). The C^{14}-HEMA was purified utilizing the "salting out" technique described earlier. The product was diluted with carrier HEMA and was then distilled by micro-vacuum techniques. The distillate was determined to have a specific activity of 9.1×10^5 dpm/ml.

To check the radioisotopic purity, a 1 ml aliquot was chromatographed on 100g Grade II alumina. The column was eluted with a linear gradient from 100% petroleum ether (250ml) to 5% methanol in diethyl ether (250ml). The radioactivity eluted in one peak. the fractions were combined and evaporated. The product exhibited an identical infra-red spectrum to control HEMA.

To initiate the polymerization of C^{14}-HEMA, azobis(methyl isobutyrate) was added (7.84 micromole/ml). The monomer was polymerized in a polypropylene mold. The mold dimensions were 50mm x 50mm x 1mm. The standard polymerization conditions were 60°C for 24 hours unless otherwise noted. After this time the mold was cooled to 0°C, and the C^{14}-pHEMA was removed and weighed. The C^{14}-pHEMA was then placed in various solvents at 37°C. Aliquots were removed at various time intervals and counted using liquid scintillation techniques. The amount of radioactivity found in the solvent was calculated as a percentage of the overall radioactivity in the polymer. Figure 3 shows the percent radioactivity extracted with time for some typical gels. Gels 1 and 2 are duplicates. Gel 6 was polymerized under identical conditions but was extracted with 95% ethanol. Gel 9 was polymerized with 45% water and extracted with water. The radioactivity of all gels extracted with water leveled out after one day, but the radioactivity extracted with ethanol (Gel 6) appeared to increase after this time at about 0.5%/week. Table IV provides a complete list of the C^{14}-HEMA polymerization conditions, extraction solvents, and the percent radioactivity extracted. The percent radioactivity extracted was calculated as the average of the isotope found in solution at points in time from 4 days to 5 weeks.

TABLE IV.
Elution of Radioactivity from C^{14}-pHEMA Gels
Equilibrated in Various Solvents

| Gel#	Polymerization Conditions	Solvent	% Radioactivity in Solvent after 5 wks.
1	24 hours @ 60°C	Distilled H_2O	4.7% ± 0.13
2	24 hours @ 60°C	Distilled H_2O	4.8% ± 0.08
3	24 hours @ 60°C	Human Reference Serum	3.6% ± 0.27
4	3 1/2 hours @ 60°C	Distilled H_2O	4.8% ± 0.14
5	66 hours @ 60°C	Distilled H_2O	2.6% ± 0.41
6	24 hours @ 60°C	95% Ethanol	9.1% ± 0.90
7	24 hours @ 60°C (Gel contained 1% unlabeled EGDMA)	Distilled H_2O	2.9% ± 0.30
8	24 hours @ 60°C (Gel contained 5% unlabeled EGDMA)	Distilled H_2O	2.3% ± 0.11
9	24 hours @ 60°C (Gel contained 45% H_2O v/v)	Distilled H_2O	1.7% ± 0.09
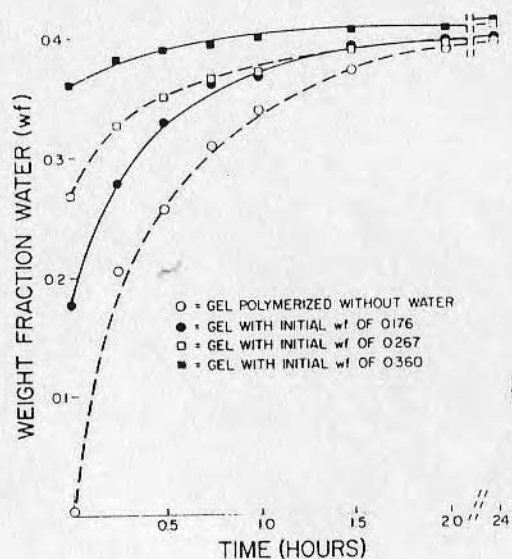
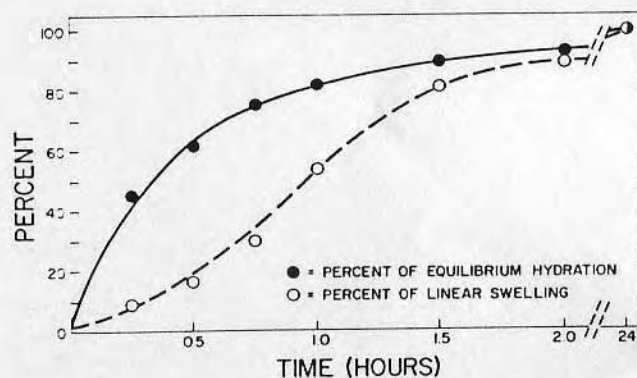Figure 4.   Water uptake of pHEMA polymerized
at different water contents

Figure 5.   Percent equilibrium hydration (0.40 w_f = 100%)
and percent equilibrium linear swelling (1.165 l_s = 100%)
plotted vs. time for pHEMA gel

Similar results are observed by Refojo for pHEMA and other gels (25). Absence of linear swelling at low water fractions is observed by us in an alternative experiment with pHEMA gels. HEMA was polymerized at various water concentrations and then allowed to equilibrate in distilled water (Figure 7). It is found that when HEMA is polymerized with a water fraction (W_f) of 0.1 or less (W_f of 0.1 is 25% of the equilibrium W_f), the gel still swells to the same degree as an anhydrous pHEMA gel.

These results indicate that there is free volume or "voids" in the hydrogels, and this volume is filled with water molecules before the gel is able to exhibit any linear expansion. This concept has been used to explain the swelling and mechanical behavior of β-keratin (26) and other biopolymers (27). Similar studies on other hydrophilic gels are in progress.

Copolymers

In order to obtain gels that would swell in water a specified amount, copolymers of the hydrophilic monomers were investigated. At the same time the water solubility of the comonomers was also studied. It was hoped that monomer solubility behavior would be useful to explain some aspects of swelling of the polymer. Figure 8 shows HEMA-MEMA comonomers and copolymers and their relationship to solubility and swelling in water. Water has a maximum solubility of 3.5% (v/v) in MEMA monomers. HEMA monomer is infinitely soluble in water. The comonomer solutions exhibit a water solubility that increases slightly as the amount of HEMA is increased up to 40% MEMA-60% HEMA. At that point the water solubility increases greatly until 20% MEMA-80% HEMA where the comonomers become infinitely soluble. The copolymers of MEMA-HEMA appear to have a linear water fraction (W_f) relationship from 0.035 water for pure pMEMA to 0.40 for pure pHEMA.

Figure 9 shows the relationship between MEEMA-HEMA and water solubility and between their copolymers and the degree of swelling in water. In this case, MEEMA monomer dissolves only about 8% water and as HEMA monomer is added, the amount of water that it dissolves increases sharply. Near a 60:40 HEMA:MEEMA ratio, water becomes infinitely soluble in the comonomers. The water swelling of the copolymers show the opposite relationship. pMEEMA swells to 63% H_2O, and as increasing amounts of HEMA are incorporated in the copolymer, the degree of swelling decreases until a 40% H_2O uptake is reached for pHEMA.

These above results indicate that the hydrophilicity of the monomer and the degree of crosslinking of the polymer (28) are not the only factors that determine the degree of water swelling of the polymer. In the methacrylate system, we have rationalized that the length of the ester chain is a third factor that should be taken into account when discussing swelling. This is probably due to the fact that the long ester functionality decreases the packing energy of the methacrylate polymer.
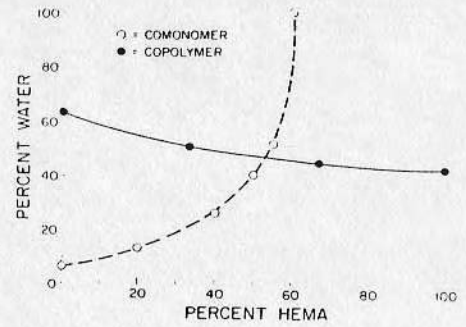
Figure 9. Water solubility of MEEMA–HEMA comonomers (v/v) and the equilibrium water weight fraction, w_f, of MEEMA–HEMA copolymers
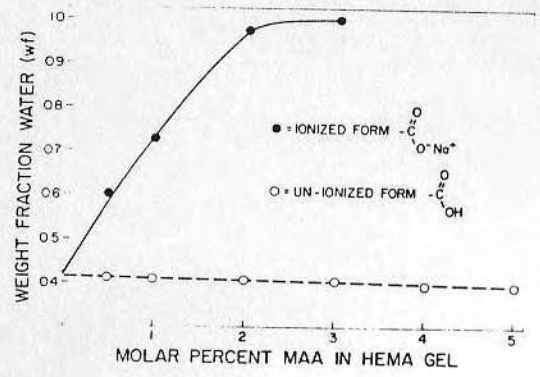

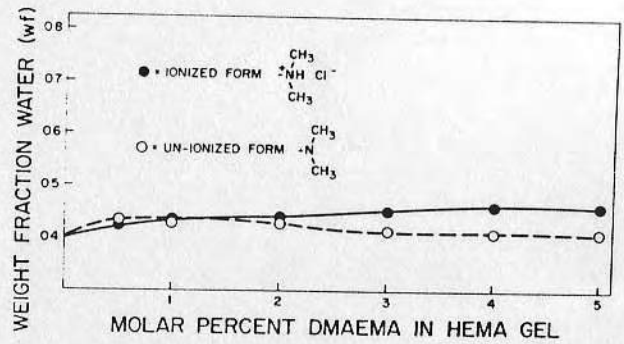*Figure 10. Equilibrium water weight fraction, w_f, of HEMA–MAA copolymers*

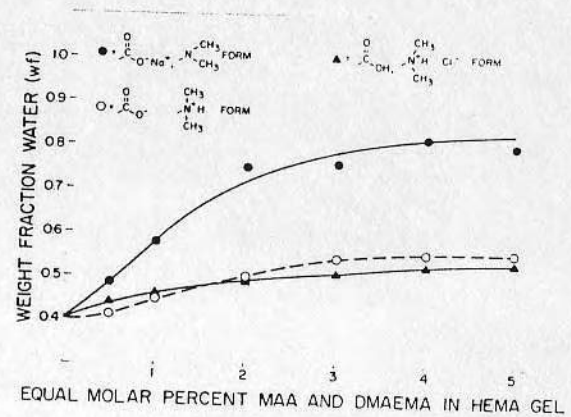*Figure 11. Equilibrium water weight fraction, w_f, of HEMA–DMAEMA copolymers*

EQUAL MOLAR PERCENT MAA AND DMAEMA IN HEMA GEL

Figure 12. Equilibrium water weight fraction, w_f, of HEMA–MAA–DMAEMA terpolymers. MAA and DMAEMA are polymerized at equal molar concentrations.

33.   Shalati, M. D. and Scott, R. M., Macromolecules, (1975) **8**, 127.

34.   Alfrey, M. D., Overberger, C. G., and Penner, S. H., J. Am. Chem. Soc., (1953) 75, 4221.

WETTABILITY OF POLYMERS AND HYDROGELS AS DETERMINED
BY WILHELMY PLATE TECHNIQUE

D.E. Gregonis*+, R. Hsu+, D.E. Buerger*, L.M. Smith*,
and J.D. Andrade*+†

*Department of Materials Science and Engineering,
+Department of Pharmaceutics, and
†Department of Bioengineering, University
of Utah, Salt Lake City, Utah 84112

ABSTRACT

Polymers and hydrogel surfaces are investigated by contact angle procedures. A comparison between underwater captive air bubble contact angles and advancing and receding water contact angles using the Wilhelmy plate technique are studied using a sequence of hydrophobic to hydrophilic model polymers. The underwater captive bubble contact angle correlates most closely with the water Wilhelmy plate receding contact angle in most of the polymer systems. Contact angle hysteresis is found in all but the most wettable of the polymers but no exact trends are found. Alkyl derivatized agarose surfaces are also studied by the Wilhelmy plate procedure; although these surfaces exhibit strong protein interactions, little change in advancing and receding contact angle is observed with increasing degree of alkyl group derivatization.

KEYWORDS

Wilhelmy plate; contact angle; hydrophilicity; contact angle hysteresis; surface wettability; alkyl agarose surfaces; polymer surfaces.

INTRODUCTION

The study of the interface between an aqueous solution and a polymer surface is of considerable interest for the investigation of biological interactions. Contact angle methods are one of the few techniques capable of measuring the polymer-water interface directly. Contact angles are determined primarily by the outermost exposed atoms, possibly the outer 10 Å of a surface (Johnson, 1969). The hydrogel-water interface, however, is more diffuse than that of a hydrophobic polymer interface and the transition region between the bulk gel and free water may be on the order of 100 Å or greater in thickness. Our previous contact angle studies have utilized the underwater air and octane captive technique in order to analyze the fully hydrated polymer surface (Andrade, 1979a, 1979b). Several drawbacks of this technique include the length of time for measurements and the difficulty to obtain reproducible angles on very hydrophilic surfaces. In addition, the captive bubble measurement provides only the static contact angle, and thus dynamic contact angles, which may offer further information about the interface, are not available.

The Wilhelmy plate technique (Wilhelmy, 1863) eliminates many of these difficulties.

Advancing and receding dynamic and static angles are easily obtained by this technique and are recorded on chart paper for permanent records. The first part of this Wilhelmy plate study correlates angles obtained with this technique and that obtained from underwater captive air bubble procedures. Poly(hydroxyethyl methacrylate) [PHEMA] and poly(methyl methacrylate) [PMMA] copolymers are used for this study. The second part of the study investigates advancing and receding angles obtained in a sequence of hydrophilic-hydrophobic triblock copolymers. These polymers were prepared by hydroboration of the butadiene block of styrene-butadiene-styrene (S-B-S) radial triblock systems. The last series of materials that were investigated consists of alkyl derivatized agarose surfaces. The alkyl agaroses bind quite strongly some proteins from an aqueous environment depending upon the size of alkyl group and the degree of group substitution and the hydrophobic character of the protein. These materials in bead form are commonly used in hydrophobic chromatography separation technique (Shatiel, 1974).

MATERIALS AND METHODS

The Wilhelmy plate apparatus incorporates a Scotts SRE500 mechanical testing machine and is used to raise and lower a beaker of 2X distilled water at a controlled speed of approximately 40 mm per minute. Situated above the beaker is a Cahn model RM-2 electrobalance which supports the test sample on a small thread. The balance is mounted separately and is vibrationally isolated. The mechanical tester and balance are contained in an insulated enclosure maintained at constant temperature (20°C) and humidity (30% RH). Electrical signals from the balance and cross head are fed to a X-Y recorder to obtain the wetting traces. Calibration of the balance is performed by the addition of a 200 mg tare weight to the sample. Other studies describe the measurement and equipment in more detail (Johnson, 1969; Smith, 1981). The captive bubble technique as performed in this work is also described elsewhere (Andrade, 1979; King, 1981).

The use of pure water in these experiments, especially when hydrating the samples for long periods of time, is very important. Water used for the wetting measurements and hydration studies found in this report is first deionized by passing it through a mixed ion exchange resin bed (Continental Water) and then distilled from a Barnsted Model YD 302 pyrogen removing still. The water is distilled a second time from an all glass system in which a small amount of potassium permanganate is added to degrade any organic substituents. The water is tested and shown to be free of pyrogens by the limulus lysate test and absent of bacteria. To this water was then added sodium azide (200 mg/l) and chlorox (30 µl/l, 1.5 ppm Cl final concentration) to prevent micro-organism recontamination. The surface tension of water is measured to be 72.6 ± 0.2 dynes/cm at 20°C using completely wetting glass microscope coverslip which was cleaned in chromic acid followed by a two minute helium radiofrequency glow discharge treatment at 200 µm Hg at 30 watts. In equation 1, θ is set equal to zero, and γ, the surface tension of water is thus calculated. For polymer hydration studies, chromic acid cleaned, all glass Coplin jars are used to store the samples.

The polymers to be studied are dip cast onto 24 x 50 mm microscope coverslips which are washed and cleaned to remove particulates and organic contaminants. The coatings are in the 1-3 micron range in thickness. Optical microscopy is used to verify surface uniformity. Polymer solutions (3% wt/vol) are filtered through 0.2 µ Fluoropore filters (Millipore Corp.) and stored in particulate free brown glass bottles. To improve polymer adhesion to the glass, silane treatments are sometimes required. A vapor phase silanization treatment, similar to that described by Haller (1978) is used. γ-Aminopropyl triethoxysilane (Aldrich Chemical) is used for the HEMA-MMA copolymer coatings and n-pentyl triethoxysilane (Petrarch Chemical) is used for the modified S-B-S triblock polymers. Agarose surfaces are deposited onto silanized clean glass coverslips. Copolymerization data for the HEMA-

MMA material is shown in Table I. Purified HEMA was donated by Hydro-Med Sciences and MMA was obtained from Aldrich Chemical Company. Copolymerization of HEMA and MMA has been shown to produce a random copolymer with a slight tendency for alternating addition (Patel, 1981; Okano, 1976).

TABLE 1 Hydroxyethyl Methacrylate (HEMA) - Methyl Methacrylate (MMA) Copolymerization Data

Copolymers (mole ratio)	Polymerization Solvent	Precipitation Solvent	Degree of Conversion
100% MMA	toluene	60-90 pet ether	34
99% MMA-1% HEMA	toluene	60-90 pet ether	44
95% MMA-5% HEMA	90% toluene - 10% ETOH	60-90 pet ether	48
75% MMA-25% HEMA	50% THF - 50% ETOH	H_2O	46
50% MMA-50% HEMA	50% THF - 50% ETOH	H_2O	44
25% MMA-75% HEMA	50% THF - 50% ETOH	H_2O	23
5% MMA-95% HEMA	ETOH	Diethyl ether	83
1% MMA-99% HEMA	ETOH	Diethyl ether	85
100% HEMA	MeOH	Diethyl ether	--

The Solprene radial S-B-S triblock copolymers were donated by Phillips Chemical Company. The styrene and butadiene homopolymers were obtained from Aldrich Chemical Company. Syndiotactic 1,2-butadiene polymer was obtained as a gift from Uniroyal Chemical Company. Characterization data of these materials is shown on Table 2. Proton nuclear magnetic resonance characterization to determine the amount and configuration of styrene and butadiene is measured on a Varian SC-300, 300 MHz instrument. Molecular weights are measured by gel permeation chromatography using μ styragel columns (Waters Associates) with nominal pore sizes of 5×10^2, 10^3, 10^4 and 10^5 Å. Tetrahydrofuran is used as the eluent and the column set was calibrated using narrow MWD polystyrene standards (Pressure Chemical). The butadiene segment of the S-B-S triblock copolymers is selectively hydroxylated using the hydroboration reagent, 9-borobicyclo [3.3.1] nonane, (9-BBN), in tetrahydrofuran. This borane is used to prevent crosslinking during the reaction which occurs when multi-reactive boranes are used (Levesque, 1971). Proton nuclear magnetic resonance shows the reaction to proceed in a quantative fashion. The polybutadiene double bonds in these polymers exist in both a cis and trans geometry with some 1,2 butadiene segments (Table 2). The hydroboration addition is non-specific for the addition across the cis or trans double bond, but adds in an anti-Markovnikov manner (Brown, 1959) (Fig. 1) to the pendant 1,2-polybutadiene segments to produce primary hydroxyl groups. It is interesting to note that the equilibrium water swelling of the hydroxylated butadiene homopolymers is greatest for the 1,2 butadiene polymer, intermediate in the cis-trans polybutadiene and lowest in the cis-polybutadiene (Table 3) and may suggest a difference in hydroboration addition between the pure cis and cis-trans polybutadiene. Also shown in Table 3 are the water contact angles obtained from 24 hour water equilibrated samples. The water content of the polymer is calculated from the weight of water in the hydrated sample multiplied by one hundred (Gregonis, 1976).

The polysaccharide agarose is a naturally occurring polymer isolated from red seaweed. It consists of a repeating 1,3 linked β-D-galactopyranose and a 1,4 linked 3,6 anhydro-α-L-galactopyranose structure as shown in Fig. 2. This polysaccharide aggregates upon cooling from an aqueous solution and produces a high water content gel with surprisingly strong mechanical properties. The agarose used in this work is obtained as uncrosslinked Sepharose 4B-200 beads (Sigma Chemical Co).

TABLE 2 Styrene-Butadiene-Styrene (S-B-S) Triblock Copolymer Analysis

Copolymer	Wt% Styrene	Butadiene Configuration %			$M_w \times 10^{-5}$	$M_n \times 10^{-5}$
		Cis	Trans	1,2-		
styrene	100	--	--	--	8.72	1.83
solprene K	77	39.7	45.5	4.8	2.31	0.23
solprene 481	48	41.7	53.1	5.2	7.23	2.64
solprene 414	40	40.8	47.3	11.9	1.70	1.39
solprene 416	30	38.4	54.5	6.1	4.79	1.15
solprene 422	20	40.5	46.5	13.0	4.43	1.65
cis, trans-butadiene	0	39.3	51.4	9.3	6.87	1.36
cis-butadiene	0	99	--	1	7.15	1.45
syndio-1,2-butadiene	0	--	--	93	1.14	0.46
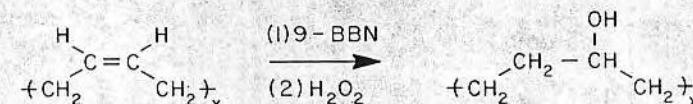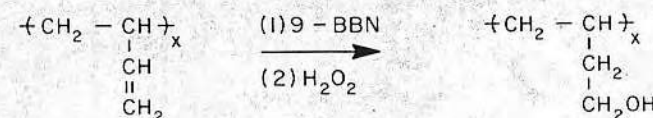
Fig. 1 Hydroxylation of olefin containing polymers by hydroboration procedures (9-BBN = 9-borobicyclo [3.3.1] nonane).

Agarose has been selectively derivatized to provide hydrophobic alkyl groups covalently linked to the polysaccharide and is used as a selective protein separation technique called hydrophobic chromatography (Svinivasen, 1980; Ochoa, 1978). Three general methods are commonly used for this derivatization procedure (Hjerten, 1974; Bethell, 1979; Cuatrecasas; 1970) but all of these procedures use or produce covalently crosslinked gels. Thus, they may be used in the configuration in which they were derivatized, but are not able to be redissolved for coating surfaces or devices. We have developed an alternate derivatization procedure which overcomes this disadvantage. In addition, our procedure provides easily prepared

radioisotopically labeled alkyl groups for measurement of the degree of derivatization. This derivatization procedure is shown in Fig. 3

TABLE 3 Hydroborated Styrene-Butadiene-Styrene (SBS) Copolymer Data

Copolymer	Wt% Styrene	% Equil. Water	Captive Air Bubble θ	Advancing θ	Receding θ	Hysteresis advθ-recθ
styrene	100	< 1	87.8±1.3	93.8±2.8	67.1± 2.9	26.7
solprene K	77	3.3±0.4	34.3±2.3	81.6±7.4	16.6± 4.6	65.0
solprene 481	48	12.1±0.4	24.8±1.5	77.4±0.8	19.7± 1.8	57.7
solprene 414	40	12.4±0.3	-------	80.5±1.2	11.8±10.2	68.7
solprene 416	30	14.0±0.6	20.4±3.4	79.3±0.8	22.3± 0.7	57.0
solprene 422	20	14.6±0.6	22.9±1.6	78.3±0.8	19.9± 2.4	58.4
cis, trans-butadiene	0	17.5±0.4	23.4±3.6	87.9±2.1	16.7± 1.4	71.2
cis-butadiene	0	11.7±0.6	25.3±2.4	86.3±1.7	22.4± 0.8	63.6
syndio, 1,2-butadiene	0	19.6±0.3	23.5±4.4	83.3±1.4	17.8± 0.5	65.5
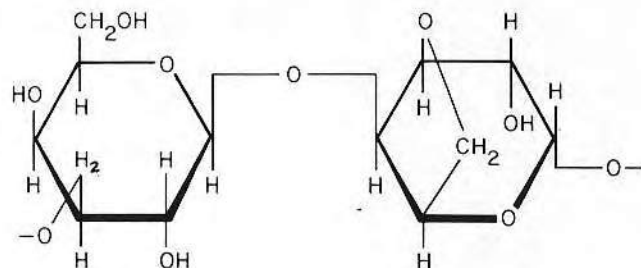
Fig. 2. Repeating sub-unit of agarose.

The key development of this reaction procedure was finding the aqueous agarose beads can be exchanged with an aprotic solvent (acetone) without changing the agarose structure. After derivatization, the beads are then re-exchanged with water for use as hydrophobic column supports or dried and then redissolved in dimethyl sulfoxide for use in solution coatings. The agarose loses its ability to redissolve in water after low amounts of alkyl group derivatization. The alkyl group-agarose bond is determined to be stable in a distilled water environment for over three months. The agarose in this study was derivatized with varying amounts of n-butyl or n-dodecyl groups. The degree of derivatization is determined by liquid scintillation procedures. The agarose beads are first digested in hydrogen peroxide-perchloric acid solution and then counted in Biofluor cocktail (New England Nuclear). The degree of derivatization is reported as μmoles alkyl group per ml packed beads. A value of 15 μmoles alkyl group per ml packed gel corresponds approximately to 0.1 moles alkyl residues per mole anhydrodisaccharide repeat unit.
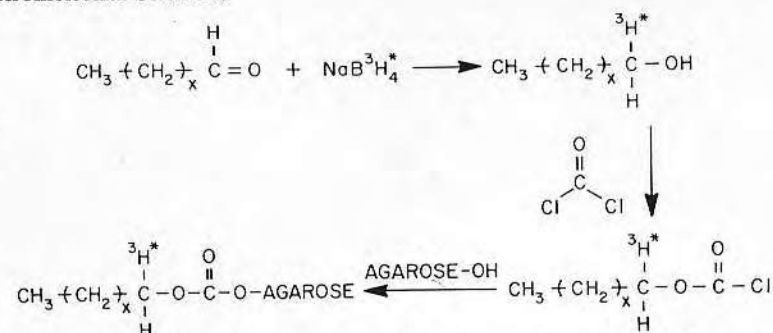
Fig. 3. Preparation and covalent bonding of α-tritiated alcohols to agarose.

DISCUSSION AND RESULTS

Contact angles may be measured by several techniques (Johnson, 1969). In this study a comparison between the underwater captive air bubble contact angle (Fig. 4) and the Wilhelmy plate method (Fig. 5) is investigated using the HEMA-MMA copolymers. In general, the angle which the water makes with the surface can be measured directly with both the captive bubble and the Wilhelmy plate technique. This is done with the captive bubble contact angle method, using a horizontal microscope and measuring drop dimensions (King, 1981), but with the Wilhelmy plate apparatus it is most convenient to measure the force on the slide as it is immersed and withdrawn from the water. The advancing and receding angles are calculated from straight line extrapolations of the advancing and receding buoyancy slopes at zero depth of immersion (Smith, 1981). By this procedure the buoyancy factor in Eq. 1 can be eliminated

$$\cos \theta = \frac{mg}{p\gamma} + \frac{V\rho g}{p\gamma}$$ [1]

where $\frac{V\rho g}{p\gamma}$ = buoyance factor

m = mass of slide as measured with electrobalance
g = local gravitational force (979.3 dynes/g)
p = perimeter of the slide (cm)
γ = surface tension of wetting liquid (water = 72.6 ± 0.2 dynes/cm at 20°C)
V = volume of immersed sample at a particular depth
ρ = density of wetting liquid (water = 0.998 g/cc at 20°C)

The angle determined from both these methods is related to interfacial energetics via the Young equation:

$$\gamma_{sa} = \gamma_{sw} + \gamma_{wa} \cos \theta$$ [2]

where γ_{sa} = solid-air interfacial free energy
γ_{sw} = solid-water interfacial free energy
γ_{wa} = water-air interfacial free energy
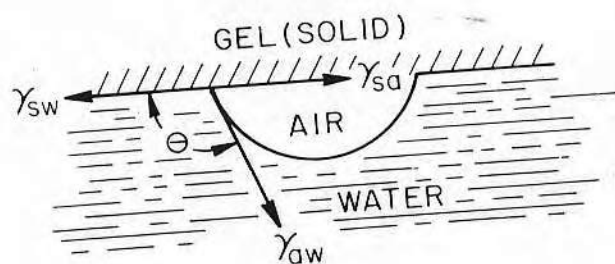θ = angle of contact measured through the water phase (Fig. 4)

Fig. 4. Captive underwater air bubble contact angle measurement. γ_{sw}, γ_{aw}, and γ_{sa} represent the solid-water, air-water and solid-air interfacial free energies.
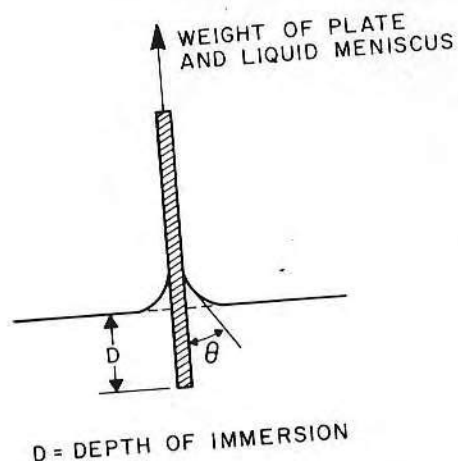

D = DEPTH OF IMMERSION

Fig. 5. Wilhelmy plate technique for contact angle determinations.

The advancing and receding of the water across the polymer surface appears to involve different mechanisms. This can be observed in the roughness of the advancing angle trace in comparison to the smooth receding angle trace with the Wilhelmy plate technique for poly(hydroxyethyl methacrylate) surface (Fig. 6). The advancing angle roughness is caused by non-uniform movement of the water over the surface. The water advance involves a rapid zipper-like action from a point of initiation and then stops and repeats the process after the advancing angle reached a certain critical angle. The receding angle measurement is smooth as a result of even, uniform movement of the water across the polymer surface.
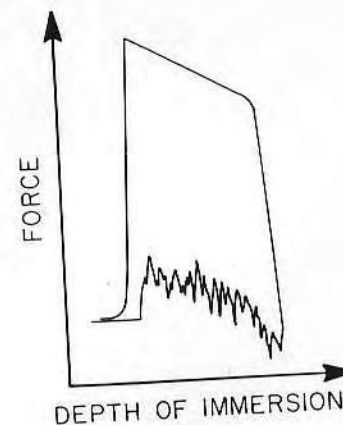
Fig. 6. Wilhelmy plate measurement of poly(hydroxyethyl methacrylate) [PHEMA] surface.

The large amount of roughness in the advancing angle measurement is not found in all polymer surfaces. In the HEMA-MMA copolymers, the advancing angle measurement roughness is minimized at 25 mole % and higher MMA content and the water advancing roughness as shown in Fig. 6 may be considered the exception rather than the rule. This advancing angle roughness is also observed in some of the alkyl derivatized agarose materials, but only at a specific range of derivatization. The roughness advancing angle measurement is observed in the HEMA materials even after prolonged hydration times but is lost from the agarose surface measurements after hydration.

METHYL METHACRYLATE-HYDROXYETHYL METHACRYLATE COPOLYMERS

The captive bubble and Wilhelmy plate contact angles were measured on surfaces prepared from the same polymer lot. At least three surfaces of the same lot were measured. The Wilhelmy plate measurements were recorded at various times of hydration, zero time, three hour hydration, 24 hour hydration and after vacuum redrying. These measurements were recorded as dynamic measurements by immersing the plate and removing it from the water at a speed of 40 mm per minute. At several points in both the advancing and receding mode of the 24 hour hydrated sample, the plate was stopped for 15 seconds. The points from the trace were then extrapolated to zero depth of immersion to obtain the static advancing and receding angle. As the depth of immersion increases, both the advancing angle decreases and the receding angle increases, both slightly; but in some cases, no change is observed between the static and dynamic contact angles. The captive air bubble measurements were measured only after 24 hour hydration times. These values are shown in Table 4.

From this study, one finds the captive air bubble angles closely follows, but is slightly higher, than the receding contact angle. It is closer to the static receding angle than the dynamic receding angle and equals this value on the 100% HEMA surface. The dynamic angle measurements always exhibit more hysteresis than the static angle measurements except for the very high HEMA content surfaces where dynamic and static angles are equal. The 24 hour hydrated contact angles are shown

in Fig. 7, along with the equilibrium water content of these copolymers which is essentially linear in regard to the HEMA-MMA mole ratio, ranging from 40% water for the pure HEMA polymer to less than 1% for the MMA polymer. Contact angle hysteresis, the difference between the advancing and receding angle, generally increase with higher HEMA content of the surface, but there are some exceptions. The advancing contact angle exhibits a minimum value at near the 50:50 copolymer ratio; however, the receding angle decreases as the HEMA content of the copolymer increases. As a function of hydration time, the receding angle shows a decrease, whereas the advancing contact angle in general remains constant, or decreases only to a very small extent.

TABLE 4   Comparison of Contact Angles as Determined by Wilhelmy Plate
and Captive Underwater Air Bubble Measurements on
HEMA-MMA Copolymer Surfaces

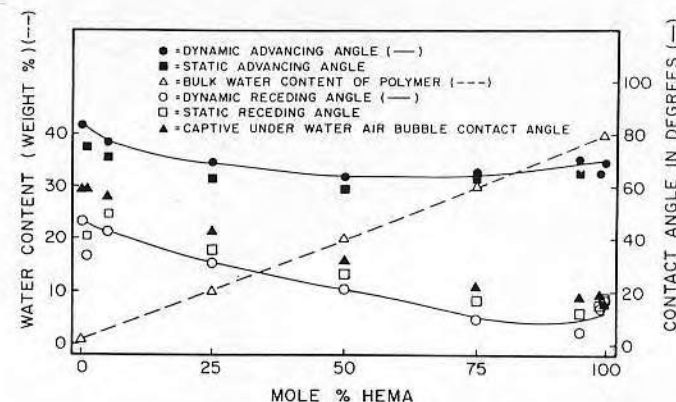| Mole % Copolymer	Angles 0 Time	Angles 3 hr. Hyd.	Angles 24 hr. Hyd.	24 hr Hyd. Hyst.	24 hr Hyd. Static Angle	Vacuum Redry	24 hr Hyd. Captive Air Bubbles
100-PMMA	θadv 82.5±1.1	83.7±1.6	83.8±2.2	36°	--	85.2±2.3	59±2
	θrec 55.8±0.2	49.1±0.9	47.8±1.0		--	50.7±1.7	
99-MMA, 1-HEMA	θadv 83.4±2.3	80.4±4.5	82.7±2.6	49.9	74.9±1.7	80.4±4.0	59±1
	θrec 54.8±1.1	51.3±2.0	33.8±1.7		40.9±2.9	48.0±1.3	
95-MMA, 5-HEMA	θadv 80.0±1.7	74.9±2.8	76.6±2.0	32.9	70.6±1.4	76.6±1.0	56±4
	θrec 51.5±1.7	45.2±1.8	43.7±1.0		49.7±1.7	50.5±0.5	
75-MMA, 25-HEMA	θadv 73.6±7.4	70.8±0.8	69.9±1.0	38.9	63.0±1.1	72.3±2.3	43±2
	θrec 40.5±0.2	31.9±0.7	31.0±3.1		36.3±2.2	37.7±2.1	
50-MMA, 50-HEMA	θadv 69.1±1.2	64.3±0.7	63.8±0.4	43.2	58.9±0.4	66.6±0.3	32±1
	θrec 28.1±2.0	20.6±1.0	20.6±1.0		26.6±0.7	28.2±1.5	
25 HEMA, 75 HEMA	θadv 65.8±1.4	65.0±1.4	65.9±1.0	56.1	63.8±1.1	71.0±5.7	22±1
	θrec 15.3±0.0	11.6±1.9	9.8±2.7		17.4±2.1	23.8±5.5	
5-MMA, 95-HEMA	θadv 69.7±1.8	72.6±1.5	70.5±3.8	66.0	65.8±4.6	73.9±1.5	18±2
	θrec 13.2±4.1	5.9±3.0	4.0±4.7		12.5±3.0	20.0±1.0	
1-MMA, 99-HEMA	θadv 68.6±0.8	74.5±2.0	65.3±5.2	49.5	65.3±5.3	71.2±0.4	19±2
	θrec 16.8±1.3	10.5±1.9	15.8±3.4		15.8±3.4	14.4±1.5	
100-HEMA	θadv 70.6±0.8	70.8±3.1	69.7±5.0	52.9	69.7±5.0	74.9±1.7	15±1
	θrec 27.0±1.4	13.3±3.4	16.8±1.3		16.8±1.3	13.2±4.1	

hyd. = hydration
hyst. = hysteresis or θadv-θrec

Fig. 7. Contact angle measurements at 24 hour hydration of methyl methacrylate [MMA] and hydroxyethyl methacrylate [MMA] copolymers using both captive air bubble and Wilhelmy plate technique. Also shown is equilibrium water content measurements of the copolymers.

HYDROPHOBIC-HYDROPHILIC-HYDROPHOBIC TRIBLOCK COPOLYMERS

The styrene-hydroxylated butadiene-styrene triblock polymer as with the underivatized polymer exists in domains due to the incompatibility of the polymer blocks (Paul, 1978). All of the polymers were solvent cast from dimethyl formamide except for polystyrene which is cast from toluene. The equilibrium bulk water content and the contact angle results on these polymer systems are shown in Table 3 and Fig. 8. As observed with the HEMA-MMA copolymer study, the captive air bubble underwater contact angle closely corresponds with the dynamic receding contact angle; however, the styrene homopolymer exhibits an anomalous point to this trend with the captive bubble angle nearer to the dynamic advancing angle. This is the only surface we observed where this is found. The receding angle, in contrast to the HEMA-MMA surfaces, does not correspond well with the bulk water content of the polymers. The bulk water content increases almost linearly with butadiene content of the polymer, but the receding contact angle decreases sharply with a small content of hydroborated butadiene and then remains constant as the butadiene content is increased. This may suggest that the underwater surface of all the block polymers is dominated by the hydroborated polybutadiene matrix. The dynamic advancing angle shows a minimum in contact angle at an intermediate butadiene content with both extremes, the polystyrene and hydroborated polybutadiene, having the highest advancing contact angles. The butadiene homopolymer data shown on Fig. 8 is obtained from the hydroborated cis, trans-configuration polymer; however, the contact angle change little from the other hydroborated butadiene configuration.

ALKYL DERIVATIZED AGAROSE SURFACES

n-Butyl or n-dodecyl alkyl groups are covalently bonded to the agarose as shown in Fig. 3. Details of this work along with protein interaction studies will be published elsewhere. The underivatized agarose dissolves in hot water but after a small amount of alkyl group coupling (6.8 μmoles butyl per ml packed gel) it is
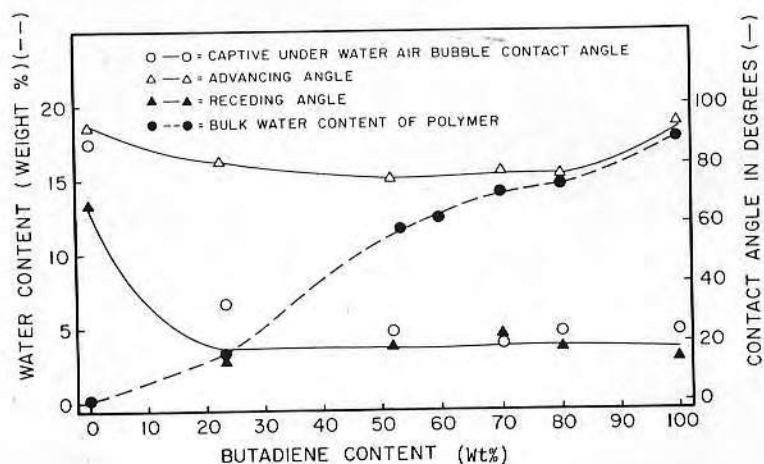
Fig. 8. Contact angle measurements at 24 hr hydration and equilibrium water content of styrene-hydroxylated butadiene-styrene triblock copolymers

no longer water soluble. All the materials are readily soluble in dimethyl sulfoxide (DMSO). After solution casting onto clean glass coverslips, the surfaces are dried in vacuum. The agarose beads contain about 95% water before and after derivatization, but the bulk water content of all the gels decreases substantially when cast and dried from DMSO. For example, the butyl derivatives and the native agarose swell to about 65% water, but the dodecyl derivatives swelling to a lesser amount, and the 60.5 µmoles/ml dodecyl agarose only swells to 43% water (Table 5). For the few agarose materials able to be cast from water, a difference is shown between the water cast and DMSO cast agarose surfaces and their corresponding contact angles.

The first measurement of the advancing angle on the dried agarose surfaces is surprisingly hydrophobic but if the slide is immediately redipped to again measure its advancing angle, the angle is changed considerably and immediately becomes more hydrophilic. These hydrated advancing angles become more difficult to measure because the extrapolated line to zero depth of immersion is many times non-linear (Fig. 9) due to rapid loss or absorption of water by the gel. Calculation of the second advancing angle as shown in Fig. 9 is in many cases not realistic. The advancing and receding contact angles of the dry agarose surface as a function of degree of derivatization is shown in Fig. 10. The contact angle measurements are shown not to be sensitive to small amounts of alkyl derivatization in the high water content gels. The 24 hour hydration data is even more difficult to interpret. The butyl agarose becomes more hydrophobic and generally exhibits larger contact angles as the degree of derivatization increases, as expected. The n-dodecyl agarose, however, shows a decrease in contact angle, in other words, the surface becomes more hydrophilic as the alkyl substitution increases. These samples have been repeated and the same trends have been observed. n-Hexyl and n-octyl derivatized agarose are presently being prepared to help clarify these results.

TABLE 5 Equilibrium Water Content and Contact Angle Data for Alkyl Derivatized Agarose Surfaces

Material	Casting Solvent	Degree of Derivatization µmol/ml	Equilibrium Water Content	Dry Surfaces		24 hr. hydrated Surfaces	
				θ Adv	θ Rec	θ Adv	θ Rec
agarose	H₂O	0	—	46.4±3.0	7.7± 1.4	0	0
agarose	DMSO	0	64	68.8±1.8	18.0± 6.5	10.8± 0.5	10.8± 0.5
n-butyl agarose	H₂O	3.9	—	102.2±3.0	9.7± 1.0	82.2± 1.2	8.9± 2.5
n-butyl agarose	DMSO	3.9	61	83.1±1.9	17.6±10.0	8.7±10.3	8.7±10.3
n-butyl agarose	H₂O	6.8	—	117.2±2.7	8.3± 2.2	85.2±5.3	10.1± 9.0
n-butyl agarose	DMSO	6.8	64	109.5±3.3	18.2± 3.1	36.0±3.0	24.6± 5.0
n-butyl agarose	DMSO	13.0	66	98.1±3.1	28.5± 3.1	64.8±6.2	29.9± 5.9
n-butyl agarose	DMSO	19.1	64	92.8±2.5	31.0± 4.0	61.1±3.0	25.6± 2.6
n-butyl agarose	DMSO	31.1	59	92.0±2.4	37.0± 1.9	—	26.2± 7.2
n-dodecyl agarose	DMSO	7.9	60	96.1±1.8	29.5± 1.0	34.6±4.0	34.6± 4.0
n-dodecyl agarose	DMSO	16.1	55	99.2±5.3	26.3± 2.4	27.3±2.0	27.3± 2.0
n-dodecyl agarose	DMSO	38.2	45	100.8±1.9	24.3± 2.4	21.2±4.0	21.2± 4.0
n-dodecyl agarose	DMSO	60.5	43	104.0±1.9	21.3± 3.1	17.8±3.3	17.8± 3.3

SUMMARY AND CONCLUSIONS

Contact angles are extremely useful measurements to determine surface energetics. The receding angle as measured by Wilhelmy plate procedures most closely approximates the underwater captive air bubble angle and correlates to the bulk water content of the systems studied. The receding angle is much more difficult to interpret and the random and block copolymers exhibit minimum angles at the intermediate (∿ 50-50) copolymer ratios. In the higher water content gels, contact angle induced surface deformation (Andrade, 1979b) may complicate the analysis. Contact angle hysteresis is observed in all but the most hydrophilic polymers studied. Surface roughness is not the cause in the surfaces studied and it has been shown that roughness is not a serious cause of hysteresis if the rugosities are less than 0.5 µ (Johnson, 1969). The hysteresis may be due to surface chemical heterogeneity (Johnson, 1964, 1979; Penn, 1980a) In the HEMA-MMA copolymers, static contact angle hysteresis is usually less than the dynamic contact angle

hysteresis. The angles between the static contact angles in a short time frame
(15 sec.) are unchanging provided that solvent evaporation is taken into account
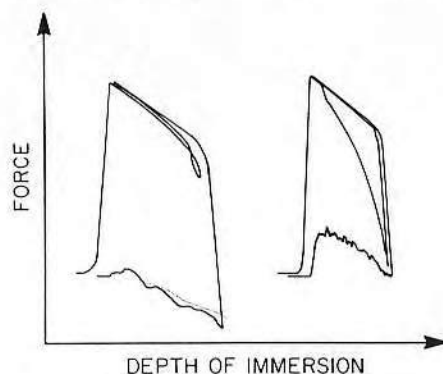and may be due to most stable or metastable intermediate states (Penn, 1980b).

Fig. 9. Wilhelmy plate measurements of agarose surfaces. The surface is
initially dry and exhibits a relatively hydrophobic advancing angle. Upon
re-immersion, the advancing angle becomes more hydrophilic and in many cases
produce non-equilibrium angles which are not readily calculated.
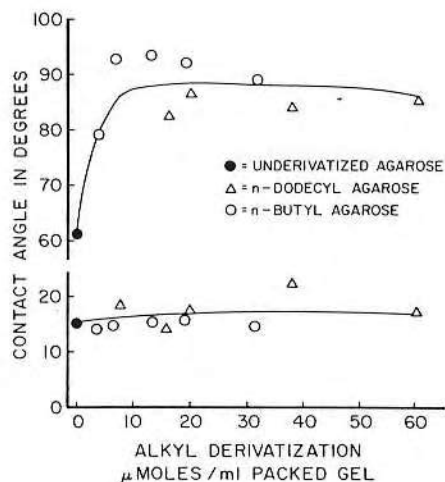
Fig. 10. Advancing (upper line) and receding (lower line) angles
n-alkyl derivatized agarose surfaces.

REFERENCES

Andrade, J.D., R.N. King, D.E. Gregonis, and D.L. Coleman (1979) *J. Polym. Sci.*,
    Polymer Symposium 66, 313-336.
Andrade, J.D., S.M. Ma, R.N. King, and D.E. Gregonis (1979) *J. Colloid Interface
    Sci.*, 72, 488-494.
Bethell, G.S., J.S. Ayers, W.S. Hancock and M.T.W. Hearn (1979) *J. Biol. Chem.*,
    254, 2572-2574.
Brown, H.C. and B.C. Subba Rao (1959) *J. Am. Chem. Soc.*, 78, 5694-5695.
Cuatrecasas, P. (1970) *J. Biol. Chem.*, 245, 3059-3065.
Gregonis, D.E., C.M. Chen and J.D. Andrade (1976) in *Hydrogels for Medical and
    Related Applications*, J.D. Andrade, Ed., ACS Symposium Series 31, American Chem-
    ical Society, Washington, D.C., 88-104.
Haller, I. (1978) *J. Am. Chem. Soc.*, 78, 8050-8055.
Hjerten, S., J. Rosengren and S. Pahlman (1974) *J. Chromat.*, 101, 281-288.
Johnson, R.E. and R.H. Dettre (1964) *J. Phys. Chem.*, 63, 1744.
Johnson, R.E. and R.H. Dettre (1969) in *Surface and Colloid Science*, Vol. 2,
    E. Matijevic, Ed., Wiley-Interscience, New York, 85-153.
King, R.N., J.D. Andrade, S.M. Ma, D.E. Gregonis, and L.R. Brostrom (1981) *J.
    Colloid Interface Sci.*, accepted for publication.
Levesque, G. and C. Pinazzi (1971) *Bull. Soc. Chim. France*, 3, 1008-1010.
Ochoa, J.-L. (1978) *Biochimie*, 60, 1-15.
Okano, T., J. Aoyagi, and I. Sinohara (1976) *Nippon Kagaku Kaishi*, 1, 161-165.
Patel, K. and W.H. Snyder (1981) *Polymer Preprints*, 22, 217-218.
Paul, D.R. and S. Newman (1978) *Polymer Blends*, Vol. 1, Academic Press, New York.
Penn, L.S. and B. Miller (1980) *J. Colloid Interface Sci.*, 77, 574-576.
Penn, L.S. and B. Miller (1980) *J. Colloid Interface Sci.*, 78, 238-241.
Shaltiel, S. (1974) *Meth. Enzymol.*, 34, 126-140.
Smith, L.M., J.D. Andrade, T. Doyle, and D.E. Gregonis (1981) *J. Appl. Polym. Sci.*,
    accepted for publication.
Srinivasan, R. and E. Ruckenstein (1980) *Separation and Purification Methods*, 9,
    267-370.
Wilhelmy, L. (1863) *Ann. Physik*, 119, 177.

Macromolecular Solutions
Solvent-Property
Relationships in Polymers

Edited by
Raymond B. Seymour
University of Southern Mississippi
G. Allan Stahl
Phillips Petroleum Company

HYDROPHOBIC HYDROGELS: PHYSICAL CHARACTERISTICS AND BLOOD INTERACTIONS.

D.E. Gregonis*, D.L. Coleman*, R. Hsu*, and D. Buerger*, Departments of
Materials Science and Engineering*, and Pharmaceutics*, University of Utah,
Salt Lake City, Utah 84112

INTRODUCTION

The nature of the interaction between blood and polymer is not complete-
ly understood. Platelet adhesion to the surface may initiate a series of bio-
chemical reactions which results in the formation of thrombus. A preliminary
event which occurs before platelet deposition is the adsorption of plasma
proteins at the blood-polymer interface. The amount, type, and orientation of
the adsorbed protein is felt to determine the overall compatibility or incom-
patibility of a polymer when interfaced with blood.

This study attempts to clarify the role protein adsorption plays in
blood-materials interactions by utilizing a model polymer system which shows
minimal protein adsorption at physiological conditions. This polymer is then
modified by various means to allow for selective protein interactions.

The polymer used in this study is the naturally occurring polysaccharide,
agarose which is obtained from Pharmacia Fine Chemicals as uncrosslinked
Sepharose[TM] 4B-200 beads. Agarose is commonly used in biochemistry for the
gel permeation chromatographic separations of protein molecules. From these
studies, the non-adsorptive nature of agarose is well documented [1]. The
overall objective of this work is to utilize the surface characteristics
exhibited by these modified polymers showing superior blood-materials inter-
actions, and engineer these properties into other more applied polymers to
improve their blood compatibility.

In this study we describe the modification of agarose with n-alkyl
groups and investigate how these hydrophobic interactions between protein and
polymer influence overall blood interactions.

EXPERIMENTAL

Although several methods are described in the literature for the deriva-
tization of agarose [2,3,4] for hydrophobic chromatographic separations, all
of these methods require the use or produce crosslinked gels. Since most of
the conventional in vitro and in vivo blood testing procedures utilize fabri-
cated surfaces, we investigated alternate procedures for alkyl derivatization
of agarose which does not produce crosslinking so the beads can be redis-
solved for use in solution casting of surfaces.

It has previously been shown that agarose beads in water can freely be
exchanged with certain organic solvents without changing their physical char-
acteristics [5]. In this study, the Sepharose 4B-200 was exchanged with
acetone to allow for greater flexibility in derivatization procedures with
the use of an aprotic solvent. Residual water concentration of the acetone
exchanged agarose was monitored by a modified Karl Fisher titration method
[6]. The agarose-acetone suspension was then allow to react with various n-
alkyl chloroformates to couple the alkyl group to the agarose via a carbon-
ate linkage as shown in Figure 1. The alkyl group is tritium labeled to aid
in the quantitation of the derivatization. The derivatized agarose is then
sequentially exchanged with water.

The carbonate linkage produced in this reaction using n-butyl chloro-
formate is stable at pH of three and higher for at least 24 hours at r.t.,
but is slightly less stable in base showing low level alkyl carbonate clea-
vage at pH of 9. Derivatized alkyl-agarose samples have been stored in dis-
tilled water at 5°C for over six months with no appreciable leakage of alkyl
group.

Protein adsorption to the agarose beads are determined by two methods: 1) A column chromatographic procedure; and 2) A stirred batch adsorption procedure. For the chromatographic procedure, the derivatized agarose is packed in a 5 ml glass column containing phosphate buffered saline (PBS). Serum (50 μl) is injected on the column and UV adsorbance flow through cell is used to monitor the eluant. The proteins which are not adsorbed are eluted with PBS; the adsorbed proteins are eluted with PBS containing 50% v/v glycerol. These fractions are characterized by gradient polyacrylamide gel electrophoresis using silver stain detection methods [7]. In the stirred batch adsorption experiment, the derivatized agarose is mixed in excess serum and washed extensively with BPS until no protein can be detected in the wash. The bound proteins are then desorbed with a 50% glycerol-50% PBS solution and again characterized by the electrophoresis procedures.

Although no protein is found to be adsorbed to the underivatized agarose, albumin starts to bind to the gel at relatively low degrees of derivatization, ~ 20 μmole alkyl group per ml packed gel. Albumin is tightly bound at derivatization levels above ~ 60 μmole/ml packed gel and other proteins as γ-globulin now start to adsorb.

Uncrosslinked agarose exhibits the characteristic of dissolution in hot water and gelatin in water below 40°C. The alkyl derivatized agarose materials are no longer water soluble at low degrees of derivatization due to the internal hydrophobic forces, but dissolve readily in dimethyl sulfoxide. Surfaces are cast from this solvent and characterized primarily by advancing-receding water contact angles to measure surface energetics and ESCA (X-ray photoelectron spectroscopy) to measure surface elemental composition.

The contact angle analysis of underivatized agarose [8] show low angles with minimal contact angle hysteresis indicating the surfaces are highly wetting. The surfaces for both the n-butyl and n-dodecyl agarose derivatized at various degree of substitution become more hydrophobic, as expected, with increasing amounts of alkyl group to a level of ~ 60 μmole alkyl group per ml of packed gel after which the contact angles become relatively constant at 80-90°C advancing and 30-40° receding angles (Figure 2).

ESCA analysis show the derivatized agarose surfaces to contain only carbon and oxygen, thus, free of other elemental contamination (ESCA does not detect hydrogen) with increasing amounts of carbon in relation to oxygen at increased derivatization values. The carbon spectra is broken down into alkyl, ether, and carbonate carbon oxidation states and correlates closely with bulk derivatization analysis.

The initial blood testing on the derivatized agarose surfaces has consisted primarily of normalized whole blood clotting time studies [9]. These tests show prolonged clotting times on agarose surfaces derivatized with both n-butyl and n-dodecyl groups above 200 μmole/ml packed gel and below 25 μmol/ml packed gel derivatization levels. The intermediate derivatized surfaces show a decrease in clotting time with a minimum value occurring about 50 μmol/ml packed gel. Future work includes additional in vitro blood studies and correlations between agarose beads and agarose surfaces of protein adsorption.

ACKNOWLEDGEMENTS

REFERENCES

1. "Gel Filtration-Theory and Practice" published by Pharmacia Fine Chemical, April 1979, Uppsala, Sweden.

2. S.C. March, I. Parikh and P. Coatrecasas, Anal. Biochem., 60, 149 (1974).

3. S. Hjerten, J. Chromatogr., 87, 325 (1973).

4. G.S. Bethell, J.S. Ayers, S.W. Hancock, and M.T.W. Hearn, J. Biol. Chem., 254, 2572 (1979).

5. T.C.J. Gribnau, C.A.G. Van Eekelen, C. Stumm, and G.I. Tesser, J. Chromatogr., 132, 519 (1977).

6. E. Scholz, Fresenius Z. Annl. Chem., 309, 30 (1981).

7. D.W. Sammons, L.D. Adams, and E.E. Hishizawa, Electrophoresis, 2, 135 (1981).

8. D.E. Gregnois, R. Hsu, D.E. Buerger, L.M. Smith, and J.D. Andrade, in "Macromolecular Solutions," R.B. Seymour and G.A. Stahl, eds., Pergamon Press, 1982, pp 120-133.

9. D.L. Coleman, D.E. Gregonis, and J.D. Andrade. J. Biomed. Materials Res., 16, 381 (1982).

$$CH_3 + CH_2 +_x \overset{H}{\underset{\,}{C}} = O \ + \ NaB^3H_4^* \longrightarrow CH_3 + CH_2 +_x \overset{^3H^*}{\underset{H}{C}} - OH$$

$$CH_3 + CH_2 +_x \overset{^3H^*}{\underset{H}{C}} - O - \overset{O}{\underset{\,}{C}} - O - AGAROSE \xleftarrow{\text{AGAROSE-OH}} CH_3 + CH_2 +_x \overset{^3H^*}{\underset{H}{C}} - O - \overset{O}{\underset{\,}{C}} - Cl$$
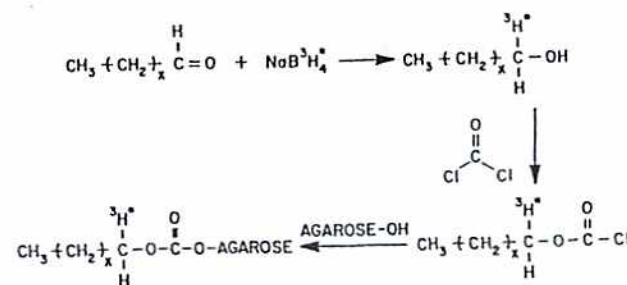
Figure 1.   Preparation and covalent bonding of α-tritiated alcohols to agarose.
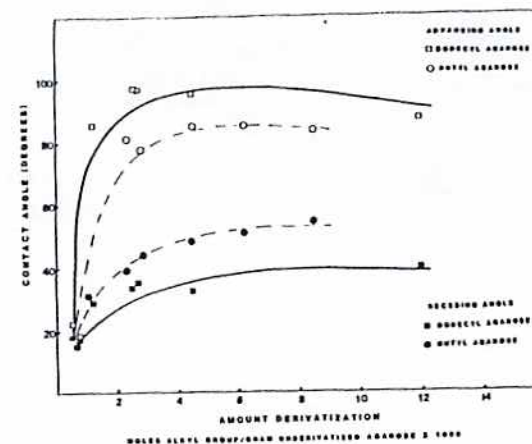
Figure 2.   Advancing-receding contact angles of alkyl derivatized
agarose surfaces hydrated four hours in distilled water.
A derivatization value of 3×10^{-3} moles alkyl group per
gram underivatized agarose corresponds to a degree of
substitution of one alkyl group per each anhydrodisac-
charide repeat unit of agarose.

646

29

SURFACES WITH MINIMAL OR SELECTIVE PROTEIN ADSORPTION INTERACTIONS AS MODEL BIOMEDICAL POLYMERS

D.E. GREGONIS, R.A. van WAGENEN, D.L. COLEMAN and J.D. ANDRADE

INTRODUCTION

The amount, type, conformation and orientation of proteins that adsorb at an interface during the first minutes of blood exposure are felt to dominate the blood compatibility response of that surface. This study attempts to clarify the role protein adsorption plays in blood-materials interactions by utilising model polymer systems which show minimal protein adsorption at physiological ionic strength and pH. One of these surfaces is then derivatised by various means to allow for selective protein interactions. Blood-materials investigations can then be studied as a function of protein interactions with this substrate.

This study utilises two different materials: agarose and poly(ethylene glycol), PEG. Purified agarose is known to be generally a non-protein adsorbing surface, at least when used as a high (>90%) water content gel for biochemical separations by size exclusion chromatography (Hjerten, 1983). Agarose has also been derivatised with various chain lengths and amounts of alkyl groups to be used in a procedure referred to as hydrophobic chromatography (Hjerten, 1973; March et al., 1974; Bethell et al., 1979) which separates biomolecules by their hydrophobic character. Thus, agarose appears to be an interesting model substrate to investigate the role protein adsorption plays in blood-materials interactions.

Covalently bound PEG surfaces were tested for protein adsorption because of the indication in the literature that PEG minimises protein adsorption (Merrill et al., 1982; Mori et al., 1982). In our studies we find PEG grafted surfaces to be superior even to the agarose surfaces for this purpose.

EXPERIMENTAL

Materials Preparation

The agarose used in this study is obtained from Pharmacia Fine Chemicals as uncrosslinked Sepharose 4B-200 beads. Although several methods are described in the literature for the derivatisation of agarose (Hjerten, 1973; March et al., 1974; Bethell et al., 1979), all these methods require the use of or produce crosslinked gels. Since most of the conventional in vitro and in vivo blood testing procedures utilise fabricated smooth surfaces, we investigated alternative procedures for alkyl derivatisation of agarose which do not produce crosslinking so the beads can be redissolved for use in solvent casting of surfaces.

It has previously been shown that agarose beads in water can freely be exchanged in certain organic solvents without changing their physical characteristics (Gribnau et al., 1977). In this study, the Sepharose 4B-200 beads were exchanged with acetone to allow for greater flexibility in derivatisation procedures with the use of an aprotic solvent. The agarose-acetone suspension was then allowed to react with various alkyl chloroformates to couple the alkyl groups to the agarose via a carbonate linkage. The alkyl group is tritium labelled to aid in quantification of derivatisation. The derivatised agarose is then sequentially exchanged with water.

Uncrosslinked agarose exhibits the characteristic of dissolution in hot water and gelation in water below 40°C. The alkyl derivatised agarose materials are no longer water soluble at low degrees of derivatisation due to internal hydrophobic forces, but dissolve readily in dimethyl sulphoxide. Surfaces are cast from this solvent.

PEG materials are readily available in a wide variety of molecular weight fractions (Bailey and Koleske, 1979). The PEG molecule is depicted as:

$$HO \ (CH_2CH_2-O)_x H$$
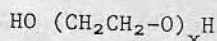
Relatively easy modification of the terminal hydroxyl group(s) results in chemical activation of the PEG molecule. A method used in this report reacts PEG with excess phosgene to produce PEG bis-chloroformates. Quartz substrates are modified by vapour phase reaction of γ-aminopropyltriethoxysilane (APS) (Haller, 1978). The APS procedure incorporates reactive amino groups at the quartz surface. The APS quartz is then immersed in a 5% solution of PEG bis-chloroformate in an inert (aprotic) solvent such as methylene chloride. After 2 hours, the quartz is removed from reaction, washed extensively with water and absolute alcohol and then dried at room temperature in vacuum.

Materials Characterisation

The resultant surfaces are characterised by advancing-receding water contact angles using the Wilhelmy plate procedure, X-ray photo-electron spectroscopy (ESCA) using a Hewlett-Packard 5950B instrument and optical microscopy. The contact angle measurements on agarose and derivatised agarose have previously been reported (Gregonis et al., 1982). Low wetting angles are observed with underivatised agarose with minimal contact angle hysteresis indicating that the surfaces are highly wetting. The surfaces of alkyl (n-butyl and n-dodecyl) agarose derivatised to various degrees of substitution become more hydrophobic with increasing amounts of alkyl group to a level of ∿60 μmol alkyl group per ml of packed agarose gel, after which the angles become relatively constant at 80°-90° advancing and 30°-40° receding angle. The PEG coupled surfaces show very little contact angle hysteresis (40° advancing, 30° receding) with little change of the angle with molecular weight of the PEG.

ESCA analysis shows the derivatised agarose surfaces to contain only carbon and oxygen, thus to be free of other elemental contamination (ESCA does not detect hydrogen) with increasing amounts of alkyl-type carbon in relation to oxygen at increasing derivatisation values. The carbon spectra are broken down into alkyl, ether and carbonate carbon oxidation states and show close correlation with bulk derivatisation analysis. The PEG grafted surfaces possess greater amounts of ether carbon at the surface with increasing molecular weight of PEG, as expected. Optical microscopy shows the surfaces to be homogeneous and particulate free.

PROTEIN ADSORPTION STUDIES

Protein adsorption to flat surfaces is monitored with the total internal reflectance intrinsic fluorescence (TIRIF) technique (van Wagenen et al., 1982). The intrinsic fluorescence of tryptophan-containing proteins, excited at 280 nm, is measured at the interface bead columns measuring ratios of unbound protein fractions (eluted with pH 7.4 phosphate buffered saline) and bound protein fractions (eluted with a hydrophobic buffer of 50:50 phosphate buffered saline:glycerol containing 1% n-butanol).

Protein adsorption to flat surfaces is monitored with the total internal reflectance intrinsic fluorescence (TIRIF) technique (Van Wagenen et al., 1982). The intrinsic fluorescence of tryptophan-containing proteins, excited at 280 nm, is measured at the interface using total internal reflectance of the excitation light. The evanescent wave which decays across the interface excites the tryptophans. The emitted fluorescence (320-350 nm) is collected as a function of time. The adsorbed proteins are measured as the increase in fluorescence intensity at 320-350 nm after exposure of the

surface to various proteins or serum and then flushing with phosphate buffered saline.

IN VITRO BLOOD INTERACTIONS

The surfaces were evaluated by normalised whole blood clotting times (Coleman et al., 1982) and by platelet adhesion. Significant differences are noted in the clotting times of the alkyl agarose surfaces as a function of derivatisation. The clotting times pass through a minimum around 40-60 µmol alkyl group per ml packed gel derivatisation. Platelet adhesiveness increases substantially with alkyl derivatisation as measured by a modified centrifugation test procedure (Mohammad et al., 1974).

The PEG surfaces show greatly prolonged clotting times over all the agarose substrates tested. Previous studies have shown that PEG surfaces minimise platelet adsorption (Merrill et al., 1982; Mori et al., 1982).

ACKNOWLEDGEMENTS

REFERENCES

Bailey, F.E., Jr. and Koleske, J.V. (1979). Poly(ethylene oxide), Academic Press, New York.

Bethell, G.S., Ayers, J.S., Hancock, S.W. and Hearn, M.T.W. (1979). A novel method of activation of crosslinked agaroses with 1,1'-carbonyldimidazole. J.Biol.Chem., 254, 2572-2574.

Coleman, D.L., Gregonis, D.E. and Andrade, J.D. (1982). Blood-materials interactions: the minimum interfacial free energy and the optimum polar/apolar ratio hypothesis. J.Biomed.Mater.Res., 16, 381-398.

Gregonis, D.E., Hsu, R., Buerger, D.E., Smith, L.M. and Andrade, J.D. (1982). Wettability of polymers and hydrogels as determined by Wilhelmy plate technique, in R.B. Seymour and G.A. Stahl (eds.), Macromolecular Solutions, Solvent Property Relationships in Polymers, Pergamon, New York, pp.120-133.

Gribnau, T.C.J., van Eekelen, C.A.G., Stumm, C. and Tesser, G.I., (1977). Microscopic observations on agarose beads. J.Chromatography, 132, 519-524.

Haller, I. (1978). Covalent attached organic monolayers on semiconduction surfaces. J.Am.chem.Soc., 26, 8050-8055.

Hjerten, S. (1973). Some general aspects of hydrophobic interaction chromatography. J.Chromatography, 87, 325-331.

Hjerten, S. (1983). High performance liquid chromatography on
    matrices of agarose, in H. Peters (ed.), Protides of the Bio-
    logical Fluids, vol.30, Pergamon, New York, pp.9-17.
March, S.C., Parikh, I. and Cuatrecasas, P. (1974). A simplified
    method for cyanogen bromide activation of agarose for affinity
    chromatography. Analyt.Biochem., 60, 149-152.
Merrill, E.W., Salzman, E.W., Wan, S., Mahmud, N., Kushner, L.,
    Lindon, J.N. and Curme, J. (1982). Platelet-compatible hydro-
    philic segmented polyurethanes from polyethylene glycols and
    cyclohexane diisocyanate. Trans.Am.Soc.artif.intern.Organs, 28,
    482-487.
Mohammad, S.F., Hardison, M.D., Glenn, C.H., Morton, B.D., Bolan,
    J.C. and Mason, R.G. (1974). Adhesion of human blood platelets
    to glass and polymer surfaces. I. Studies with platelets in
    plasma. Haemostasis, 3, 257-270.
Mori, Y., Nagaoka, S., Takiuchi, H., Kikuchi, T., Noguchi, N.,
    Tanzawa, H. and Noishiki, Y. (1982). A new antithrombogenic
    material with long polyethyleneoxide chains, Trans.Am.Soc.
    artif.intern.Organs, 28, 459-463.
van Wagenen, R.A., Rockhold, S. and Andrade, J.D. (1982). Probing
    protein adsorption: total internal reflectance intrinsic fluor-
    escence. Adv.Chem.Ser., 199, 353-370.

Model Polymers for Probing Surface and Interfacial Phenomena

D. E. Gregonis and J. D. Andrade

1. INTRODUCTION

This chapter will review the use of model polymer systems for studying surface and interfacial properties. It is not intended to be all inclusive in regard to the overall chemistry of the systems, or even to review each and every polymer which has been investigated. This chapter is meant to provide a condensed overview of the bulk and surface characteristics of selected systems. Generally these model polymers are systematically prepared in order to change the bulk composition of polymeric material. The bulk composition is then extrapolated to the interface. It must be emphasized that this extrapolation is often not direct. The tendency is for the polymer to minimize its interfacial energies; thus, a polymer cast against a clean (high energy) glass surface may exhibit different surface properties than the same polymer's air-exposed surface. These effects are more pronounced in block copolymers which may have large domains of different surface properties. A polymer with high glass transition temperature may retain its surface energies for extended periods of time or until annealing. Polymers with their glass transition below room temperature may reorient quite rapidly upon exposure to different environments and may have different groups exposed in an air environment as compared to an aqueous environment. (See Chapter 2.)

Plasticization of a polymer generally decreases the glass transition temperature. A hydrogel, such as poly(hydroxyethyl methacrylate), can have a high glass transition temperature $(115°C)$[1] in the dry state but becomes a highly flexible polymer when swollen with water. Even polymers

D. E. Gregonis and J. D. Andrade ● Department of Bioengineering, University of Utah, Salt Lake City, Utah 84112.

that are not highly swollen in the aqueous environment may experience enough plasticization of the polymer chains at the interface to have different thermal motions as compared to the polymer chains found in the bulk.

What must be emphasized is that extrapolation from bulk polymer measurements to surface properties is not direct. The ability to measure the top ten angstroms of the polymer interface are limited; most of the available techniques measure the dry, nonhydrated polymer surface. However, until surface measurement techniques become more advanced, knowledge of the bulk polymer system is still important for investigating surface trends.

2. STEREOREGULAR POLYMERS

2.1. PURPOSE (STEREOCHEMISTRY)

All addition polymers which have unsymmetrical groups off the main chain exhibit asymmetrical centers along the polymer chain. The orientation of these groups in relation to adjacent neighbors is referred to as stereoregularity. Polymers such as polyethylene, polyisobutylene, and poly(vinylidene chloride) have symmetric pendant groups, and thus do not exhibit stereoisomerism. Although several forms of stereoisomerism exist,[2] only the methacrylate polymer system, which can exist in isotactic, heterotactic, and syndiotactic configuration, will be covered here. Even though it seems reasonable that the stereochemistry of the polymer may influence its biological interactions, no systematic study of these polymeric systems has been done to substantiate this hypothesis.

One of the most studied systems, the methacrylates, has a methyl group and a carboxylic acid or derivatized carboxylic acid group attached to every other carbon atom along the main chain. Thus, if the polymer chain is stretched, in the extreme cases of tacticity the same group is always on the same side (isotactic) or on alternate sides (syndiotactic) of the polymer chain. Random orientation of the groups is referred to as atactic (Figure 1).

The stereoregularity of the polymer usually has a strong influence on bulk characteristics. For example, the glass transition (T_g) for poly(methylmethacrylate) is 41.5°C for isotactic, 125.6°C for syndiotactic, and 104°C for atactic polymer.[3] Tactic polymers generally show detectable changes in properties such as density, solubility, rate and extent of solubility, crystallinity, thermal and mechanical transitions, and spectroscopic characteristics such as infrared and nuclear magnetic resonance (NMR) spectra and X-ray diffraction patterns. Although many of these methods have been used to quantitate stereoregularity, the NMR technique is most sensitive for exact measurements in most polymer systems.[4]

2.2. CHEMISTRY

The synthesis of methyl and other alkyl methacrylates has been widely studied. The stereoregularity can be varied by both radical and anionic initiation methods. Under identical reaction conditions, the stereochemistry of the resulting polymer can be strongly influenced by the size of the ester substituent.

In general, for poly(methyl methacrylate) and other small ester methacrylates, the tacticity of the polymer polymerized free radically produces a 60% syndio, 40% hetero, 0% isotactic configuration.[5] Decreasing the temperature of polymerization results in a greater degree of syndiotacticity (Table 1). For example, poly(hydroxyethyl methacrylate) polymerized by radical means at −40°C produced a 84% syndio, 16% hetero, and <1% isotactic configuration.[6]
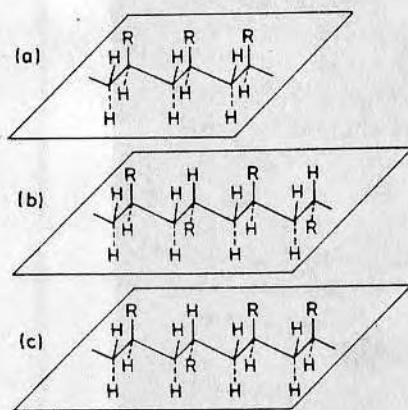

FIGURE 1. Zig-zag planar conformation of the main chain of vinyl polymers having different types of stereoregularity: (a) isotactic chain; (b) syndiotactic chain; (c) atactic chain [reprinted with permission from Reference (76)].

TABLE 1
Effect of Temperature on Tacticity in Radical Polymerization of Methyl Methacrylate[a]

Temperature (°C)	Fraction of syndiotactic placement(s)
−40	0.86
60	0.76
100	0.73
150	0.67
250	0.64

[a] From Reference (74).

TABLE 2
Effect of Solvent on Tacticity of Poly(methyl methacrylate)[a]

Polymerization system	Tacticity (triad analysis)		
	Iso	Hetero	Syndio
Radical, bulk polymerization at 60°C	0.08	0.33	0.59
n-C$_4$H$_9$Li at −78°C			
% Tetrahydrofuran in toluene:			
0	0.78	0.16	0.06
2.5	0.30	0.31	0.39
5	0.24	0.34	0.42
10	0.13	0.35	0.52

[a] From Reference (74).

TABLE 3
Glass Transition as a Function of Tacticity of Poly(methyl methacrylate)[a]

Glass transition temperature T(°C)	Tacticity (triad analysis)		
	Iso	Hetero	Syndio
41.5	0.95	0.05	
54.3	0.73	0.16	0.11
61.6	0.62	0.20	0.18
104.0	0.06	0.37	0.56
114.2	0.10	0.31	0.59
120.0	0.10	0.20	0.70
125.6	0.09	0.36	0.64

[a] From Reference (3).

The anionic polymerization technique provides much more versatility in preparation of these tactic polymers. The polymerization is much more sensitive to reaction conditions, e.g., temperature, solvent composition, order and possible rate of addition of reactants.[7] One of the more common anionic initiators is n-butyl lithium. When polymerization takes place in an apolar solvent such as toluene, highly isotactic product results; but upon addition of the polar solvent tetrahydrofuran to the reaction, a syndiotactic polymer results, as shown in Table 2. The polar solvent acts to increase the distance between the gegen ion from the propagating anion, negating its stereochemical influence on the incoming monomer. This effect is also noted in ether-containing monomers, such as methoxyethyl methacrylate. When anionically polymerized in an apolar solvent, the formation of syndiotactic polymer results due to ether solvation of the gegen ion.[8]

Stereoregular poly(hydroxyethyl methacrylate) hydrogels have been prepared using the above concepts. The hydroxyl group was protected as the benzoate ester during anionic polymerization, and then removed by selective hydrolysis. The isotactic polymer exhibits a more strongly temperature-dependent aqueous swelling profile than the syndiotactic polymer.[6]

2.3. BULK PROPERTIES

As mentioned above, the bulk properties are generally different for polymers of different stereoregularity. It has been proposed that isotactic poly(methyl methacrylate) exists as a double helix[9]; however, this recently has been questioned.[10] The relation between the tacticity of poly(methyl methacrylate) and glass transition temperature is shown in Table 3.

2.4. SURFACE CHARACTERIZATION

The surface wettability of tactic polymers as measured by critical surface tension contact angle methods exhibits no difference between isotactic and atactic poly(methyl methacrylate) ($\gamma_c = 36$ dyn/cm); however, isotactic poly(α-chloroethyl methacrylate) and poly(phenyl methacrylate) show lower γ_c by about 4 dyn/cm than those of the atactic polymer.[11] It is postulated that this effect is due to specific conformation requirements of the bulkier ester group which would minimize hydrogen bonding interactions between the methacrylate carbonyl and wetting liquids. The smaller methyl ester substituent would minimize this effect.

Methacrylate polymers and copolymers may show time-dependent interfacial properties in contact with water. This effect has been discussed in some detail in Chapter 2 and will not be repeated here. It is important to point out, however, that surface properties may and generally are time, temperature, and environment dependent.

3. HYDROXYETHYL METHACRYLATE COPOLYMERS

3.1. PURPOSE (SYSTEMIC HYDRATION)

The methacrylate system offers the versatility of providing a wide range of polymer properties by varying the side chain ester functionality. Many of these monomers are commercially available or can be conveniently prepared in the laboratory. A system which has been widely studied[12] is the poly(methyl methacrylate–hydroxyethyl methacrylate) (MMA–HEMA)

copolymer system. Poly(methyl methacrylate) is a hard, rigid glassy polymer that absorbs approximately 1–2% water when hydrated. Poly(hydroxyethyl methacrylate) in the dry state is also a hard, glassy polymer; it becomes a hydrogel by absorbing 40% by weight of water when hydrated. Other hydrophobic comonomers have been substituted for MMA in this system, for example, ethyl methacrylate[13] and methoxyethyl methacrylate, resulting in relatively similar properties to those of the copolymers.

3.2. CHEMISTRY

The polymers of MMA and HEMA are polymerized generally by radical initiators. For biomedical applications, azobisisobutyronitrile (AIBN) or AIBN derivatives are generally preferred due to the similarity of the initiating group to the methacrylate backbone, and the absence of charge. The chemistry of the hydroxyethyl methacrylate system has recently been reviewed.[12,14]

The reactivity ratios of HEMA to MMA, ethyl methacrylate (EMA), and n-butyl methacrylate (BMA) have been reported by Varma et al.[15,16] for bulk polymerizations; they report a higher reactivity of the HEMA radical relative to the HEMA monomer and a higher reactivity for the MMA and other hydrophobic methacrylate radicals relative to the HEMA monomer.

The monomer reactivity of HEMA with hydrophobic methacrylates at 60°C using the Fineman–Ross method is:

r_1HEMA	r_2MMA	r_1HEMA	r_2EMA	r_1HEMA	r_2BMA
1.054	0.296	1.87	0.55	2.08	0.45

This indicates that the initial polymer produced is higher in HEMA composition in comparison to the monomer feed. However, other reports[17] indicate the reactivity ratios of HEMA and MMA to be r_1(HEMA), 0.66, and r_2(MMA), 0.86, indicating this copolymer tends toward an alternating system.

Soluble polymers of the methacrylate system are obtained by polymerization at high solvent dilution, typically one part monomer to ten parts solvent. Polymers prepared by this method at 60°C are ~60% syndio, 40% hetero, and <1% isotactic. The soluble polymers are generally used for preparation of solvent cast films. It should be mentioned that uncrosslinked PHEMA, although it swells in water, will not dissolve due to the hydrophobic nature of the methacrylate backbone.
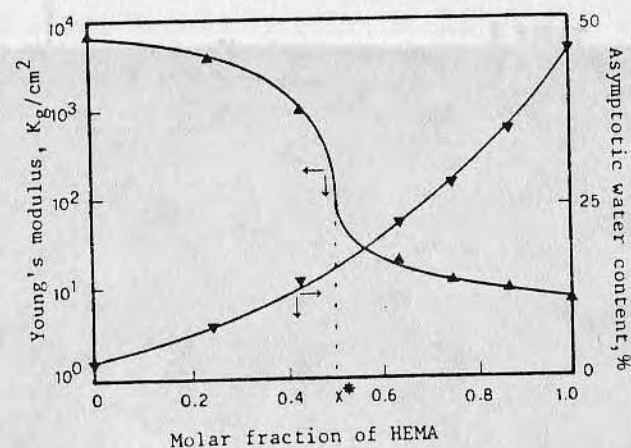
FIGURE 2. Water content and modulus of elasticity as a function of molar fraction of HEMA in HEMA–MMA copolymers [reprinted with permission from Reference (18)].

3.3. BULK PROPERTIES

The aqueous swelling of HEMA and MMA or methoxyethyl methacrylate (MEMA) copolymers results in a linear relationship when volume percentages of HEMA and MEMA are copolymerized.[12] The water fraction of MEMA homopolymer is 0.035% water and pHEMA homopolymer is 0.40% water. When molar fractions of MMA and HEMA are polymerized, the water content again increases with increasing percentage of HEMA; however, this does not follow exactly a linear relationship. Young's modulus undergoes a sharp decrease at near equal molar ratio.[18] This is the transition region where the hydrated copolymer changes from a glass to a plasticized rubbery polymer as shown in Figure 2.

3.4. SURFACE CHARACTERISTICS

The interface between a hydrogel and water is more diffuse when compared to a hydrophobic polymer–water interface.[19] It has been shown that contact angle methods can lead to local dimensional changes of the highly deformable gel surface.[20] (See Chapter 7.)

Captive underwater air and octane droplet data have been reported for the HEMA–MMA and HEMA–EMA copolymers.[21] This study utilized the Hamilton procedure[22,23] for calculation of dispersion and polar components at the interface and the surface–water interfacial free energies as shown in Figure 3. The surface–water interfacial free energies approach zero at values as low as 30% water suggesting that the hydrophilic phase dominates the underwater interface.
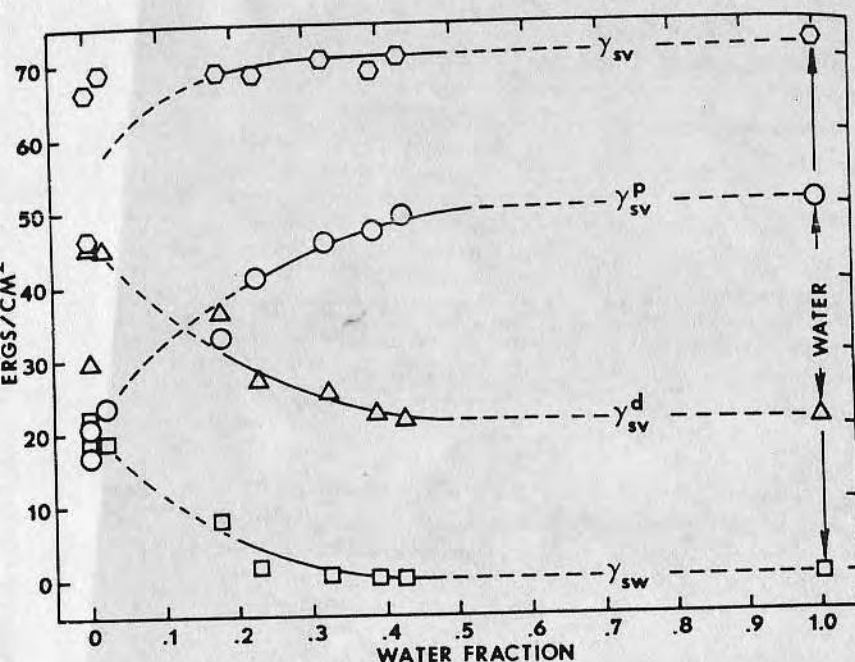
FIGURE 3. γ_{sv}^d, γ_{sv}^p, γ_{sv}, and γ_{sw} as a function of water fraction for methacrylate polymers of various bulk water contents. The data at water fraction = 1.0 are for pure water [reprinted with permission from Reference (21)].

The aqueous wetting character of HEMA–MMA copolymers has also been reported as a function of the mole ratio of HEMA as in Figure 4.[24] In this study, the wetting characteristics are measured both by the Wilhelmy plate procedure and the captive underwater air bubble procedure. The dynamic advancing and receding Wilhelmy angles are recorded as the surface is immersed and removed from the water liquid at a rate of 40 mm/min. To obtain the static Wilhelmy plate angles, the surface was stopped for 15 seconds at several points in both the advancing and receding mode, before measurements were made. The receding contact angle changes created at higher amounts of hydroxyethyl methacrylate in the copolymer. The advancing contact angle shows less change over the copolymer range. The underwater captive air bubble closely approximates the receding contact angle measurements of the Wilhelmy plate.

Analysis of ethyl methacrylate–HEMA copolymers by X-ray photoelectron spectroscopy (ESCA) have been reported on solvent cast and radiation grafted surfaces.[13]
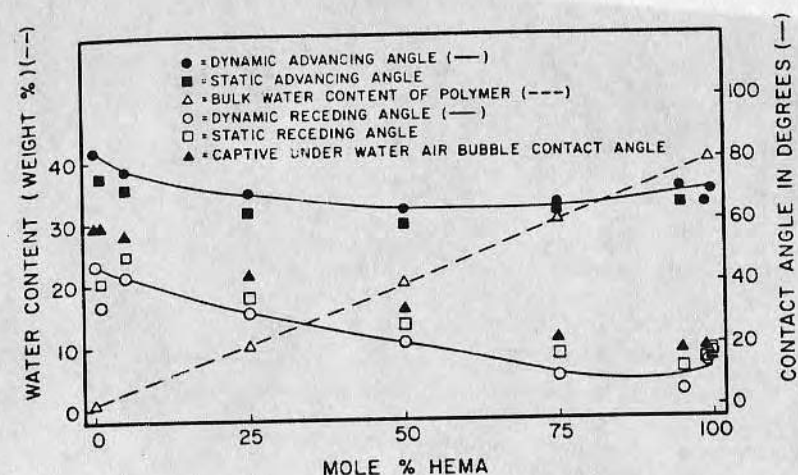

FIGURE 4. Contact angle measurements at 24-hour hydration of methyl methacrylate [MMA] and hydroxyethyl methacrylate [HEMA] copolymers using both captive air bubble and Wilhelmy plate techniques. Also shown are equilibrium water content measurements of the copolymers [reprinted with permission from Reference (24)].

4. BLOCK COPOLYMERS

Mixtures of two homopolymers are usually not compatible; that is they phase separate into macroscopic domains consisting of essentially pure homopolymers.[25] If these two polymeric materials were covalently coupled, they would still be phase separated, but the phase domains will be limited to the molecular weight of the polymeric chains and the relative molecular weight ratios of the two polymers. The polymeric blocks can be arranged in various structures, i.e., A—B, A—B—A, and (A—B)$_n$ blocks, so-called diblocks, triblocks, and multiblock polymeric systems.

4.1. PURPOSE (MORPHOLOGY)

Block copolymer systems permit the control of morphology for the study of protein interactions and cellular adhesion. For example, if one investigates the general detail of A—B diblocks or A—B—A triblock copolymers, and changes the volume fraction of the blocks, one finds a systematic order of the phases as shown in Figure 5.

If the morphology of these polymers extends to the interface, the nature of protein adsorption is expected to change compared to that on a homogeneous surface. When a protein molecule diffuses to the vicinity of

A SPHERES   **A CYLINDERS**   **A, B LAMELLAE**   **B CYLINDERS**   **B SPHERES**
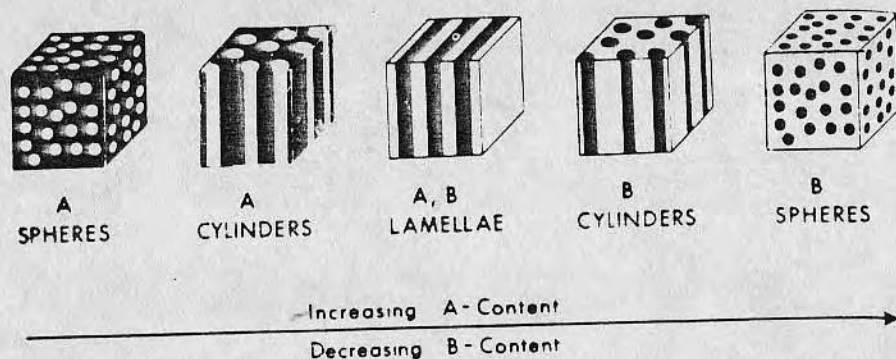
→ Increasing A - Content

Decreasing B - Content

FIGURE 5. Schematic illustration of various phase structures composed of components A and B [reprinted with permission from Reference (77)].

the polymer-solution interface, it may adsorb on either phase A, B, or even the A—B interface bridging the two phases. Table 4 shows the techniques which are useful for the differentiation of block copolymers versus homopolymer blends. (See Chapters 10 and 13.)

Several block copolymer materials are of commercial importance. These include the styrene-butadiene or styrene-isoprene A—B and A—B—A block systems produced by Shell Chemical Company (Kratons) and Phillips Petroleum Company (some grades of Solprenes). Several (A—B)$_x$ materials are commercially available including the polyether-polyester blocks produced by DuPont Co. (Hytrels) and the polyurethanes, which may be poly(ester-urethane) blocks, poly(ether-urethane) blocks, poly(ether-urethane-urea) blocks, etc. Makers of these polyurethanes include Upjohn Corp. (Pellethanes), DuPont Co. (Lycra), Mobay Co. (Texins), and B. F. Goodrich (Estanes). Because of the biomedical importance of the urethanes, they are included in a separate listing in this chapter.

4.2. STYRENE–HYDROXYLATED BUTADIENE–STYRENE TRIBLOCKS

Styrene–butadiene–styrene triblock materials are commercially available from Shell Chemical Co. (Kraton) and from Phillips Petroleum Co. (Solprene) in a wide variety of molecular weight and composition ratios. Several groups have used these materials to prepare hydrophilic-hydrophobic segments by oxidation of the butadiene block either by peracid followed by hydrolysis[26,27] or by hydroboration procedures.[28,29] The peracid method leads primarily to dihydroxylation of the double bond as shown in Figure 6, whereas the hydroboration leads to anti-Markovnikov monohydroxylation of the double bond as shown in Figure 7. Due to the nature of

TABLE 4
Techniques for Block Copolymer Characterization^a

Block copolymer versus homopolymer blend

1. Solubility characteristics
   a. Solid phase extraction
   b. Solution fractionation
2. Film clarity
3. Solution compatibility
4. Molecular weight distribution
   a. Density gradient ultracentrifugation
   b. Gel permeation chromatography
5. Rheological characteristics

Block copolymer versus random copolymer

1. Proton magnetic resonance
2. Infrared spectroscopy
3. Dynamic mechanical behavior
4. Differential scanning calorimetry
5. Electron microscopy
6. Small-angle X-ray scattering
7. Mechanical properties
8. Rheological characteristics
9. Crystallinity characteristics
10. Solution light scattering
11. Thermomechanical analysis

Molecular structure

1. Osmometry
2. Solution light scattering
3. Ultracentrifugation
4. Gel permeation chromatography
5. Solution viscometry
6. Oligomer analysis
7. Selective degradation

Architecture and purity

1. Elastic recovery
2. Rheological characteristics
3. Gel permeation chromatography
4. Density gradient ultracentrifugation

Supermolecular structure

1. Dynamic mechanical behavior
2. Differential scanning calorimetry
3. Rheological characteristics
4. Electron microscopy and scanning electron microscopy
5. Wide-angle X-ray scattering
6. Small-angle X-ray scattering
7. Birefringence
8. Small-angle light scattering
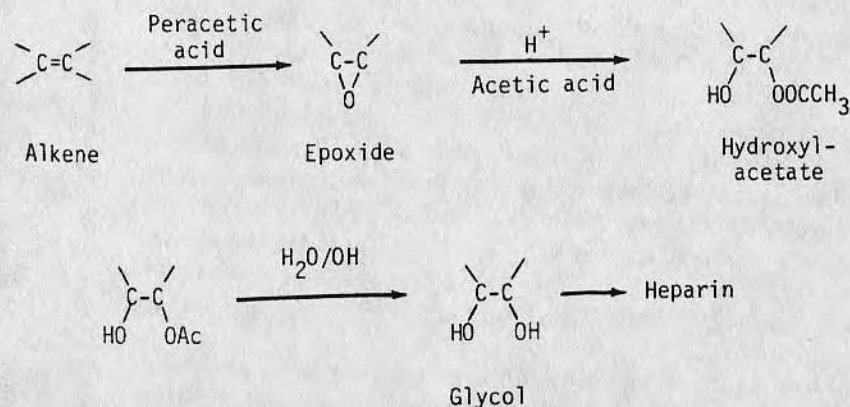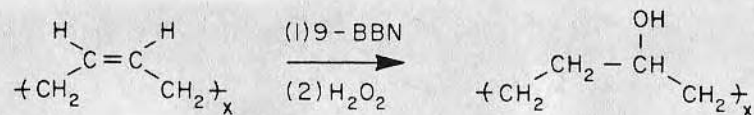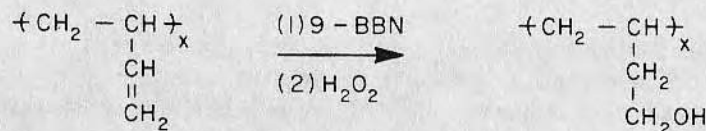
^{a} From reference (43).

FIGURE 6. Hydroxylation reaction scheme for polybutadienes [reprinted with permission from Reference (6)].

CIS AND TRANS
1, 4 − POLYBUTADIENE

1, 2 − POLYBUTADIENE

FIGURE 7. Hydroxylation of olefin-containing polymers by hydroboration procedures (9-BBN = 9-borobicyclo[3.3.1]nonane) (reprinted with permission from Reference (24)).

the peracid method, which proceeds through a reactive epoxide intermediate, crosslinked polymer inevitably results; the hydroboration procedure leads to uncrosslinked polymer.

The butadiene segments of the S—B—S triblock polymers of different styrene–butadiene ratios were hydroborated and the bulk water content and aqueous wetting angles were measured[24] (Figure 8). The receding contact angle shows the most change and becomes highly wetting at or above 20%
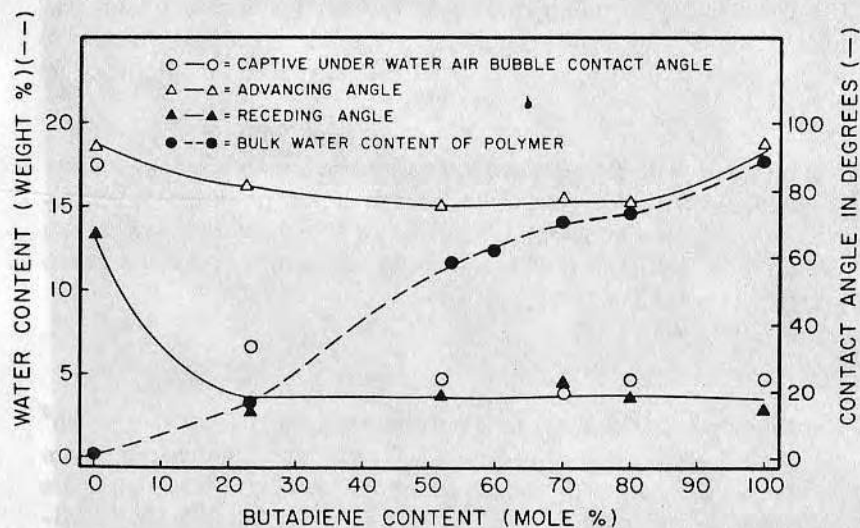

FIGURE 8. Contact angle measurements at 24-hour hydration and equilibrium water content of styrene-hydroxylated butadiene-styrene triblock copolymers [reprinted with permission from Reference (24)].

hydroxylated butadiene content. The advancing contact angle, however, changes very little over the entire copolymer composition.

4.3. HEMA–STYRENE–HEMA TRIBLOCKS

Preparation of these A—B—A block polymers with the blocks having different wetting character has been reported.[27,28] The (A) blocks consist of hydroxyethyl methacrylate segments; the (B) block consists of poly-styrene. This material was prepared from an amino-terminated poly(hydroxyethyl methacrylate) and a bis-isocyanate-terminated styrene in order to couple the blocks by urea functionalities as shown in Figure 9.
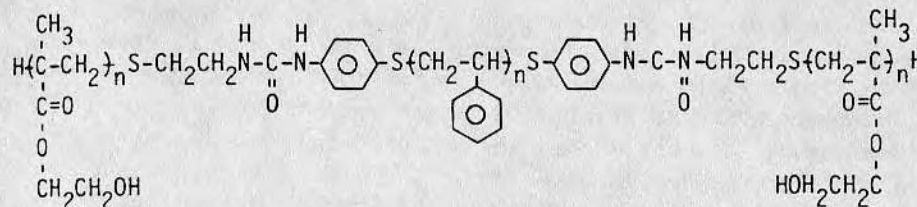

FIGURE 9. Chemical structure of HEMA-Styrene ABA-type block copolymers [reprinted with permission from Reference (78)].

The wetting characteristic using a water droplet on the dry polymeric surface is shown in Figure 10 for both the A—B—A triblock system along with the HEMA-styrene random copolymer wetting characteristics. This contact
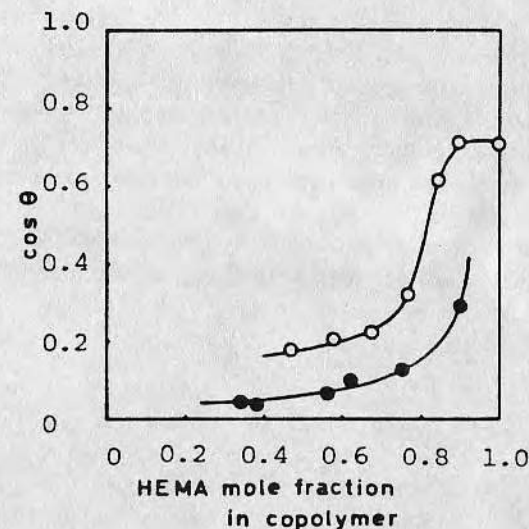

FIGURE 10. Relation between wettability and copolymer composition: (●) HEMA-Styrene ABA-type block copolymer system; (○) HEMA-Styrene co-oligomer system [reprinted with permission from Reference (31)].

angle measurement gives results approximating the advancing contact angle measurement of the Wilhelmy plate procedure. The contact angle becomes more wetting above 0.8 mole fraction HEMA in copolymer.
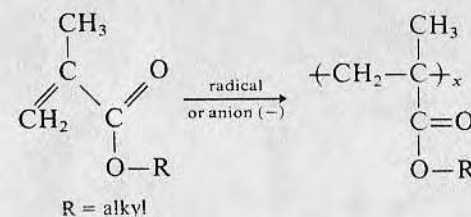
5. ALKYL METHACRYLATES

5.1. PURPOSE (SYSTEMATIC CHANGE IN T_g)

Polymer science is aware of the importance of polymer main chain and side chain segmental mobility on the physical and mechanical properties of polymers. It is very reasonable that such characteristics would significantly influence the interfacial interactions of solute molecules with the polymer surface. (See Chapter 2.) One can think of this in terms of an entropic argument: if a protein molecule were to adsorb on a highly mobile polymer surface, it would influence the polymer surface locally and the mobility of the polymer would be constrained. Therefore, from the entropic point of view, adsorption would not be favorable assuming all other factors are constant.[32]

The mobility of polymer molecules is expressed via a very commonly measured bulk property of polymers, the glass transition temperature (T_g). The T_g of a polymer is that temperature at which large segments of the molecule or entire polymer molecules can move within the solid. At temperatures considerably below the glass transition temperature, the mobility is constrained or does not occur, and as a result the polymer is relatively brittle and not deformable. If the polymer is crosslinked to a three-dimensional network, then above the glass transition temperature the network will generally have elastic character. Thus, all of our common elastomers and rubbers are three-dimensional polymer networks whose glass transition temperature is considerably below room temperature. Merrill[32] has suggested that such a surface is in constant motion and would be relatively unfavorable for protein adsorption. It is difficult to vary T_g in most systems without varying the chemistry of the system. The family of methacrylate polymers with different length alkyl ester side chains provides a means of being able to vary T_g without greatly altering surface wetting characteristics.

5.2. CHEMISTRY

The chemistry of the methacrylates has been reviewed.[33,34] The methacrylates can be polymerized either by radical or anionic means as shown opposite:

R = alkyl

Many of the alkyl methacrylate monomers and polymers are commercially available, although preparation of specific alkyl methacrylate monomers is easily accomplished.[35] For highly pure polymers it is usually advisable to purify the monomer and polymerize it in the lab rather than to obtain the commercial polymer. The polymer is most useable in the uncrosslinked form, because it can be solubilized and solvent cast. Uncrosslinked polymer can be prepared by polymerizing the monomer at relatively high dilution (1 to 10) in a good solvent such as toluene or tetrahydrofuran (for these n-alkyl methacrylates) using a radical initiator such as AIBN (azobisisobutyronitrile). The polymer is isolated by precipitation in a non-solvent such as methanol and then purified by redissolving and reprecipitation.

### 5.3. BULK CHARACTERISTICS

The glass transition temperatures of the n-alkyl methacrylates are shown in Table 5. The brittle point temperatures of the acrylates and methacrylates are plotted as a function of the alkyl ester functionality in Figure 11.

The T_g of the methacrylates reaches a minimum with the n-octyl ester and then increases with temperature due to interactions of the longer alkyl ester side chains. The accurate measurement of the polymer transitions requires the complete removal of all solvent or other additives which can function as plasticizers. This is done by heating the sample in vacuum above its glass transition temperature.

5.4. SURFACE CHARACTERISTICS

The critical surface tension of the polymers will range from 35 ergs/cm^2 for poly(methyl methacrylate) to around 24 ergs/cm^2 for the long chain length ester methacrylates. Air and octane underwater contact angles[36] are shown for various chain length methacrylate esters in Table 6. The solid-water interfacial energies are determined from these values along with the dispersion and polar components from these surfaces. The dispersion component of the surface shows little change over the entire range (from methyl

TABLE 5
Glass Transition Temperatures (T_g) of Alkyl Methacrylate Polymers

$$\begin{array}{c} CH_3 \\ | \\ +CH_2-C+ \\ | \\ C=O \\ | \\ O-R \end{array}$$
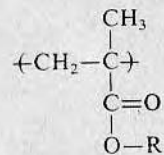
R =	Name	$T_g(°C)$
$-CH_3$	methyl methacrylate (MMA)	105
$-CH_2CH_3$	ethyl methacrylate	47, 65
$-(CH_2)_2CH_3$	n-propyl methacrylate	33
$-(CH_2)_3CH_3$	n-butyl methacrylate (BMA)	17
$-C-(CH_3)_3$	t-butyl methacrylate	107
$-(CH_2)_5CH_3$	n-hexyl methacrylate (HMA)	−5
$-(CH_2)_7CH_3$	n-octyl methacrylate (OMA)	−70
$-(CH_2)_{11}CH_3$	n-dodecyl methacrylate (DDMA)	−65
$-(CH_2)_{17}CH_3)$	n-octadecyl methacrylate (ODMA)	<+60

[a] From Reference (75).

to n-octadecyl) of n-alkyl methacrylates. The polar force component shows a slight decrease with increasing alkyl ester chain length. (See also Chapter 2.)

6. DERIVATIZED AGAROSE

6.1. PURPOSE (MODIFICATION FOR SYSTEMIC HYDROPHOBICITY)

The adsorption of plasma proteins on various surfaces can lead to activation of the blood coagulation, complement, and fibrinolytic systems. The adsorbed plasma proteins may also influence the deposition of platelets and other blood cellular components at a surface. Although investigators have initially investigated hydrogels for minimizing interactions with blood components, it is now known that hydrogels such as poly(hydroxyethyl methacrylate) show fairly strong interactions with certain blood proteins.

There are, however, certain hydrogels which are demonstrated to show little protein adsorption. These are hydrogels such as crosslinked dextran, crosslinked polyacrylamide, and agarose gels used by biochemists for gel permeation chromatography of proteins.[37] The gel permeation process relies upon size separation of molecules and minimal or non-interaction of
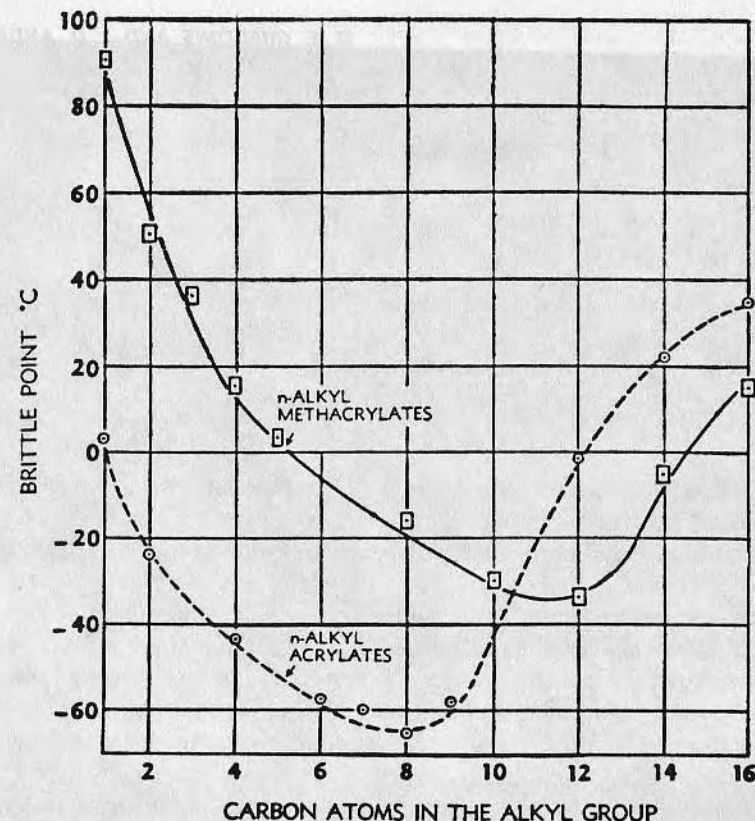

FIGURE 11. Brittle points of polymeric n-alkyl acrylates and methacrylates [reprinted with permission from Reference (75)].

TABLE 6
Surface Characterization of Alkyl Methacrylates[a]

Methacrylate ester polymer	T_g (°K)	Water contact angle (degrees)		Surface energetics (ergs/cm²)			
		θ(air)	θ(octane)	γ_{SW}	γ^P	γ^d	γ^P/γ^d
methyl	332/368	62 ± 1.1	87 ± 2.4	19.2	17.6	35.4	0.50
n-butyl	310/312	72 ± 3.2	103[b]	29.5	11.8	40.0	0.30
n-hexyl	265/257	76	110[b]	32.9	9.9	40.4	0.25
n-octyl	192/175	73	105[b]	29.9	11.2	38.6	0.29
n-dodecyl	NA	82	118[b]	36.2	7.7	38.5	0.20
n-octadecyl	185/179	90	130[b]	41.1	4.9	36.1	0.14

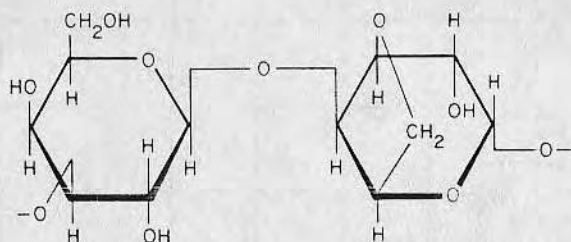[a] From Reference (36).
[b] Estimated values.

FIGURE 12. Repeating subunit of agarose [reprinted with permission from Reference (24)].

the protein with the stationary chromatography support is a requirement for the gel permeation process.

The agarose material is a polysaccharide containing a repeating 1,3-linked β-D-galactopyranose and 1,4-linked 3,6-anhydro-α-L-galactopyranose structure (Figure 12). All the other gel chromatographic supports require chemical crosslinked structures to maintain their gel properties: agarose, however, gels by self-aggregation due to helical chain interactions and by hydrogen bonding and hydrophobic interactions. Agarose is soluble in hot water (>80–$90°C$) but forms a porous, mechanically strong network upon cooling to 30 to $40°C$.

A modification of the agarose gel network to cause selective protein interactions is a technique now known as hydrophobic chromatography.[38-40] This is accomplished by various procedures to covalently bond aryl or various chain length alkyl groups to the agarose network. All of these previous procedures have resulted in the formation or require the use of chemically crosslinked agarose chromatography supports. Thus, the resulting derivatized agarose materials can no longer be dissolved for solvent casting of films.

6.2. CHEMISTRY

We developed a procedure to overcome the crosslink formation upon alkyl derivatization.[24] To accomplish this, the agarose beads were exchanged with dry acetone. It has previously been shown that this acetone exchange does not disrupt the agarose structure.[41] The agarose can now be reacted with alkyl and aryl chloroformates to covalently bond the hydrophobic group to the agarose molecule via a carbonate linkage. This linkage is shown to be quite stable in aqueous environments from pH 3 to 8. The derivatized agarose has been stored at $5°C$ in distilled water for over six months without detectable alkyl group hydrolysis. The degree of alkyl group coupling to the agarose can be measured using tritiated alkyl alcohols
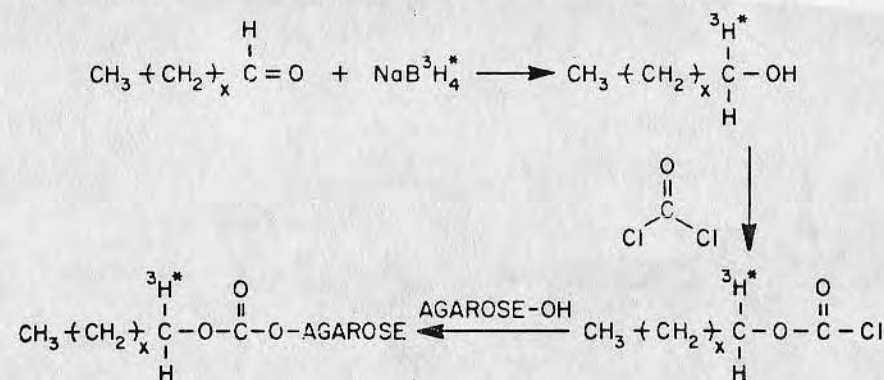
FIGURE 13. Preparation of α-titriated alcohols and covalent bonding to agarose (reprinted with permission from Reference (24)].

which are readily prepared by the reduction of alkyl aldehydes with tritium-labelled borohydride. This procedure is outlined in Figure 13.

The agarose and derivatized agarose materials are soluble in dimethyl sulfoxide which is used for solvent casting of surfaces. The derivatized agarose is quantitated in terms of μmoles alkyl group per ml of packed gel for aqueous suspensions of the beads or moles alkyl group per mole anhydrodisaccharide repeat unit for dried agarose powders. The latter terminology is a more exact representation of coupling at high derivatization since the gel structure starts to collapse in water due to the increased internal hydrophobic forces above a value of ~ 70 μmole/ml packed gel.

6.3. BULK CHARACTERISTICS

Spectroscopic measurements such as transmission infrared and 300 MHz ^{1}H-nuclear magnetic resonance spectroscopy confirm the alkyl coupling to the agarose structure and can be used as quantitative procedures to determine the degree of coupling. For example, in infrared analysis the ratio of the hydroxyl absorption at $3400\ cm^{-1}$ ($2.9\ \mu m$) to the carbonate absorption at $1750\ cm^{-1}$ ($5.7\ \mu m$) correlates with the percentage of alkyl group coupling. The carbonate functional group is attached to the agarose structure by the alkyl chloroformate coupling reaction.

Proton nuclear magnetic resonance (NMR) has been used by us and others to quantitate the amount of alkyl group coupling. The agarose samples are dried and then dissolved in a solvent consisting of 25% D_2SO_4 using 0.1 g agarose per 0.5 ml. Typical NMR spectra of the underivatized and derivatized agarose are shown in Figure 14. The area of the signals as shown in spectrum C of Figure 14 are ratioed according to the following
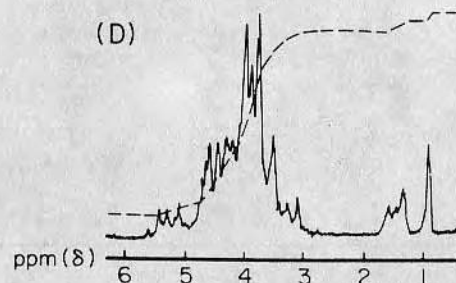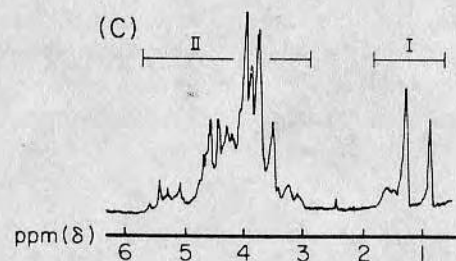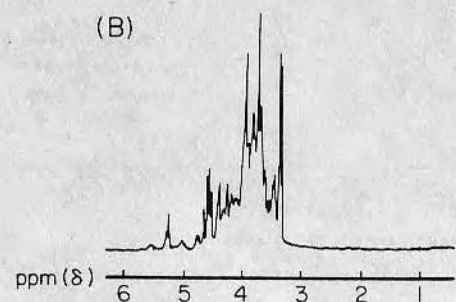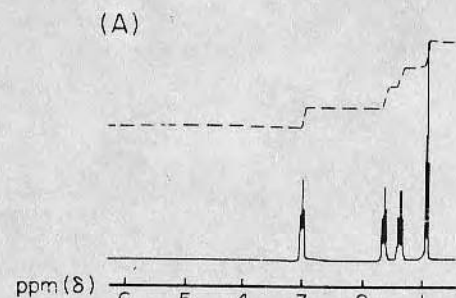
(A)

ppm (δ)

(B)

ppm (δ)

(C)

II   I

ppm (δ)

(D)

ppm (δ)

FIGURE 14. 300 MHz ^{1}H-NMR analysis of agarose and alkyl-derivatized agarose (spectra taken in 25% D_2SO_4 in D_2O): (A) n-butylamine standard; (B) Sepharose 4B-200; (C) n-hexyl agarose; (D) n-butyl agarose.

TABLE 7
300 MHz ^{1}H-NMR Analysis of n-Alkyl Agarose Derivatives

Derivative	1st analysis[a]	2nd analysis[a]
Hexyl agarose 1	18.7	17.1
Hexyl agarose 2	28.3	28.1
Butyl 1	11.1	10.4
Butyl 2	17.2	18.3
Butyl 3	30.0	30.9
Butyl 4	12.7	13.1
Butyl 5	21.1	16.8
Butyl 6	29.6	29.4

[a] Reported in μmole alkyl group/ml packed gel.

equation[42]:

$$\frac{\text{moles alkyl group}}{\text{moles anhydrodisaccharide}} = \frac{I/Z}{\left(II - \frac{2I}{Z}\right)\Big/7}$$

where $Z = 2n - 2$ for $NH_2-(CH_2)_n-CH_3$ or $HO-(CH_2)_n-CH_3$ and I and II correspond to areas shown in Figure 14C.

The reproducibility of the technique appears to be quite good. Duplicate analyses of derivatized agarose by the NMR method are shown in Table 7. The NMR results have also been compared with radioisotopic quantitation methods (the radiolabeled samples were obtained from Dr. Herbert Jennissen, Ludwig-Maximilians-Universitat Munchen, Munich, West Germany).

As seen in Table 8, good correlations are observed for the hexyl agarose samples; however, not quite as good results were observed for the butyl samples. We haven't been able to determine if this discrepancy is due to the radiolabeled samples or the NMR quantitation method.

6.4. SURFACE CHARACTERISTICS

The surface characterization of the agarose and derivatized agarose films were done primarily by two methods, ESCA (Chapter 5) and advancing/receding water contact angles (Chapter 7). The ESCA technique measures the top 50 ± 20 Å of the surface of the polymer, whereas the contact angle method (Wilhelmy plate) measures the top 10 Å for most surfaces. The contact angle method as applied to hydrogels is not very well

TABLE 8
Comparison of NMR Method and Radioisotope Method for Analysis
of Alkyl-Derivatized Agarose

	Derivatization: NMR method[a]	Derivatization: radioisotope method[b]
Hexyl agarose 1	12.2	14.1 ± 0.3
Hexyl agarose 2	17.1, 18.7	20.7 ± 1.0
Hexyl agarose 3	28.1, 28.3	28.3 ± 4.6
Butyl agarose 1	10.4, 11.1	21.3 ± 0.8
Butyl agarose 2	18.3, 17.2	34.1 ± 2.5
Butyl agarose 3	30.9, 30.0	45.9 ± 1.3

[a] Average of 2 determinations.
[b] Average ± standard deviation for 3 determinations.

modeled due to the diffuse water–bulk gel interface and the problem of contact angle-induced surface deformation (Chapter 7).

The ESCA studies used a Hewlett–Packard 5950B X-ray photoelectron spectrometer utilizing Al $K\alpha$ radiation (1487 eV) and a vacuum of 10^{-8} to 10^{-9} torr at ambient temperature. Water contact angles utilized a Wilhelmy plate apparatus built in our labs. The agarose samples were solvent cast and dried on glass plates from 0.2-μ-filtered dimethyl sulfoxide solutions.

The contact angles of butyl and dodecyl agarose after one hour of hydration are plotted versus the degree of derivatization in Figure 15. The underivatized agarose is, of course, very hydrophilic and exhibits essentially no hysteresis and essentially a zero contact angle. After relatively low degrees of derivatization (a value of 3×10^{-3} moles alkyl group per gram underivatized agarose corresponds to one alkyl group per each anhydrodisaccharide unit repeat of agarose), the advancing and receding contact angles remain constant. It is interesting to note that the advancing and receding contact angles of the butyl agarose always show less hysteresis than those of the longer alkyl chain dodecyl agarose surfaces.

ESCA analysis was done on underivatized agarose samples and n-butyl, n-hexyl, n-octyl, and n-dodecyl agarose coupled at approximately 40 μmole/ml packed gel. These samples were prepared on 1-cm² glass plates by solvent casting from dimethyl sulfoxide. The solvent was evaporated under nitrogen atmosphere at 60°C overnight. A survey scan for sulfur showed that all the solvent was removed by this process.

The carbon ESCA peaks are shown in Table 9. It is observed that the underivatized agarose, which should only contain ether-like carbons, contains a substantial amount of alkyl carbon contaminants. This may not be unexpected since high-energy surfaces are known to pick up a hydrocarbon layer in normal laboratory environments.
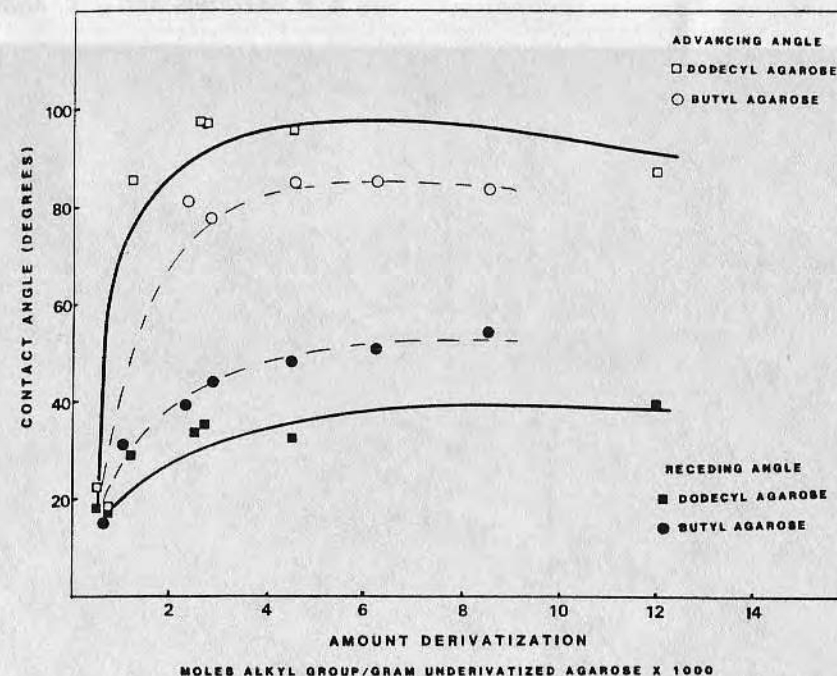
FIGURE 15. Contact angle changes with alkyl derivatization for n-butyl and n-dodecyl agarose.

Note that the relative percentage of ether carbon decreases as the length of the alkyl chain increases and the alkyl carbon peak area increases as the alkyl chain length increases. The ratio of the ether carbon peak to the carbonate carbon peak remains relatively constant, which would be expected since they are derivatized to essentially the same degree.

TABLE 9
ESCA Analysis of Derivatized Agarose Surfaces

	Alkyl carbon (%)	Carbonate carbon (%)	Ether carbon (%)	Ether carbon: carbonate carbon ratio
Agarose	33.9	0	55.3	—
n-Butyl agarose	31.3	6.8	49.8	7.3
n-Hexyl agarose	36.6	5.0	43.6	8.7
n-Octyl agarose	47.2	6.2	39.1	6.3
n-Dodecyl agarose	52.5	4.1	35.6	8.7

7. POLYURETHANES

7.1. PURPOSE (PRACTICAL BIOMEDICAL ELASTOMERS)

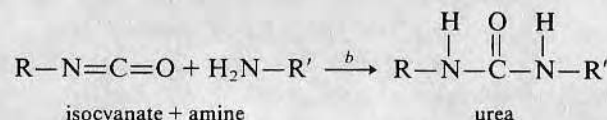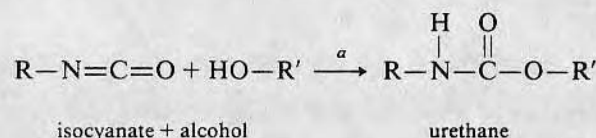Polyurethanes have been studied fairly extensively as biomedical polymers. They can be prepared with a wide range of mechanical properties, from flexible elastomers to rigid plastics. The poly(ether urethanes) exhibit greater hydrolytic stability than the poly(ester urethanes) and, thus, find greater use in biomedical applications. The elastomeric urethanes are particularly suited for flexing membranes as used in artificial heart and heart assist devices due to their adequate blood compatibility, good elastomeric properties, and ability to undergo repeated flexing without failure.

7.2. CHEMISTRY

Polyurethane chemistry involves primarily the chemistry of the isocyanate group. This will be discussed here for background purposes, but has been reviewed extensively in the literature.[43,44] Isocyanates react with alcohols by route (a) to form urethane structures and with amines by route (b) to form urea structures.

$$R-N=C=O + HO-R' \xrightarrow{a} R-\overset{\overset{\displaystyle H}{|}}{N}-\overset{\overset{\displaystyle O}{||}}{C}-O-R'$$

isocyanate + alcohol   urethane

$$R-N=C=O + H_2N-R' \xrightarrow{b} R-\overset{\overset{\displaystyle H}{|}}{N}-\overset{\overset{\displaystyle O}{||}}{C}-\overset{\overset{\displaystyle H}{|}}{N}-R'$$

isocyanate + amine   urea

Both urethane and urea structures are found in various biomedical urethanes. The basic polyurethane structures of interest here are prepared by the reaction of three components: diisocyanates, polyols, and chain extenders. The chain extenders may be either a diol or a diamine. Polyols are linear polyethers terminated at both ends by hydroxyl groups. The molecular weights of the polyols which exhibit suitable mechanical properties in polyurethane formulations are in the range of 500 to 5000 Daltons. By using different diisocyanates, polyols, and chain extenders, a large number of possible polymer structures can be formed. A common feature of all these polymers is the phase morphology of the material due to the

incompatibility of the segments and aggregation of the hard segments due to hydrogen bonding. The hard segments refer to the diisocyanate and the chain extender moiety in the polymer; the soft segment consists of the polyol portion of the polymer. In general, the higher the molecular weight of the polyol used in the polymer, the softer, more elastic the resulting polyurethane.

Most of the biomedical polymers use similar components. The diisocyanate most used is methylene-4,4'-diphenyl diisocyanate, commonly referred to as MDI. The polyol used most commonly is poly(tetramethylene glycol), PTMG, of molecular weight from 500 to 3000. The chain extender can be a diol such as 1,4-butanediol or a diamine such as ethylenediamine. The diamine chain extender gives generally better mechanical properties and greater phase separation of the segments due to the stronger hydrogen bonding nature of the urea as compared to the urethane unit.[45] Most injection moldable (thermoplastic) urethanes are diol chain extended which produces weaker hydrogen bonding interactions in the hard segment, allowing it to melt below the degradation temperature.
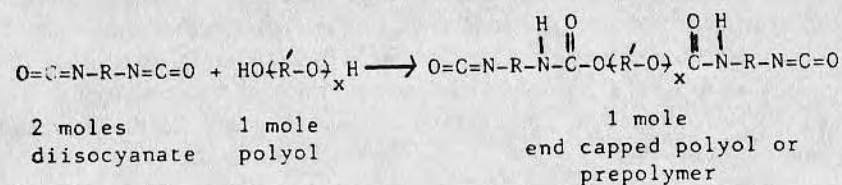
The addition and stoichiometry of the components can be combined in a variety of methods. For small batch biomedical polymers, the polyurethanes are generally prepared by a two-step process. One mole of polyol is "end capped" with two moles of diisocyanate in the first stage. This is followed by the addition of one mole of chain extender in the second stage as shown in Figure 16.

It is noted that the diamine chain extender results in a poly(ether urethane urea) polymeric structure. Other combinations of this stoichiometry may be used. For example, a 3:2 ratio of diisocyanate to polyol results in a dimeric, end capped polyol under the proper conditions which is then polymerized using one mole of chain extender.

For larger-volume production of polyurethanes, it is more economical to mix the polyol and chain extender together and combine with the diisocyanate in absence of solvent to form the polyurethane. The chain extender in this case is a diol to provide equal reactivity with the polyol. The segments of the blocks are not quite as well defined in this case resulting in a statistical linking of the components.

Other components used in urethane polymers are diisocyanates such as 2,4-toluene diisocyanate (TDI) and methylene-bis(4-dicyclohexyl isocyanate), a hydrogenated form of MDI. The hydrogenated MDI diisocyanate yields polymers with better photooxidative stability. Poly(propylene glycol) and poly(ethylene glycol) have been used as polyol components for the polyurethanes. The poly(ethylene glycol)-containing polyurethane becomes more hydrophilic with increasing molecular weight of the polyol and can be prepared as a hydrogel formulation.

1st Step – End Capping Polyol

$$O=C=N-R-N=C=O \;+\; HO(R'-O)_x H \;\longrightarrow\; O=C=N-R-\overset{H}{\underset{}{N}}-\overset{O}{\underset{}{C}}-O(R'-O)_x \overset{O}{\underset{}{C}}-\overset{H}{\underset{}{N}}-R-N=C=O$$

2 moles   1 mole
diisocyanate   polyol

1 mole
end capped polyol or
prepolymer

2nd Step – Chain Extension

$$O=C=N-R-\overset{H}{\underset{}{N}}-\overset{O}{\underset{}{C}}-O(R'-O)_x \overset{O}{\underset{}{C}}-\overset{H}{\underset{}{N}}-R-N=C=O$$

1 mole
end capped polyol

$$+\; H_2N-R''-NH_2 \;\longrightarrow\; \left[N-\overset{O}{C}-N-R''-N-\overset{O}{C}-N-R-N-\overset{O}{C}-O(R'-O)_x \overset{O}{C}-N-R \right]_y$$

poly(urethane-urea)

1 mole
diamine chain
extender

or

$$+\; H-O-R''-OH \;\longrightarrow\; \left[N-\overset{O}{C}-O-R''-O-\overset{O}{C}-N-R-N-\overset{O}{C}-O(R'-O)_x \overset{O}{C}-N-R \right]$$
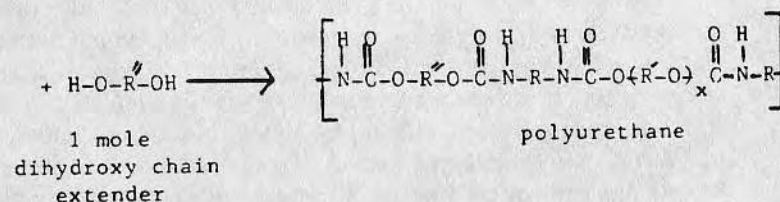
polyurethane
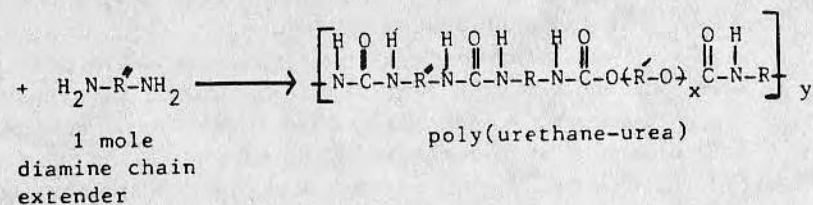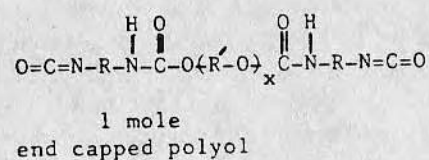
1 mole
dihydroxy chain
extender

FIGURE 16. Two-step preparation of polyurethanes.

7.3. BULK PROPERTIES

Considerable work has been reported on structure–property relationships of segmented polyurethanes.[46-48] Much of this work has investigated the domain morphology of these materials, which is quite complex and dependent upon solvent casting temperatures and on annealing conditions. Usually the diamine chain extended polymers have better phase separation than the diol extended polymer. Phase separation is also dependent upon the molecular weight of the polyol. The morphology has been studied by wide- and small-angle X-ray diffraction,[49] infrared spectroscopy,[50]

infrared dichroism,[51] low-angle light scattering,[46,52] and stress birefringence.[53]

7.4. SURFACE CHARACTERISTICS

The surface characteristics of the polyurethanes have been studied by internal reflection infrared spectroscopy[54] and by ESCA techniques.[55,56] Both of these techniques show changes between the surface and the bulk structure of the polyurethanes. The infrared data show differences between the molecular and secondary (hydrogen) bonding nature of the surface. The surface nature of polyurethanes has been studied by Ratner,[57,58] Cooper,[59] Merrill,[55] and Knutson and Lyman.[60] Surface structure depends on the preparation conditions, including casting substrate, solvent removal rate, and the environment in which the surface characterization is made, i.e., air, water, etc. The surface properties are also, of course, highly dependent on the nature of the soft segment, i.e., PEG, PPG, or PTMG, as well as its molecular weight. There is inconsistency among some of the various studies in the literature. The surface nature of biomedical polyurethanes is not yet fully understood.
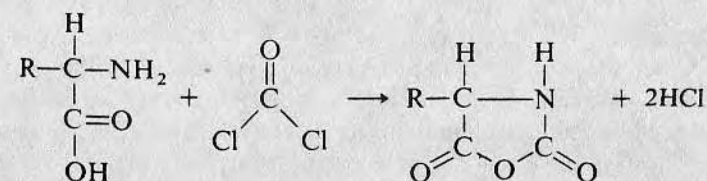
8. POLY(α-AMINO ACIDS)

### 8.1. PURPOSE (NATURALLY OCCURRING REPEAT UNITS)

Polymers of a wide variety of characteristics can be prepared from over 20 commonly occurring amino acids. They can be made as hydrogels or very hydrophobic polymers and be either biodegradable or biostable. Biodegradable poly(amino acids) have been proposed for use in sutures,[61] sustained release drug systems,[62] and artificial skin substitutes.[63] The more stable poly(amino acids) have been suggested for use in hemodialysis and blood oxygenator membranes.[64]

8.2. CHEMISTRY

The most useful reaction for the preparation of synthetic poly(α-amino acids) involves n-carboxy anhydrides (Leuchs anhydrides) prepared by reaction of α amino acids with phosgene.[65,66]

$$\begin{array}{c} H \\ | \\ R-C-NH_2 \\ | \\ C=O \\ | \\ OH \end{array} \;+\; \begin{array}{c} O \\ \| \\ C \\ Cl \quad Cl \end{array} \;\longrightarrow\; \begin{array}{c} H \quad\; H \\ | \quad\;\; | \\ R-C-N \\ | \quad\quad | \\ O=C \quad C=O \\ \;\;\diagdown O \diagup \end{array} \;+\; 2HCl$$

With amino acids containing other reactive groups, such as glutamic acid and lysine, the groups must be blocked prior to the n-carboxy anhydride formation. The n-carboxy anhydrides react with nucleophiles such as water or amines to yield high-molecular weight poly(amino acids), liberating carbon dioxide in the process.
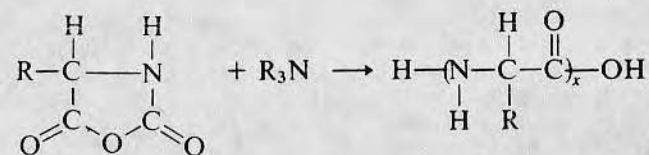
The polymerization initiation mechanism may differ depending upon the type of nucleophile used[67]; the exact reaction mechanism is still not completely understood.

Co-polymers of the amino acids are also prepared from the n-carboxy anhydride intermediates. For the preparation of random copolymers, the n-carboxy anhydrides of two different amino acids are both mixed in the same reaction vessel before initiation. The usual procedure is to polymerize the n-carboxy anhydrides to near 100% conversion, isolate the copolymer, and measure the average amino acid composition. Depending upon the particular amino acid n-carboxy anhydrides used, the reactivity of the comonomers may be close to unity, leading to an essentially random copolymer, or be widely different resulting in a very heterogeneous polymer composition. The solvent used for polymerization can also exert an effect on the comonomer reactivities.

Block copolymers have also been prepared from amino acid n-carboxy anhydrides by polymerizing n-carboxy anhydride monomer almost to completion, and then adding a second monomer. The size of the blocks are controlled by the stoichiometry of the initiator and n-carboxy anhydride-amino acid ratios.

The hydrophobicity of the poly(α-amino acids) can be controlled by the amount and type of amino acid incorporated into the polymer. Hydrogels or water-soluble poly(α-amino acids) are prepared by using glutamic acid or aspartic acid and derivatives such as hydroxyethyl and hydroxypropyl glutamine, prepared from nucleophilic displacement of poly(α-benzyl glutamate) with the corresponding hydroxyalkyl amine.[68]

The crosslinking of poly(α-amino acids) has been accomplished by two methods. One method uses a hexamethylene diisocyanate poly(oxyethylene glycol) to transesterify with poly(L-glutamic acid).[69] Alternatively the formation of hydrogels can be accomplished by the displacement of poly(γ-benzyl glutamate) with ω-hydroxyalkyl amines with α,ω-diaminoalkanes amino added to function as crosslinker.[70,71]

TABLE 10

Water Contact Angles on Copolypeptide Films[a] (from Ref. 73)

Material[b,c]	Casting solvent	Conformation	Contact angle (average) (degrees)
GL 1:1	CHCl₃	α-helix	80
GA 4:1	TFA	α + (random)	71
GA 1:1	CHCl₃ + Tr TFA	α-helix	58
GL 4:1	CHCl₃	α-helix	63.5
ZL 4:1	CHCl₃	α-helix	53.5
ZL 1:1	CHCl₃	α-helix	60
ZL 1:4	CHCl₃ + Tr TFA	α-helix	63
G(OH)V 4:1	TFA	α + (random)	37
G(OH)V 1:1	TFA	α + (random)	38
G(OH)V 1:4	TFA	β-sheet	47
G(OH)L 1:1	TFA	α-helix	40

[a] From Reference (73).
[b] G = γ-benzyl-L-glutamate; L = L-leucine; A = L-alanine; Z = ε-carbobenzoxy-L-lysine; V = L-valine; G(OH) = L-glutamic acid.
[c] Note that conformation of the G(OH) polypeptides may change slightly on hydration. Anhydrous film conformations are listed.

8.3. SURFACE ANALYSIS

The surface analysis and characterization of poly(amino acid) films has been limited to optical microscopy, scanning electron microscopy,[72] and some contact angle analysis.[73]

The contact angle measurements were advancing water droplets measured in air after ten minutes of contact (Table 10). As expected, the more hydrophilic copolypeptides which contain L-glutamine acid result in lower wetting angles.

9. SUMMARY/CONCLUSIONS

We have briefly reviewed a series of different polymer systems which have been used and can be used as model materials for probing biosurface phenomena. Although a wide variety of other polymer systems exist and can potentially be used as models, the ones reported here allow some study of stereochemistry, hydrophilicity, morphology, side chain and main chain mobility, hydrophobicity, and related properties. In addition, the hydroxyethyl methacrylate copolymer systems and the poly(α-amino acid) copolymer systems can also be used to probe surface charge phenomena, although this was not emphasized here.

It is clear that by application of suitable model systems and by careful quality control and surface property evaluation, coupled with careful biomedical interaction measurements such as *in vitro* blood interactions, one can indeed obtain significant correlations between the surface properties of materials and their biological behavior.[36]

ACKNOWLEDGMENTS

REFERENCES

1. Y. K. Sung, D. E. Gregonis, G. A. Russell, and J. D. Andrade, Effect of water and tacticity on the glass transition temperature of poly(2-hydroxyethyl methacrylate), *Polymer* **19**, 1362–1363 (1978).
2. A. D. Jenkins, Stereochemical definitions and notations relating to polymers, *Pure Appl. Chem.* **51**, 1101–1121 (1979).
3. J. Brandrup and E. H. Immergut, *Polymer Handbook*, 2nd ed., Wiley, New York (1975).
4. F. A. Bovey, *High Resolution NMR of Macromolecules*, Academic Press, New York (1972).
5. F. A. Bovey and G. V. D. Tiers, Polymer NSR spectroscopy, *J. Polym. Sci.* **44**, 173–182 (1960).
6. D. E. Gregonis, G. A. Russell, J. D. Andrade, and A. C. deVisser, Preparations and properties of stereoregular poly(hydroxyethyl methacrylate) polymers and hydrogels, *Polymer* **19**, 1279–1284 (1978).
7. H. Yuki and K. Hatada, in: *Advances in Polymer Science* (H.-J. Cantow, G. Dall'Asta, K. Dušek, J. D. Ferry, H. Fujita, M. Gordon, W. Kern, G. Natta, S. Okamura, C. G. Overberger, T. Saegusa, G. V. Schulz, W. P. Slichter and J. K. Stille, eds.), Vol. 31, pp. 1–45, Springer-Verlag, New York (1979).
8. P. Vlcek, D. Doskocilova, and J. Trekoval, Anionic copolymerization of methacrylates, *J. Polym. Sci. Symp.* **42**, 231–238 (1973).
9. H. Kusangi, H. Tadokoro, and Y. Chatani, Double strand helix of isotactic poly(methyl methacrylate), *Macromolecules* **9**, 531–532 (1976).
10. R. Lovell and A. H. Windel, Structure of noncrystalline isotactic poly(methyl methacrylates). Evidence against double helices, *Macromolecules* **14**, 211–212 (1981).
11. M. Toyama and T. Ito, Studies of surface wettability of stereospecific poly(methacrylic acid esters), *J. Colloid Interface Sci.* **49**, 139–142 (1974).
12. D. E. Gregonis, C. M. Chen, and J. D. Andrade, in: *Hydrogels for Medical and Related Applications*, (J. D. Andrade, ed.), Am. Chem. Soc. Symp. Ser. **31**, 88–104 (1976).
13. B. D. Ratner and A. S. Hoffman, in: *Adhesion and Adsorption of Polymers* (L. H. Lee, ed.), Part B, pp. 691–706, Plenum, New York (1980).
14. O. Wichterle, Hydrogels, *Encyclopedia of Polymer Science* **15**, 273–291 (1971).
15. M. S. Choudhary and I. K. Varma, Copolymerization of 2-hydroxyethyl methacrylate with alkyl methacrylates, *Eur. Polym. J.* **15**, 957–959 (1979).
16. I. K. Varma and S. Patnaik, Copolymerization of 2-hydroxyethyl methacrylate with alkyl acrylates, *Eur. Polym. J.* **12**, 259–261 (1976).
17. T. Okano, J. Aoyagi, and I. Shinohara, The wettability and composition of 2-hydroxyethyl methacrylate copolymers. *Nippon Kagaku Kaishi* **1976(1)** 161–170 (1976).

18. C. Migliaresi, L. Nicodemo, and L. Nicolais, 2-Hydroxyethyl methacrylate/methyl methacrylate copolymers for biomedical use, *Society for Biomaterials Abstracts*, 8th Annual Meeting, p. 123 (1982).
19. A. Silberberg, in: *Hydrogels for Medical and Related Applications* (J. D. Andrade, ed.), Am. Chem. Soc. Symp. Ser. **31**, 198–205 (1976).
20. J. D. Andrade, R. N. King, D. E. Gregonis, and D. L. Coleman, Surface characterization of poly(hydroxyethyl methacrylate) and related polymers, *J. Polym. Sci. Symp.* **66**, 313–336 (1979).
21. J. D. Andrade, S. M. Ma, R. N. King, and D. E. Gregonis, Contact angles at the solid–water interface, *J. Colloid Interface Sci.* **72**, 488–494 (1979).
22. W. C. Hamilton, A technique for the characterization of hydrophilic solid surfaces, *J. Colloid Interface Sci.* **40**, 219–222 (1972).
23. W. C. Hamilton, Measurement of the polar force contribution to adhesive bonding, *J. Colloid Interface Sci.* **47**, 672–675 (1974).
23. W. C. Hamilton, Measurement of the polar force contribution to adhesive bonding, *J. Colloid Interface Sci.* **47**, 672–675 (1974).
24. D. E. Gregonis, R. Hsu, D. E. Buerger, L. M. Smith, and J. D. Andrade, in: *Macromolecular Solutions* (R. B. Seymour and G. A. Stahl, eds.), pp. 120–133, Pergamon, New York (1982).
25. D. R. Paul and S. Newman, *Polymer Blends*, Vol. 1, Academic Press, New York (1978).
26. M. F. Sefton and E. W. Merrill, Surface hydroxylation of styrene–butadiene–styrene block copolymers for biomaterials, *J. Biomed. Materials Res.* **10**, 33–45 (1976).
27. M. F. Sefton and E. W. Merrill, Infrared spectroscopic analysis of complex polymer systems, *J. Appl. Polym. Sci.* **20**, 157–168 (1976).
28. H. C. Brown, *Organic Synthesis via Boranes*, J. Wiley, New York (1975).
29. C. P. Pinazzi, A. Menil, J. C. Rabadeax, and A. Pleurdeau, Polyisoprene and polybutadiene derivatives of potential biomedical interest, *J. Polym. Sci. Symp.* **52**, 1–7 (1975).
30. T. Okano, M. Ikemi, and I. Shinohara, The viscosity behavior of ABA-type block copolymer composed of 2-hydroxyethyl methacrylate and styrene in organic solvent mixture, *Polym. J.* **10**, 477–484 (1978).
31. T. Okano, M. Katayama, and I. Shinohara, The influence of hydrophilic and hydrophobic domains on water wettability of 2-hydroxyethyl methacrylate–styrene copolymers, *J. Appl. Polym. Sci.* **22**, 369–377 (1978).
32. E. W. Merrill, Properties of materials affecting the behavior of blood at their interfaces, *Ann. N.Y. Acad. Sci.* **283**, 6–16 (1977).
33. L. S. Luskin in: *Encyclopedia of Industrial Chemical Analysis* (F. D. Snell and C. L. Hilton, eds.), Vol. 4, pp. 181–218, Interscience, New York (1967).
34. R. S. Corley, in: *Monomers* (E. R. S. Blout and H. Mark, eds.), Interscience, New York (1951).
35. C. E. Rehberg and C. H. Fisher, Preparation and properties of *n*-alkyl acrylates, *J. Am. Chem. Soc.* **66**, 1203–1207 (1944).
36. D. L. Coleman, *In Vitro Blood–Materials Interactions: A Multi-Test Approach*, Ph.D. Thesis, Department of Pharmaceutics, University of Utah, August, 1980.
37. H. Determan, *Gel Chromatography*, Springer-Verlag, New York (1968).
38. S. Shaltiel, Hydrophobic chromatography, *Methods Enzymol.* **34**, 126–140 (1974).
39. J. L. Ochoa, Hydrophobic (interaction) chromatography, *Biochimie* **60**, 1–15 (1978).
40. B. H. J. Hofstee and N. F. Otillio, Non-ionic adsorption chromatography of proteins, *J. Chromatogr.* **159**, 57–70 (1978).
41. T. C. J. Gribnau, C. A. G. van Ekelen, C. Stumm, and G. I. Tesser, Microscopic observations on agarose beads, *J. Chromatogr.* **132**, 519–524 (1977).
42. J. Rosengren, S. Pahlman, M. Glad, and S. Hjerten, Hydrophobic interaction chromatography on noncharged sepharose derivatives, *Biochem. Biophys. Acta* **412**, 51–61 (1975).

43. A. Noshay and J. E. McGrath, *Block Copolymers, Overview and Critical Survey*, Academic Press, New York (1977).

44. D. C. Allport and W. H. James, *Block Copolymers*, Wiley, New York (1973).

45. G. L. Wilkes, T. S. Dziemianowicz, Z. H. Ophir, E. Artz, and R. Wildnauer, Thermally induced time dependence of mechanical properties in biomedical grade polyurethanes, *J. Biomed. Materials Res.* **13**, 189-206 (1979).

46. K. A. Pigott, in: *Kirk Othmer Encycl. Chem. Technol.* (H. Mark, ed.), Vol. 21, pp. 56-106, Interscience, New York (1970).

47. J. M. Buist and H. Gudgeon, *Adv. Polyurethane Tech.* Wiley, New York (1968).

48. C. S. Schollenberger and K. J. Dinberg, Thermoplastic urethane molecular weight-property relations, *J. Elastoplast.* **5**, 222-251 (1973).

49. C. S. P. Sung, C. B. Hu, and C. S. Wu, Properties of segmented poly(urethane ureas) based on 2,4-toluene diisocyanate, *Macromolecules* **13**, 111-116 (1980).

50. C. S. P. Sung and C. B. Hu, Orientation studies of segmented polyether poly(urethane urea) elastomers by infrared dichroism, *Macromolecules* **14**, 212-215 (1981).

51. C. S. P. Sung and N. S. Schnedier, Infrared studies of hydrogen bonding in toluene diisocyanate based polyurethanes, *Macromolecules* **8**, 68-73 (1975).

52. S. L. Samuels and G. L. Wilkes, Anisotropic superstructure in segmented polyurethanes as measured by photographic light scattering, *Polym. Lett.* **9**, 761-766 (1971).

53. R. W. Seymour, G. M. Estes, D. S. Huh, and S. L. Cooper, Rheo-optical studies of polyurethane block polymers, *J. Polym. Sci.* **10**, 1521-1527 (1972).

54. K. Knutson and D. J. Lyman, Morphology of block copolyurethanes. II. FTIR and ESCA techniques for studying surface morphology, *Organic Coatings and Plastics Preprints* **42**, 621-627 (1980).

55. V. S. da Costa, D. Brier-Russell, D. W. Salzman, and E. W. Merrill, ESCA studies of polyurethanes: blood activation in relation to surface composition, *J. Colloid Interface Sci.* **80**, 445-452 (1981).

56. B. D. Ratner, ESCA and SEM studies on polyurethanes for biomedical applications, *Polymer Preprints* **21**, 152-153 (1980).

57. B. D. Ratner in: *Photon, Electron, and Ion Probes of Polymer Structure and Properties* (D. W. Dwight, T. J. Fabish, and H. R. Thomas, eds.), Am. Chem. Soc. Symp. Ser. **162**, 371-382 (1981).

58. B. D. Ratner in: *Physicochemical Aspects of Polymer Surfaces* (K. L. Mittal, ed.), Vol. 2, pp. 969-983, Plenum, New York (1983).

59. M. D. Lelah, L. K. Lambrecht, B. R. Young, and S. L. Cooper, Physiochemical characterization and *in vivo* blood tolerability of cast and extruded biomer, *J. Biomed. Materials Res.* **17**, 1-22 (1981).

60. K. Knutson and D. J. Lyman in: *Biomaterials: Interfacial Phenomena and Applications* (S. L. Cooper and N. A. Peppas, eds.), Advan. Chem. Ser. **199**, 109-132 (1982).

61. T. Miyamae, S. Mori, and Y. Takeda, Poly-L-glutamic acid surgical sutures, U.S. Patent 3,371,069 (1968).

62. R. V. Peterson, C. G. Anderson, S. M. Fang, D. E. Gregonis, S. W. Kim, J. Feijen, J. M. Anderson, and S. Mitra in: *Controlled Release of Bioactive Materials* (R. Baker, ed.), pp. 45-60, Academic Press, New York (1980).

63. C. W. Hall, M. Spira, F. Gerow, L. Adams, E. Martin, and S. B. Hardy. Evaluation of artificial skin models: presentation of three clinical cases, *Trans. Am. Soc. Art. Int. Org.* **16**, 12-16 (1970).

64. E. Klein, P. D. May, J. K. Smith, and N. Leger, Permeability of synthetic polypeptide membranes, *Biopolymers* **10**, 647-655 (1971).

65. F. Fuchs, Uber N-carbonsaure-anhydride, *Chem. Ber.* **55**, 2943 (1922).

66. A. C. Farthing, Synthetic polypeptides, *J. Chem. Soc.*, 3213-3217 (1950).

67. H. R. Kricheldorf, Mechanisms of NCA polymerization, *Makromol. Chem.* **178**, 905-939 (1977).

68. N. Lupu-Lotan, A. Yaron, A. Berger, and M. Sela, Conformational changes in the nonionizable water soluble synthetic polypeptide poly-N5(3-hydroxypropyl) L-glutamine, *Biopolymers* **3**, 625-655 (1965).

69. T. Tanaka, T. Mori, K. Ogawa, and R. Tanaka, Heterogeneous network polymers. IX. Poly(L-glutamic acid) crosslinked with polyether diisocyanates, *Polymer J.* **11**, 731-736 (1979).

70. T. Sugie, J. M. Anderson, and P. A. Hiltner, Structure and deformation of a crosslinked poly(α-amino acid), *Polymer Preprints* **20**, 439-441 (1979).

71. T. Sugie and A. Hiltner, Structure and deformation of a crosslinked poly(α-amino acid), *J. Macromol. Sci., Phys.* **B17**, 769-785 (1980).

72. D. D. Solomon, D. H. Cowan, J. M. Anderson, and A. G. Walton, Platelet interaction with synthetic copolypeptide films, *J. Biomed. Materials Res.* **13**, 765-782 (1980).

73. D. D. Solomon, D. H. Cowan, and A. G. Walton in: *Colloid and Interface Science*, Vol. 5 (M. Kerker, ed.), pp. 1-21, Academic Press, New York (1976).

74. G. Odian, *Principles of Polymerization*, McGraw-Hill, New York (1970).

75. E. H. Riddle, *Monomeric Acrylic Esters*, Reinhold, New York (1954).

76. P. Pino and R. Mulhaupt, Stereospecific polymerization of propylene: an outlook 25 years after its discovery, *Angew Chem., Int. Ed. Engl.* **19**, 857-875 (1980).

77. S. L. Aggarwal, *Block Copolymers*, Plenum, New York (1970).

78. T. Okano, M. Shimada, I. Shinohara, K. Kataoka, T. Akaike, and Y. Sakurai, in: *Biomaterials 1980*, (G. D. Winters, D. F. Gibbons, and H. Plenk, Jr., eds.), pp. 445-450, John Wiley, New York (1982).

Surface and Interfacial Aspects of Biomedical Polymers

Volume 1
Surface Chemistry and Physics

Edited by
Joseph D. Andrade
University of Utah
Salt Lake City, Utah

1985

PLENUM PRESS • NEW YORK AND LONDON